

Assessment of adaptation limits in the water sector under a changing climate

GEO 511 Master's Thesis

Author Fiona Federer 18-703-231

Supervised by Dr. Randy Muñoz Asmat

Faculty representative Prof. Dr. Christian Huggel

Acknowledgment

First, I would like to express my gratitude to my supervisor Dr. Randy Muñoz Asmat for his support during the past year. His guidance, expertise in fields initially unknown to me, and constructive and encouraging feedback were crucial for me to write this thesis. In addition, he furnished essential data for the Quillcay catchment study, encompassing scanned reports, georeferenced data, and the script for the hydrological model. His profound local knowledge and connections were indispensable in obtaining otherwise inaccessible information. Second, I also would like to thank Prof. Dr. Christian Huggel, who accompanied my work as faculty representative and enriched it with his insightful advice. Further, I thank Isabel Hagen for sharing insights from her qualitative research on constraints and limits to adaptation in Peru, which provided valuable input for my thesis. Last, my deepest gratitude goes to my family and friends for their unconditional support, care, and encouragement throughout my studies and the writing of this thesis. I'm especially grateful to my fellow students, whose companionship, countless hours spent writing together in G10, and shared coffee breaks have brightened this year.

i

Abstract

The mountain cryosphere is a crucial water source for downstream populations. However, climate change is progressively reducing the seasonal buffering capacity of glacial runoff, increasing the vulnerability of downstream populations to insufficient water supply. In response, decision-makers are designing and implementing adaptation measures to avoid water scarcity, but the Intergovernmental Panel on Climate Change (IPCC) recognizes adaptation limits beyond which risks become intolerable, leading to irreversible damage and behavioral change. Therefore, decision-makers in water management need a basic understanding of the factors that drive water scarcity and the conditions that can lead to limits to adaptation. Nonetheless, there is an imbalance in the methods used to study the adaptation limits to climate change. While existing studies are predominantly qualitative, focusing on the present situation that causes limits to adaptation, they often fail to consider the dimension of the uncertain future. To address this challenge, this thesis aims to adapt Exploratory Modeling and Analysis (EMA) to the new context of adaptation limits. EMA is a quantitative approach used to explore multiple scenarios that capture the full extent of uncertainties, and it has been applied to study climate change adaptation measures in various fields. More specifically, the goal is to assess to what extent EMA can support the identification and quantification of critical factors and conditions that influence water scarcity in mountain regions. In a case study in the Quillcay catchment area (Cordillera Blanca, Peru), 6000 simulations of the hydrological model Shaman are conducted from 2020 - 2050. These simulations consider a range of potential climatic and socioeconomic scenarios spanning from optimistic to pessimistic, to account for uncertainty. Thus, all possible scenarios are explored without focusing on the most probable, allowing for robustness of the identified conditions where water demand is not met. The main drivers of water scarcity are found to be the adaptation measure of water use efficiency, alongside future domestic water allocation. As the range of socioeconomic scenarios narrows, the influence of climatic factors on water scarcity increases. This underscores the necessity of defining feasible socioeconomic scenario ranges and establishing pertinent thresholds for water scarcity. It is of the utmost importance to involve local stakeholders in this process to ensure a context-specific definition of water scarcity, while also considering the limitations of the models and assumptions used. The research illustrates how the novel method EMA offers valuable insights, particularly when combined with qualitative, local research. For decisionmakers in regions like the Quillcay watershed, EMA can provide crucial information on future water management, influencing not only water scarcity responses but also broader climate change mitigation and adaptation strategies.

Resumen

La criosfera montañosa es una fuente de agua crucial para los habitantes aguas abajo. Pero el cambio climático está reduciendo la capacidad de amortiguación estacional de la escorrentía glaciar, lo que aumenta la vulnerabilidad de las poblaciones aguas abajo a un suministro insuficiente de agua. En respuesta, los responsables de la toma de decisiones están diseñando y aplicando medidas de adaptación para evitar la escasez de agua, pero el Grupo Intergubernamental de Expertos sobre el Cambio Climático (ingl. IPCC) reconoce límites de adaptación más allá de los cuales los riesgos se vuelven intolerables, provocando daños irreversibles y cambios de comportamiento. Así pues, los responsables de la gestión del agua deben tener un conocimiento básico de los factores que provocan la escasez de agua y de las condiciones que pueden conducir a límites de adaptación. Sin embargo, existe un desequilibrio en los métodos utilizados para estudiar los límites de adaptación al cambio climático. Mientras que los estudios existentes son principalmente cualitativos y están centrados en el presente que causa límites de adaptación, a menudo no consideran la incertidumbre futura. Para abordar este reto, esta tesis aspira a adaptar "Exploratory Modeling and Analysis" (ingl. EMA) a un nuevo contexto. EMA es un método cuantitativo utilizado para explorar múltiples escenarios que capturan todo el espectro de incertidumbres, y se ha aplicado para estudiar medidas de adaptación al cambio climático en diversos sectores. Más concretamente, el objetivo es evaluar hasta qué punto EMA puede contribuir a identificar y cuantificar los factores y condiciones clave que influyen en la escasez de agua en las regiones montañosas. En un estudio de caso en la cuenca del Quillcay (Cordillera Blanca, Perú), se realizan 6000 simulaciones del modelo hidrológico Shaman entre 2020 y 2050. Estas simulaciones consideran una serie de posibles escenarios climáticos y socioeconómicos desde optimistas a pesimistas, para tomar en cuenta la incertidumbre. Así, se exploran todos los escenarios posibles sin centrarse en los más probables, lo que permite la robustez de las condiciones identificadas en las que no se satisface la demanda de agua. Los factores que más influyen la escasez de agua son la eficiencia en el uso del agua como medida de adaptación y la futura dotación de agua para uso doméstico. Al reducirse la gama de escenarios socioeconómicos, aumenta la influencia de los factores climáticos en la escasez de agua. De ahí la necesidad de definir gamas de escenarios socioeconómicos realistas y de establecer umbrales pertinentes para la escasez de agua. Es fundamental implicar a actores locales en este proceso para garantizar una definición de la escasez de agua adaptada al contexto, sin olvidar las limitaciones de los modelos y supuestos aplicados. La tesis muestra cómo el nuevo método EMA ofrece perspectivas valiosas, especialmente al combinarse con la investigación cualitativa local. Para los responsables de la toma de decisiones en regiones como la cuenca de Quillcay, EMA puede ofrecer información esencial sobre la futura gestión del agua, influyendo no sólo en las respuestas a la escasez de agua, sino también en estrategias más amplias de mitigación y adaptación al cambio climático.

Table of Contents

List	of Fig	gures	s and Tables	vi
Fi	gures	3		vii
Ta	ables			x
List	of Ab	brev	iations	xii
1.	Intro	ducti	on	1
1.	1.	Rele	evance of mountain cryosphere in future water resource management	1
1.	2.	Red	lucing climate risks by understanding limits to adaptation	2
1.	3.	Res	earch question	3
2.	Stud	y Are	ea	4
2.	1.	Clin	natological and hydrological context	4
2.	2.	Soc	ioeconomic context	6
3.	State	e of t	he art	7
3.	1.	Sha	red Socioeconomic Pathways and Representative Concentration Pathways	7
3.	2.	Key	concepts on limits to adaptation and constraints	8
	3.2.1	١.	Risks	8
	3.2.2	2.	Limits to adaptation	9
	3.2.3	3.	Constraints	11
3.	3.	Trac	ditional methods to identify limits to adaptation	12
3.	4.	Con	nplementary methods to identify limits to adaptation	14
3.	5.	Ехр	loratory Modeling and Analysis (EMA)	15
	3.5.1	١.	Structuring the analysis with the XLRM-framework	15
	3.5.2	2.	Modeling future pathways by defining ranges of uncertain variables	16
	3.5.3	3.	Exploring the analysis with stress testing	16
4.	Meth	nod		18
4.	1.	Inte	gration of the XLRM-framework in the case study	18
	4.1.1	۱.	Uncertainties X: climate scenario and socioeconomic data	20
	4.1.2	2.	Policy levers L: efficiencies	30
	4.1.3	3.	Relation R: Shaman model	31
	4.1.4	١.	Metric M: water scarcity indicator	37

	4.	2.	Inte	gration of uncertainty ranges in the case study	38
	4.	.3.	Inte	gration of stress testing in the case study	40
		4.3.1	١.	Threshold setting	41
		4.3.2	2.	Sensitivity Analysis operationalized with Feature Scoring	42
		4.3.3	3.	Scenario Discovery operationalized with PRIM	42
5	•	Resu	ults		43
	5.	1.	Disc	charge modeling	43
	5.	2.	Stre	ss testing: Sensitivity Analysis operationalized with Feature Scoring	46
		5.2.1		Impacts of irrigation efficiency and uncertainty variables on the water balance	46
		5.2.2	2.	Impacts of irrigation efficiency and uncertainty variables on water scarcity	47
		5.2.3	3.	Impacts of domestic efficiency and uncertainty variables on water scarcity	51
	5.	.3.	Stre	ss testing: Scenario Discovery operationalized with PRIM	53
		5.3.1		Threshold sensitivity shaping non-operational ranges	53
		5.3.2	2.	The lack of informative results	54
		5.3.3	3.	Unrealistic operational ranges	54
		5.3.4	l.	Interactions between adaptation measures and socioeconomic uncertainties	55
		5.3.5	5.	Interactions between adaptation measures and climatic uncertainties	56
6		Disc	ussio	on	58
	6.	1.	Fact	tors driving water scarcity and potential adaptation limits in the Quillcay catchment	58
		6.1.1		Insights from the Sensitivity Analysis	58
		6.1.2	<u>)</u> .	Insights from the Scenario Discovery	59
	6.	2.	Limi	tations of integrating EMA to identify key drivers of water scarcity	59
		6.2.1		Adapting EMA to the Quillcay catchment: assumptions and their limitations	59
		6.2.2	<u>)</u> .	Boundaries of EMA in the case study: analytical capabilities and constraints	63
	6.	.3.	Adv	ancing adaptation and risk assessments with EMA: insights and recommendations	65
7	•	Cond	clusic	on	71
8	-	Refe	renc	es	73
9		Appe	endix		84
	9.	.1.	Data	3	84
		911		GIS data	84

9.	1.2.	Historical data	85
9.	1.3.	Future projections	86
9.2.	Stat	istics	87
9.:	2.1.	Trend detection	87
9.:	2.2.	Statistical differences between historical and projected data	87
9.3.	Add	itional figures	88
10.	Persor	nal Declaration	90

List of Figures and Tables

Figures

Figure 1: left: Santa watershed. right: Quillcay catchment with the three main glacial valleys (Motschmann et al., 2020a)
Figure 2: Visualization of pathways combining different RCPs and SSPs and their indicative temperature and mitigation trajectories according to the IPCC (Chen D. et al., 2021)
Figure 3: Acceptable, tolerable and intolerable risks in relation to adaptation limits (Dow et al., 2013; based on Klinke and Renn, 2012)
Figure 4: Key risks propeller and the conceptualization of limits to adaptation in the solution space for climate resilient development (O'Neill et al., 2022)
Figure 5: Four-dimensional view of limits to adaptation designed by (Juhola et al., 2024) 11
Figure 6: Schematic representation of the workflow to operationalize RDM (own illustration; based on Vaghefi et al., 2021; Muñoz et al., 2024b).
Figure 7: Schematic representation of step i) in the EMA workflow: the XLRM-framework set for the analysis of future water scarcity (own illustration; based on Vaghefi et al., 2021; Muñoz et al., 2024a).
Figure 8: left: Effect of MBCn bias-correction on the average of the GCM compared to the multiannual monthly average precipitation of PISCOv2p1. right: Bias-corrected multiannual monthly average temperature data based on the average of the GCM (own illustration)
Figure 10: left: Historical and future total annual precipitation based on the different GCMs. right: Multiannual monthly average precipitation. The bold line represents the SSP average derived for each GCM, whilst the shaded areas illustrate the standard deviation from the climate models used for each climate scenario (own illustrations).
Figure 11: Comparison between historical and future precipitation patterns. The box groups 50% of the data equally around the median (horizontal line) and the whiskers extend to the 10% and 90% of the data respectively (own illustration)

Figure 12: Bias-corrected multiannual monthly average evapotranspiration data based on the
historical average of the GCM. The bold line represents the GCM average derived from the three
climate scenarios (SSP1-2.6, SSP3-7.0, and SSP5-8.5), whilst the shaded areas illustrate the
standard deviation from the climate models used for each climate scenario (own illustration) 24
Figure 13: left: Average annual temperature. right: Glacier extent. In both figures, the bold line
represents the GCM average derived from the three climate scenarios (SSP1-2.6, SSP3-7.0, and
SSP5-8.5), whilst the shaded areas illustrate the standard deviation from the climate models used
for each climate scenario (own illustration)
Figure 14: left: Quillcay catchment and its location within the political district borders and main urbar
settlement area (own illustration, data: delineation from Geo Perú "Ríos y Quebradas" and "Google
Satelital" (2024), Quillcay catchment; Jarvis et al. (2008), Cordillera Blanca; ANA (2023), ESRI living
atlas; Esri (n.d.). right: Drinking water network of the city of Huaraz in 2024 of Empresa Prestadora
de Servicios de Saneamiento (EPS, Enterprise providing sanitation services) Chavín; EPS Chavír
S.A. (2024)
Figure 15: Schematic representation of Shaman model (Muñoz et al., 2021; Muñoz et al., 2024c)
Figure 16: Environmental flow requirements (EFR) based on the observed runoff (1981 – 2014). The
methods are persistence at 95% of total runoff used as environmental flow (95), minimal monthly
average runoff (min), and 50% of the minimal monthly average runoff (50%min)
Figure 17: Total runoff and glacier contribution in the calibration and validation period. Calibration
(R ² : 0.93, Nash: 0.86, Nash-In: 0.76), validation (R ² : 0.92, Nash: 0.84, Nash-In: 0.78)
Figure 18: Schematic representation of step ii) in the EMA workflow: applied range definitions A, B
and C on the uncertainties and policy levers. Variables (X, L) that are not listed are not subject to
different range scenarios
Figure 19: Applied range definitions of the uncertain variables in part ii) of EMA 40
Figure 20: Fuzzy space of acceptable intolerable risks in relation to the metric and threshold setting
operationalized in EMA, adapted from Dow et al. (2013) (based on Klinke and Renn (2012)). In the
way EMA has been adapted, the frequency of water scarcity (WS) can be changed by varying the
threshold, thus the analyzed black point can be moved on the black dotted line. The continuous colo
gradient of acceptable and intolerable risks represents the gradual change in perception from
acceptable to tolerable to intolerable risk and illustrates the concept rather than the exac
manifestations41

Figure 21: Multiannual monthly average discharge colored based on the three different climate scenarios. left: Historical PISCO data. right: Simulated historical data. The bold line represents the GCM average derived from the three climate scenarios (SSP1-2.6, SSP3-7.0, and SSP5-8.5), whilst the shaded areas illustrate the standard deviation from the climate models used for each climate scenario (own illustrations).
Figure 22: left: Average annual discharge. right: Average dry season discharge. Both datasets are based on the three different climate scenarios and simulated historical data. The bold line represents the GCM average derived from the three climate scenarios (SSP1-2.6, SSP3-7.0, and SSP5-8.5), whilst the shaded areas illustrate the standard deviation from the climate models used for each climate scenario (own illustrations).
Figure 23: Comparison between historical and future discharge patterns. The box groups 50% of the data equally around the median (horizontal line) and the whiskers extend to the 10% and 90% of the data respectively (own illustration)
Figure 24: Concept of peak water. The gray-shaded area represents the evolution until 2020 for an analysis in the upper Santa river (Guittard et al., 2020; based on Baraer et al., 2012)
Figure 25: Comparison of water demand based on sectors from 2020 to 2050 (L = irrigation efficiency). The bold line represents the average of all monthly simulations, whilst the shaded areas illustrate the standard deviation
Figure 26: Comparison of water demand (multiannual monthly mean) based on sectors of all simulations from 2020 – 2050. The bold line represents the average of all simulations, whilst the shaded areas illustrate the standard deviation.
Figure 27: Historical and future total annual temperature, precipitation based on the three different climate scenarios. In both figures, the bold line represents the GCM average derived from the three climate scenarios (SSP1-2.6, SSP3-7.0, and SSP5-8.5), whilst the shaded areas illustrate the standard deviation from the climate models used for each climate scenario (own illustration) 51
Figure 28: Scenario discovery outputs showing non-operational ranges on the upper horizon and pair scatter (range scenario B. left: $t \ge 0.2$ with coverage = 0.648 and density = 0.947; right: $t \ge 0.15$ with coverage = 0.79 and density = 0.982). The term True is counterintuitive, meaning successful or metric outcomes above the threshold.
Figure 29: Scenario discovery outputs showing non-operational ranges (range scenario C, $t \ge 0.2$ with coverage = 0.819 and density = 0.588)
Figure 30: Scenario discovery outputs showing non-operational ranges (range scenario C, $t \ge 0.2$ with coverage = 0.603 and density = 0.76)

Figure 31: Scenario discovery outputs showing pair scatter (range scenario C, $t \ge 0.2$). The term True is counterintuitive, meaning successful or metric outcomes above the threshold
Figure 32: Scenario discovery outputs showing non-operational ranges and pair scatter (range scenario A, $t \ge 0.22$ with coverage = 0.630 and density = 0.634)
Figure 33: Scenario discovery outputs showing pair scatter (range scenario A, $t \ge 0.22$). The term True is counterintuitive, meaning successful or metric outcomes above the threshold
Figure 34: Different risk definition that have an implication of the scaling of the threshold. They are spanned between an axis of scale from individual to global and humanity and an axis of the the severity of how the subjects are impacted by Huggel et al. (2022)
Figure 35: Comparison between historical and future precipitation patterns. The box groups 50% of the data equally around the median (horizontal line) and the whiskers extend to the 10% and 90% of the data respectively (own illustration)
Figure 36: Average dry season discharge. Both datasets are based on the three different climate scenarios and simulated historical data. The bold line represents the SSP average for each GCM, whilst the shaded areas illustrate the standard deviation (own illustrations)
Figure 37: Historical and future glacier extent. The bold line represents the average area for each GCM, whilst the shaded areas illustrate the standard deviation(own illustration)
Tables
Table 1: Overview of constraint categories with a possible example in the context of the adaptation to water scarcity in the Andes based on Thomas et al. (2021)
Table 2: Traditional methods to assess limits to adaptation with their strengths and limitations 13
Table 3: Strengths and weaknesses of RDM to assess robust adaptation strategies 14
Table 4: Description of the uncertainties (X), policy levers (L), and the metric (M) and constants of the model (R) used in this study. The column "Data / Reference" gives an overview of the source of the defined ranges. More information about original data ("raw data") and modified data ("processed data") in appendix 9.1.
Table 5: Reclassification logic for all existing land cover classes in the original data 34
Table 6: Comparison of different land cover fractions derived from analysis and reports 35
Table 7: P-values from the Mann-Kendall test (α = 0.05) applied to historic (1981-2014) and average scenario (2015 - 2050, 2020 – 2050 for simulated discharge) time series. Simulated historical runoff

data were used to isolate the contributions of climate scenarios from discrepancies between simulated and observed data
Table 8: P-values for testing statistical significance and post hoc test results are reported for significant findings, with a significance level of $\alpha = 0.05$ for all tests
Table 9: Results from Feature Scoring according to the applied script (combined climate variables / split climate variables) and range scenarios (A / B / C) with the policy leverage being irrigation efficiency.
Table 10: Number and share of experiments considered as water-scarce depending on threshold setting and range setting
Table 11: Results from Feature Scoring with $t \ge 0.2$ and $t \ge 0.15$ according to the range scenarios (A / B / C) with the policy leverage being irrigation efficiency
Table 12: Number and share of experiments considered as water-scarce depending on threshold setting and range setting
Table 13: Results from Feature Scoring with $t \ge 0.2$ and $t \ge 0.15$ according to the range scenarios (A / B / C) with the policy leverage being domestic efficiency
Table 14: Raw GIS data used for the analysis
Table 15: Processed GIS data used in for the analysis
Table 16: Raw historical data. The variables are color-coded according to their impact on the water balance: Variables that influence supply = blue; demand = orange; both = yellow
Table 17: Processed historical data. The variables are color-coded according to their impact on the water balance: Variables that influence supply = blue; demand = orange; both = yellow
Table 18: Raw future scenarios. The variables are color-coded according to their impact on the water balance: Variables that influence supply = blue; demand = orange; both = yellow
Table 19: Processed future scenarios. The variables are color-coded according to their impact on the water balance: Variables that influence supply = blue; demand = orange; both = yellow 86
Table 20: P-values from the Mann-Kendall test (α = 0.05) applied to historic (1981-2014) and average scenario (2015 - 2050, 2020 - 2050 for simulated discharge) time series. Simulated historical runoff data were used to isolate the contributions of climate scenarios from discrepancies between simulated and observed data.
Table 21: P-values for statistical significance and post hoc test results are reported for significant

List of Abbreviations

ANA Autoridad Nacional del Agua (National Water Authority)

BASD-CMIP6-PE Bias-Adjusted and Statistically Downscaled CMIP6 projections for

Peru and Ecuador

DEM Digital Elevation Model

DAPP Dynamic Adaptive Policy Pathways

DMDU Decision Making under Deep Uncertainty

EMA Exploratory Modeling and Analysis

FAO Food and Agriculture Organization of the United Nations

FLH Freezing Level Height
GCM Global Climate Model

IAM Integrated Assessment Models

INAIGEM Instituto Nacional de Investigación en Glaciares y Ecosistemas de

Montaña (National Institute for Research in Glaciers and

Mountain Ecosystems)

INEI Instituto Nacional de Estadística e Informática (National Institute

of Statistics and Informatics)

IPCC Intergovernmental Panel on Climate Change

L&D Loss(es) and Damage(s) method

MIDAGRI Ministerio de Desarrollo Agrario y Riego (Ministry of Agricultural

Development and Irrigation)

MINAM Ministerio del Ambiente (Ministery of the Environment)

NDVI Normalized Difference Vegetation Index

PISCO Peruvian Interpolated data of the SENAMHI's Climatological and

hydrological Observations

PROFODUA Proyecto de Formalización de la Propiedad Rural y Desarrollo de

Catastro Rural (Project for the Formalization of Rural Property

and Development of Rural Cadaster)

RCP Representative Concentration Pathway

RDM Robust Decision Making

SENAMHI Servicio Nacional de Meteorología e Hidrología del Perú (National

Service of Meteorology and Hydrology of Peru)

SLF Sustainable Livelihood Framework

TPA Tipping Point Analysis

SSP Shared Socioeconomic Pathway

WHO World Health Organization

1. Introduction

1.1. Relevance of mountain cryosphere in future water resource management

The mountain cryosphere is a critical water resource for downstream populations and economies (Motschmann et al., 2020b). It represents not only a water resource for domestic and agricultural use supporting people's livelihood but also a cultural value (Motschmann et al., 2020b). However, the mountain cryosphere and consequently glacial runoff are strongly affected by climate change (Huss and Hock, 2018). The IPCC's mid to long-term risks (2041 - 2100) point out that the risk of declining physical water availability will continue to increase in all assessed regions at higher global warming. Specifically, snowmelt water availability for irrigation in agriculture is projected to decline in some snowmelt-dependent river basins by up to 20% at approximately 2°C global warming, and global glacier mass also has its contribution to water availability for sectors, such as agriculture and domestic water supply (IPCC, 2022a).

Yet, modeling future glacio-hydrological processes in mountainous regions is highly challenging: due to data scarcity of historical data series and limited process understanding (Muñoz et al., 2024b). The remoteness of the areas makes it difficult to install and to maintain a comprehensive hydrometeorological network (Salzmann et al., 2013), which for the example of the Peruvian Andes is already limited by insufficient funding (Llauca et al., 2023). Additionally, high natural variability, e.g. in precipitation at high altitudes, complicates the identification of long-term trends, as well as the limited ability of regional climate models and downscaling methods to capture the nuanced interactions between large-scale climate shifts and local processes influenced by complex terrain (Hock et al., 2019; Fernandez-Palomino et al., 2024). A lack of socioeconomic data to model local economic development, changes in water demand, and future population growth also limits the modeling process in general (Berkhout et al., 2014). Finally, the wide range of future climate and socioeconomic projections presents a challenge to a meaningful assessment of glacio-hydrological modeling.

Adaptation to climate change and its limits, discussed in the next section, is a critical and complex research challenge, particularly in the highly affected region of South America (Thomas et al., 2021), with significant implications for climate policy (Berkhout and Dow, 2022) due to the relevance of the mountain cryosphere.

1.2. Reducing climate risks by understanding limits to adaptation

Human-induced climate change, including more frequent and intense extreme events, is putting ecosystems and human systems at risk, which can result in an existential threat to the livelihood of billions of people worldwide (Huggel et al., 2022). The *Sixth Assessment Report* (AR6) of the *Intergovernmental Panel on Climate Change* (IPCC) highlights the challenges and vulnerabilities faced by different regions and sectors due to climate change. Adaptation to climate change is essential to reduce exposure and vulnerability and thus reduce risk. Nonetheless, the IPCC recognizes limits to societal adaptation, beyond which risks become intolerable, leading to irreversible loss, damage, and radical changes in human behavior, such as land abandonment or migration (Berkhout and Dow, 2022). Some ecosystems have already reached the limits of adaptation, and as global warming intensifies, losses and damage to both human and natural systems will increase (IPCC, 2022b).

The terminology of limits to adaptation remains not yet clearly defined, often being vague, abstract, and at times contradictory in literature (Dow et al., 2013; Barnett et al., 2015; Leal Filho et al., 2021; Hagen et al., in review). In general, one can understand limits to adaptation as mentioned above as a point beyond which no more adaptation will be possible (IPCC, 2022b; Juhola et al., 2024). Adaptation action can be restricted or impeded by constraints (IPCC, 2022b), also referred to as *obstacles* or *barriers* (Moser and Ekstrom, 2010; Ologeh et al., 2018; Leal Filho et al., 2021; Thomas et al., 2021). Limits to adaptation vary across ecological sectors, such as water resources, and human domains, including human health and urban planning (Thomas et al., 2021). According to Thomas et al. (2021) Central and South America emerge as regions where there is strong evidence of limits, particularly the adaptation measures taken by small-scale farmers in these regions are limited (Acevedo-Osorio et al., 2017; Gerlicz et al., 2019; Harvey et al., 2014; Jezeer et al., 2019; Warner, 2016).

Limits have not yet been widely incorporated into adaptation policy (Berkhout and Dow, 2022). The motivation for quantifying adaptation limits is that their existence has far-reaching implications (Dow et al., 2013): If the ability of different social actors to adapt is assumed to be unlimited, the effort to reduce greenhouse gas emissions is weakened and replaced by considerations of costs and benefits (Dow et al., 2013). Furthermore, it is worth noting that the majority of climate finance is directed towards mitigation efforts (Locatelli et al., 2016), while adaptation finance is often overlooked. Consequently, a better understanding of adaptation limits could be crucial to address this financial disparity. In addition, poorly designed or ineffective adaptation can undermine social equity and ultimately lead to maladaptation (Bezner Kerr et al., 2022; IPCC, 2022b). Maladaptation can be avoided through inclusive, flexible, long-term planning (IPCC, 2022b). To conclude, it is essential to understand the limits to adaptation, but also its constraints, in order to make informed decisions and avoid maladaptation.

1.3. Research question

Significant theoretical, methodological, and empirical advances are needed in research on adaptation limits, especially for social systems (Adger et al., 2009; Juhola et al., 2024). This is underpinned by Aggarwal et al. (2022), who argue for an additional focus on mountain areas. Moreover, Berkhout and Dow (2022) call for a more coherent, interdisciplinary, and methodologically diverse approach to research on limits. The methodologies for identifying limits as studied by Thomas et al. (2021), show a reliance on qualitative, actor-centered approaches. Consequently, this study aims to address the research gap in quantitative methods which would also facilitate more general research as proposed by Berkhout and Dow (2022) that is robust to an uncertain future. Yet, a basic understanding of the conditions that give rise to risks in the first place is needed in addition to, or as a basis for, identifying the limits to adaptation.

Therefore, the overarching goal of this Master's thesis is to assess to what extent *Exploratory Modeling and Analysis* (EMA; a component of *Decision Making under Deep Uncertainty*) can support the identification and quantification of critical factors and conditions that influence water scarcity in mountain regions. The *Decision Making under Deep Uncertainty* (DMDU) approach is designed to support better decisions under conditions of deep uncertainty. In the context of climate change in water management, it can be asserted that policymakers face deep uncertainty not only regarding the climate change scenarios but also regarding the actions of different stakeholders (Lempert, 2019).

The thesis begins with a case study exploring potential future water scarcity during the dry season in the Peruvian Andes, more specifically in the Quillcay watershed, addressing the following questions:

- 1. How can EMA be used to identify and quantify key drivers of future water scarcity within the social-ecological system of the Quillcay catchment?
- 2. What factors within the social-ecological system of the Quillcay catchment drive water scarcity and potentially represent a limit to adaptation?

Following the case study, the research adopts a broader conceptual approach to address an additional research question:

3. How can EMA be integrated or complement existing risk and adaptation frameworks to assess and quantify constraints and limits to adaptation?

This will provide insights on how EMA might be integrated into existing risk and adaptation frameworks and where are collaborative intersections with methodologically diverse research most needed.

2. Study Area

2.1. Climatological and hydrological context

The case study is located in the data-scarce Quillcay catchment, which is situated in the southern tropical Andes, more specifically in the mountain range Cordillera Blanca in Northern Peru. The Cordillera Blanca is a subsystem of the Cordillera Occidental. A dominant climatic feature of the southern tropical Andes is the seasonality of the precipitation on an intra-annual timescale (Martinez et al., 2011). At the same time, the hydroclimatic patterns across the tropical Andes remain highly complex and influenced by various factors (Fernandez-Palomino et al., 2024). For instance, elevation and topography play major roles in shaping local climate (Martinez et al., 2011). Whether a location is in the Cordillera Oriental (eastern range) or Cordillera Occidental (western range) influences precipitation patterns and temperature variations (Martinez et al., 2011). The catchment spans from 3050 m.a.s.l. until the highest elevation, the Nevado Cojup at 6250 m.a.s.l. and has an area of 250 km² (Quesquén Rumiche, 2008). The upper catchment is characterized by high-altitude Andean alpine landscapes and glacial lakes with an extensive glacierized area of 12% (2016) (ANA, 2018a; Motschmann et al., 2020) (cf. appendix 9.1.1.). The upper basin is part of the Huascarán National Park, while the lower part, between 3000m and 4000m, is used for small-scale agriculture and in the lowest area of the catchment the land cover is dominated by the urban infrastructure of the city Huaraz (Meza et al., 2016).

Hydrographically the catchment is influenced by seasonality and the mountain cryosphere. The precipitation pattern in the catchment is in line with the characteristics of southern tropical Andes showing a strong seasonality with the majority of the precipitation falling from October to April and a pronounced dry season from May to September (Bury et al., 2011; Mark et al., 2017). From 1981 to 2014, the total annual precipitation spans from approximately 900 to 1100mm (cf. Figure 9) The hydrographic network has its source in the glacierized gorge Cojup, which downstream forms the river Paria; after the confluence with the river Auqui, it is called Quillcay, which crosses the city of Huaraz before flowing into the river Santa (Meza et al., 2016). The Santa basin eventually drains into the Pacific Ocean (cf. Figure 1) (Meza et al., 2016). In the lower catchment area, the Quillcay has a multiannual monthly average runoff between 1.6 and 15.5 m³/s (1981 - 2014), while the average runoff is around 6.4 m³/s (cf. Figure 21, 22). As in other regions of the Andes, the study area benefits from the natural storage of precipitation in glaciers and groundwater, which is a key factor in mitigating the mismatch between supply and demand (Salzmann et al., 2013; Buytaert et al., 2017; Grupo Banco Mundial, 2023). Glacial meltwater contribution varies significantly by season. This is due to the fact that precipitation in the majority of regions within the tropical Andes exhibits seasonal fluctuations, whereas temperatures within the region remain relatively consistent throughout the year. This results in a tendency for year-round melting. Furthermore, the period of maximum ablation coincides with the catchment's dry season. As a consequence of the low precipitation levels, the proportion of glacial meltwater becomes increasingly significant. This is also reflected in the relative contribution of glacial meltwater to the water supply in Huaraz of 19% as an annual average, but the monthly maximum contribution of glacial meltwater can reach up to 67% in the dry season. Consequently, the vital role played by the cryosphere in the livelihoods of downstream populations is once again emphasized (Buytaert et al., 2017).

Globally, climate change has a strong impact on the cryosphere in high mountainous regions (Huggel et al., 2018; Huss and Hock, 2018) and, consequently, the glacio-hydrological characteristics of this study area, both now and in the future. Seehaus et al. (2019) observed a glacier area loss of 29% from 2000 to 2016 on a national scale. For the tropical Andes, the outlook by Hock et al. (2019) shows high confidence in a decline in long-term meltwater contributions from glaciers; however, the impact on future human water use remains uncertain. This underlines the need to consider the interplay between hydroclimatic and socioeconomic factors in the catchment.

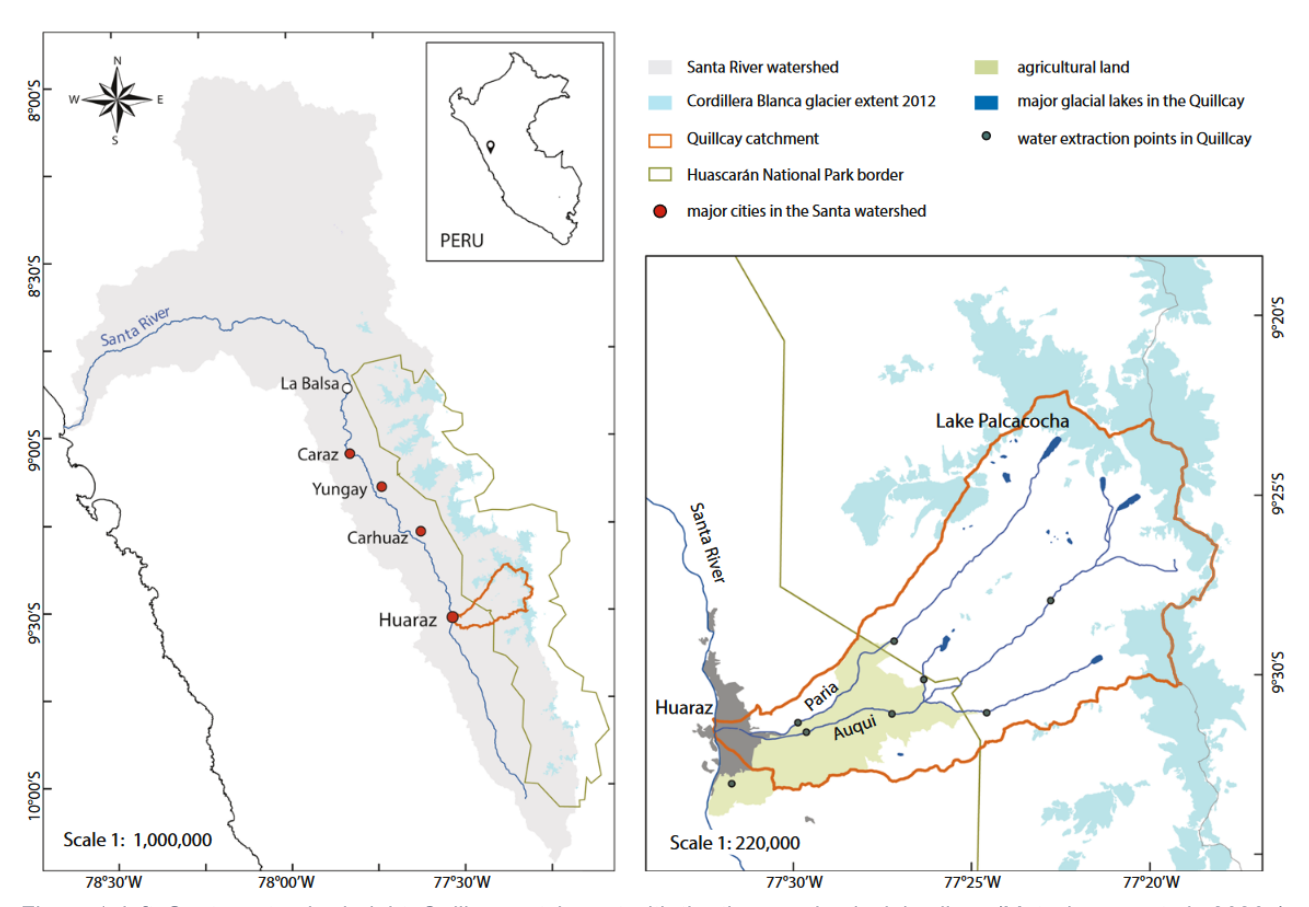


Figure 1: left: Santa watershed. right: Quillcay catchment with the three main glacial valleys (Motschmann et al., 2020a).

2.2. Socioeconomic context

Politically the Quillcay watershed is located in the department of Áncash, more specifically in the districts of Huaraz and Independencia (Meza et al., 2016). The city of Huaraz, the region's principal urban center, is host to a diverse economic landscape, encompassing mining and other industrial activities. It serves as the center of business, commerce, finance, and tourism. Moreover, agriculture not only represents an important sector of the regional economy, but it is also highly relevant to the population: 80% of the population's main income is from livestock production and small-scale farming (Mark et al., 2010; Motschmann et al., 2020b).

The agricultural and domestic sector are the principal consumers of water in the catchment and depend strongly on glacial meltwater. In the entire Santa Valley, water is distributed as follows: 86% for agriculture, 7% for population, 6% for industry, and 1% for mining (ANA, 2015). In addition, the *Ley de Recursos Art. 62* (Resources Law) establishes that the order of priority, after the population's use of water, in the event of competing uses, is as follows: a) agricultural, aquacultural and fishing uses; b) energy, industrial, medical and mining uses; c) recreational, tourism and transport uses (ANA, 2009). In 2021, 91.8% of the population had access to drinking water from the public network in the department of Áncash (INEI, 2023). Given the distribution of water use and the priorities identified, agricultural and domestic use are critical to the overall water availability in the region.

The self-subsistent farming is precipitation-fed during the wet season and depends on glacial meltwater in the dry season (Mark et al., 2010). In fact, 96% of the agricultural area is irrigated (Rivas et al., 2014). Most crops are grown in the wet season, with wheat, barley, and potatoes occupying the largest areas, followed by other traditional crops (Quesquén Rumiche, 2008). In the dry season, the area is much smaller, and only lucerne, beans, peas, capulin, and onions are grown (Quesquén Rumiche, 2008). Water from the Quillcay River is used to irrigate these areas, whose farmers are organized in *Usuarios de Agua de Riego* (Irrigation Water User Committees), which currently hold licenses from the *National Water Authority* (ANA) (Meza et al., 2016). Residents interviewed by Hagen et al. (in review), who conducted qualitative research in the upper Santa catchment, described the visible reduction in glacier extent and linked it to their diminishing water resources. Their main climate-related concern is insufficient water availability, especially during the dry season (Hagen et al., in review). The livelihoods of farmers in the study area are therefore highly vulnerable to disruptions in rainfall or glacier-fed river flows (Heikkinen, 2017), as they rely on these to produce crops for both local market sales and subsistence (Motschmann et al., 2020b).

3. State of the art

3.1. Shared Socioeconomic Pathways and Representative Concentration Pathways

Future scenarios of a world under a changing climate are influenced by a climate and a socioeconomic dimension. These dimensions are represented by illustrative Representative Concentration Pathways (RCPs) and Shared Socioeconomic Pathways (SSPs) scenarios (IPCC, 2022b). The RCPs are used in climate science to project plausible future scenarios for radiative forcing, the change in the energy balance of the Earth's atmosphere (van Vuuren et al., 2011). RCPs provide a range of possible trajectories for the main drivers of climate change: concentrations and emissions of greenhouse gases and air pollutants, as well as changes in land use (van Vuuren et al., 2011). The SSPs have been introduced by O'Neill et al. (2014) to examine how demographics, human development, economy and lifestyle, policies and institutions, technology, environment, and natural resources might develop over the next century. SSP1 ("Sustainability") envisions a world moving towards inclusive, sustainable development, where economic and social growth prioritizes well-being, equality, and environmental sustainability over high rates of economic growth. Mitigation and adaptation challenges are low due to cooperative global governance. SSP3 ("Regional Rivalry") describes a fragmented world dominated by nationalism and regionalism, where societal focus is on local and regional security, with little global cooperation or progress on sustainability. In this narrative, challenges to both mitigation and adaptation are high due to weak global institutions and dependence on fossil fuels. SSP5 ("Fossil-fueled Development") envisions a world focused on rapid economic growth driven by fossil fuel use and technological innovation. Mitigation challenges are high due to continued reliance on fossil fuels, while adaptation challenges are relatively low due to robust economic and technological capacity. SSPs 1, 3, and 5 are the primary scenarios used in this study. However, SSP2 and SSP4 also appear to incorporate socioeconomic uncertainties, representing either a future where social and economic trends broadly follow historical patterns (SSP2), or a world characterized by growing inequality within and between countries, where mitigation is readily achievable as elites prioritize technological progress and carbon reduction (SSP4). In combination with the RCPs, they are employed in climate research to span and explore the prospective future space in which society may navigate with respect to adaptation and mitigation strategies (cf. Figure 2). In line with the IPCC, the SSPs throughout this thesis are referred to as 'SSPx-y', where 'SSP-x' indicates the SSP, hence the socioeconomic trend, whereas 'y' refers to the approximate level of radiative forcing [W/m2] in the year 2100 (Calvin et al., 2023; O'Neill et al., 2014; O'Neill et al., 2017).

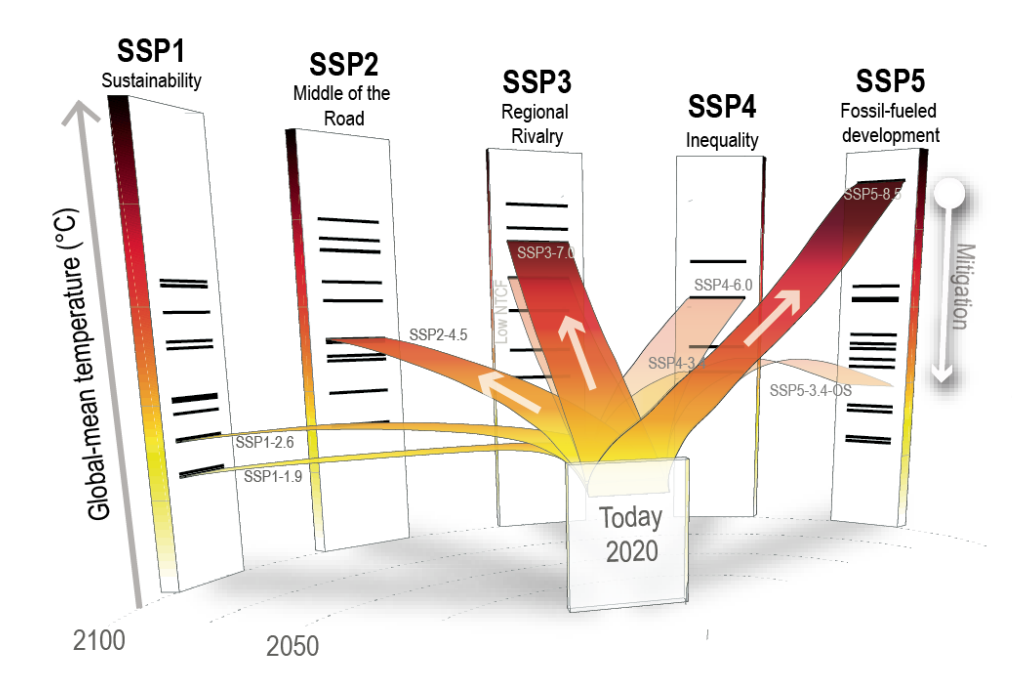


Figure 2: Visualization of pathways combining different RCPs and SSPs and their indicative temperature and mitigation trajectories according to the IPCC (Chen D. et al., 2021).

3.2. Key concepts on limits to adaptation and constraints

As definitions of adaptation limits and constraints remain vague, terms are used interchangeably, and some of the conceptualizations, however, have been challenged in the last years (Juhola et al., 2024; Hagen et al., in review), the concepts that are used in this study are clarified in this section.

3.2.1. Risks

According to the IPCC (2022b) climate-related risks arise from the interactions between hazards, exposure, and vulnerability of affected communities and ecological systems. Scholars express risks in terms of damages, and economic and non-economic losses. Adaptation to climate-related risks can happen autonomously in ecological systems, but in human systems, there are different paths depending on the type of development and timing: it can be anticipatory or reactive as well as incremental or transformational, meaning it can change the system (IPCC, 2022b).

Defining what constitutes an acceptable or intolerable risk is crucial for further clarifying the definition of limits of adaptation, but it remains a challenge. Dow et al., (2013) argue, that risks have two dimensions, the first is material and can e.g. be quantified by the *Losses and Damage* (L&D) approach (cf. Surminski and Lopez, 2015; Huggel et al., 2018; McNamara and Jackson, 2019a; Mechler et al., 2020). The second dimension is socially and culturally constructed, leading to different perceptions down to an individual level of what is tolerable or not (Dow et al., 2013). In an actor-centered case study, this subjectivity leading to a fluid adaptation limit is emphasized (Warner, 2016). Figure 3 illustrates the categories of risk (acceptable, tolerable, and intolerable), in a two-dimensional

space depending on the relationship between the perceived probability and intensity of climate change-induced impacts. However, it can be criticized that the outer edges, i.e. what happens in very intense or very frequent events, are not discussed and are not unequivocally presented in this Figure. It may be outdated compared to other risk frameworks, but it highlights the often-contested zones between the categories: Shading around boundaries indicates that actors' views of what constitutes acceptable, tolerable, or intolerable risk may differ (Dow et al., 2013).

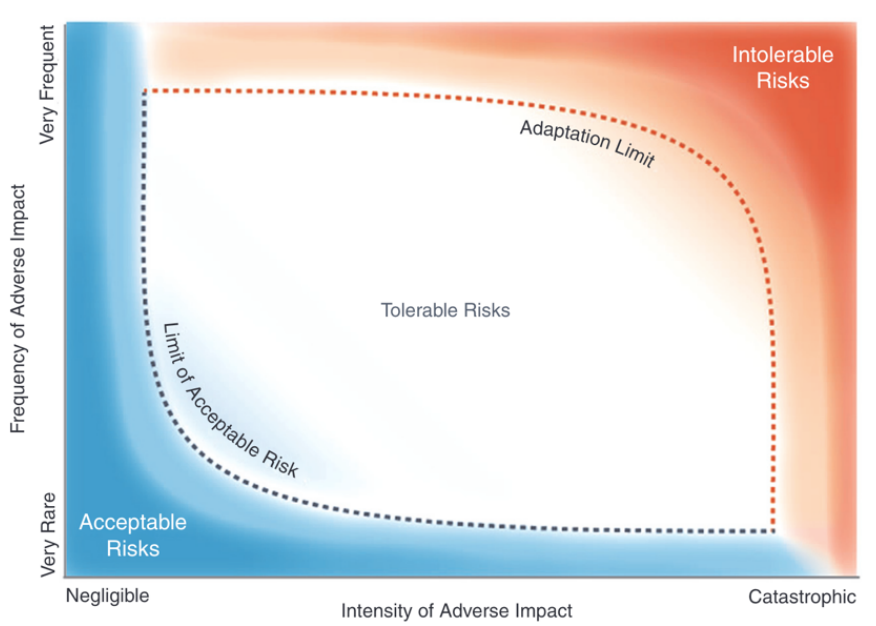


Figure 3: Acceptable, tolerable and intolerable risks in relation to adaptation limits (Dow et al., 2013; based on Klinke and Renn, 2012).

Moreover, Juhola et al. (2024) recommend conceptualizing risks from an ethical perspective, considering social justice and suggest that the categorization of risks as either tolerable or intolerable should be determined on the basis of the judgments made by those involved in the process of adaptation.

3.2.2. Limits to adaptation

In contemporary academic discourse, scholars have often adopted the term *limits to adaptation* as defined by the IPCC (Dow et al., 2013; Thomas et al., 2021; Berkhout and Dow, 2022;). It distinguishes between soft and hard limits. Soft limits are associated with human systems and can be overcome through adaptive action, whereas hard limits are related to biophysical factors and occur when risks become intolerable (Berkhout and Dow, 2022). It is important to note, that for soft limits, adaptation options may exist, but their current unavailability hinders adaptive action while risks are intolerable (IPCC, 2022b).

In the IPCC AR6, key risks are defined as potentially severe climate-related risks that may intensify over time. As in the classical risk framework, they are composed of hazards, exposure and

vulnerability (cf. Figure 4). However, their severity may also increase due to inadequate adaptation and mitigation measures (O'Neill et al., 2022).

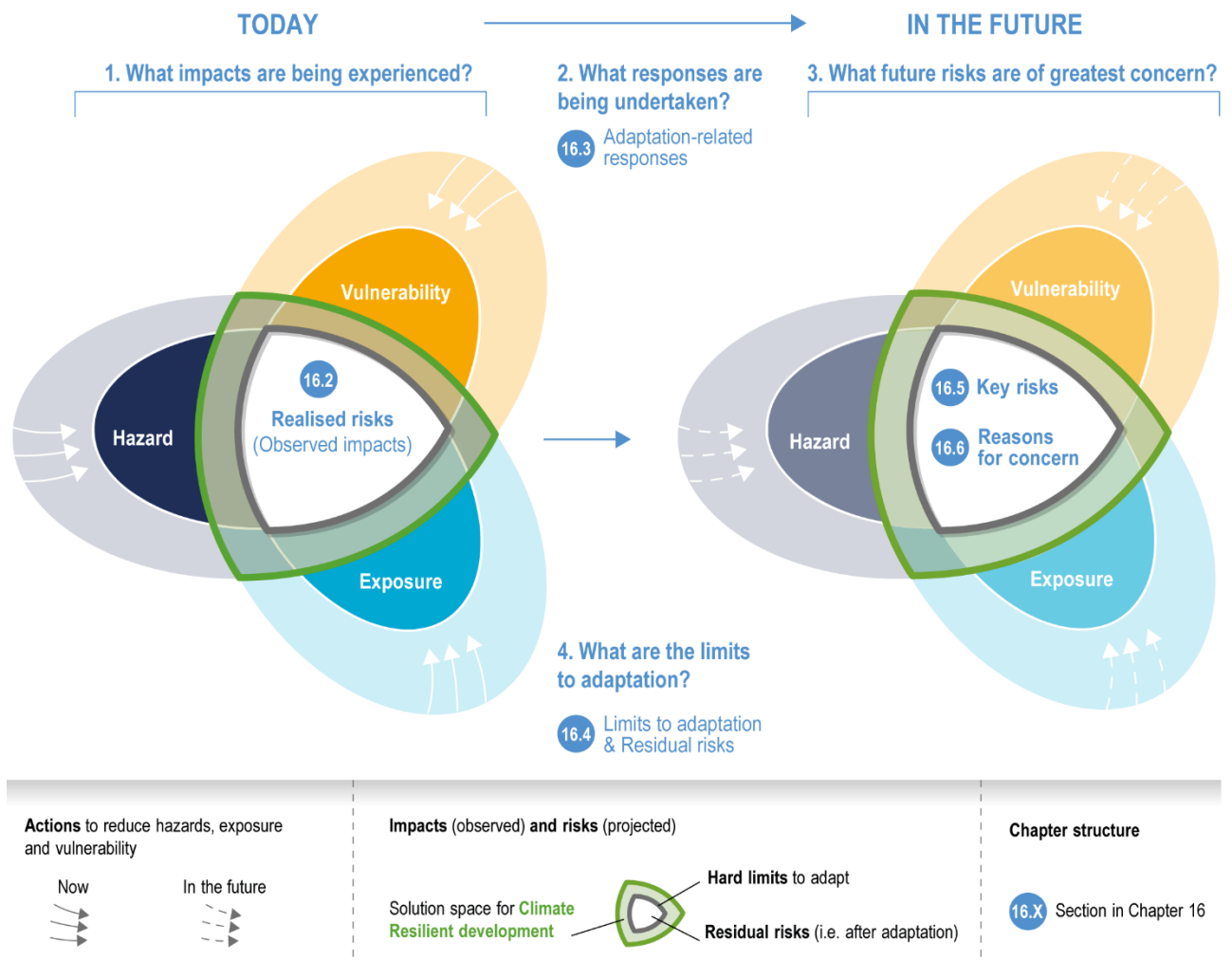


Figure 4: Key risks propeller and the conceptualization of limits to adaptation in the solution space for climate resilient development (O'Neill et al., 2022).

Figure 4 also incorporates the concept of limits to adaptation, which are shaped not only by the magnitude of climate hazards, such as the amount of glacier area loss, but also by exposure, vulnerability and societal thresholds. These thresholds include physical, infrastructural and social tolerances, as well as adaptation choices made by actors – for example, whether to invest in protective measures or to migrate from severely affected areas. While the subjective perceptions of adaptation limits by different actors are not directly addressed, the dynamic nature of these limits is emphasized. Their evolution depends on the interaction between socioeconomic systems, the changing physical climate and the adaptation choices that societies make over time (O'Neill et al., 2022).

Juhola et al. (2024) have developed a theoretical framework that also distinguishes between hard and soft limits, while emphasizing their interlinked nature (cf. Figure 5, vertical plane, distinguishable by colors) and hence, challenging the widely accepted concept used in the IPCC. Moreover, it is also differentiated between actor-level and system-level objectives (cf. Figure 5, horizontal plane).

Limits on adaptation on an actor level occur when e.g. basic needs, but also basic ecosystem functions needed for human survival are not fulfilled and adaptation actions are constrained by ecological and social characteristics of actor or system objectives. On a system level, limits occur when ecological functions or governance institutions fail to support adaptation actions. This four-dimensional view of limits to adaptation is shown in Figure 5. To address the interlinked nature, they propose, among others, translating biophysical and socioeconomic data into quantitative metrics that reflect the objectives of the social system. These indicators are then placed on a sufficiency scale that spans from meeting basic human needs to more complex societal goals such as social justice. This approach allows for assessing sufficiency across ecological and social dimensions, highlighting the interconnectedness of human needs and broader sustainability goals (Juhola et al., 2024).

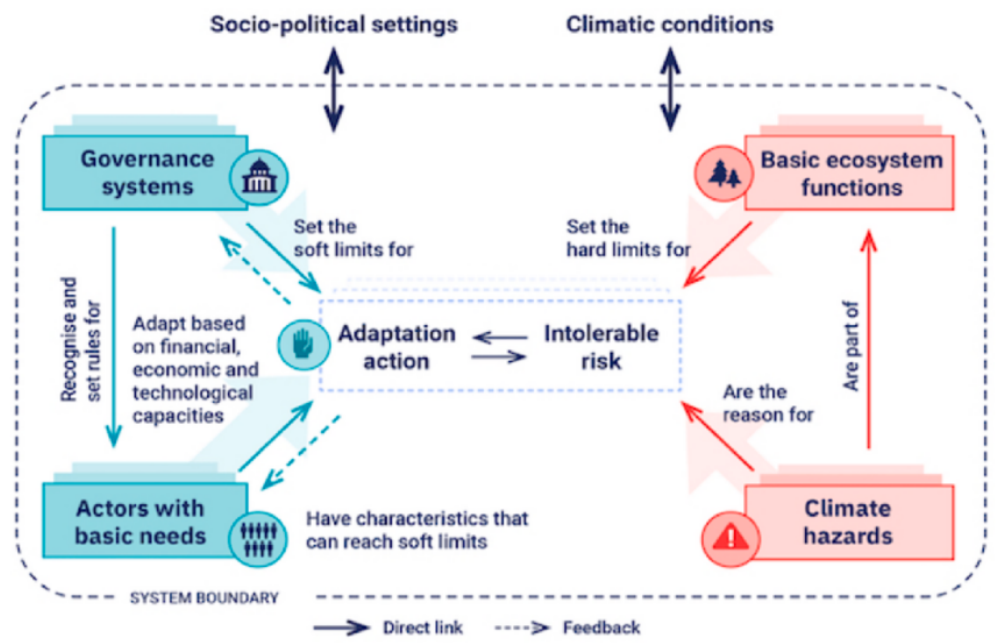


Figure 5: Four-dimensional view of limits to adaptation designed by (Juhola et al., 2024).

The distinction between soft and hard limits is critiqued by (Hagen et al., in review) on the grounds that it gives the misleading impression that a soft limit can be simply eliminated. Furthermore, it is argued that the categorization of such limits is too deterministic (Hagen et al., in review). To finish, well-being is also a factor that should be included in the framework, instead of focusing on a simple survival threshold (Hagen et al., in review). The suggested conceptual extension is also supported by Warner's case study-based findings, where well-being was identified by actors as one of the most important issues when it comes to the limits of adaptation (2016).

3.2.3. Constraints

Constraints are categorized into groups based on the research of Thomas et al. (2021) and show the diversity of factors that impede the implementation of adaptation measures (cf. Table 1).

Table 1: Overview of constraint categories with a possible example in the context of the adaptation to water scarcity in the Andes based on Thomas et al. (2021).

Constraint category	Description and example
Cultural / social	 social norms / identity / beliefs / values / education: e.g. preference from local communities for traditional farming methods over newly in- troduced practices
Economic	existing livelihoods: e.g. agricultural practices reliant on irrigation
Financial	 lack of financial resources: e.g. limited funding to implement irrigation systems with a higher efficiency
Technical	lack of technology: inadequate access to modern irrigation systems such as drip irrigation
Biological	unsuitable biological features: e.g. increasing acidity of drinking water
	•
Information / awareness	lack of awareness or access to information: e.g. limited reliable data on water availability and quality for management purposes
Human capacity	 individual, organizational, and societal capabilities to set and achieve adaptation objectives over time: e.g. limited capacity to train and edu- cate
Governance / institutions / policy	existing laws and regulations: e.g. environmental conservation regulations that prohibit the construction of reservoirs

The next section offers an overview of how constraints and limits to adaptation are identified and analyzed, focusing on the different methods used in current research.

3.3. Traditional methods to identify limits to adaptation

There is currently an imbalance in the methods used to study the limits to adaptation to climate change, leading to a research gap. The predominant research approach for identifying limitations is qualitative. This observation is consistent with the systematic research conducted by Thomas et al. (2021) and the research agenda of Berkhout and Dow (2022). More recent papers on limits to adaptation that follow a quantitative methodology align with the approach recommended by certain scholars for a broader disciplinary and methodological approach (Berkhout and Dow, 2022).

Qualitative methodology can be applied using various methods or frameworks, such as actor-centered or stakeholder-centered approaches, as well as the sustainable livelihood framework. It is typically conducted through case studies. Those methods are valuable due to their inclusion of local contexts, involving the consideration of actors, and political and economic situations (Herrador-Valencia and Paredes, 2016). Furthermore, as stated by Aggarwal et al. (2022), half of the studies on the limitations to adaptation cite social conditions as the primary contributing factor. Qualitative scientific work is therefore also necessary as the complexity of social conditions cannot be adequately represented by numerical measures and to understand the dynamic interplay between various social factors (Adger et al., 2009). However, the overview of methods and identified limits highlights a significant issue with qualitative assessments (cf. Table 2). While they may identify potential limits, they

fail to quantify at what point the limits are reached, for example when and under what conditions they occur. This impression is confirmed by Thomas et al. (2021), who point out that there are few studies that provide detailed information on when limits arise.

Quantitative methodology has the advantage of transferability to other regions in the world and has standardized outputs compared to qualitative methods. Nonetheless, they often focus on a specific aspect such as the economic dimension (McNamara and Jackson, 2019b), simplifying the context and leaving intangible factors such as culture unexamined (Mechler et al., 2020; Cortignani et al., 2021).

Furthermore, numerous studies have examined adaptation strategies and their limitations in the past and present but often fail to consider future outlooks (e.g. Leal Filho and Nalau, 2018). If the future is considered in studies, the literature review highlights a common issue of non-robustness of the method to uncertainty. When considering climate change uncertainties in the case studies, only a small number of scenarios were used, fewer than 10 in all the papers analyzed. The IPCC (2022b) recommends that decision-makers follow a climate-resilient development path to avoid maladaptation. To achieve this, a long-term component should be included in the decision-making process. As long-term climate change projections follow different emission and socioeconomic scenarios, policymakers face deep uncertainty not only regarding climate change scenarios but also regarding the actions of different stakeholders. It is therefore crucial to develop complementary methodologies that can deal with uncertainty. An overview of the mentioned and additional strengths and weaknesses of the methods are listed in Table 2.

Table 2: Traditional methods to assess limits to adaptation with their strengths and limitations.

Method	Strengths	Limitations
Qualitative: SLF / actor-centred / stake-holder-centred comparative case study	 broadly applicable in various research contexts (regions and fields) (Dow et al., 2013) intuitive results (Dow et al., 2013) local context and perspectives are considered (Herrador-Valencia and Paredes, 2016; Bezner Kerr et al., 2022) individuality of limits are considered, e.g. with the SLF one can illustrate that the limits are different depending on the individual (McNamara et al., 2017) 	case studies: data collection is time-consuming. case studies: context specific. no transferability not robust to a variety of socioeconomic and climate change scenarios
	Goal: explore the perception of the limits to ad	laptation by (different) actor(s)
Quantitative: Econometric / L&D	 transferability standardized, numerical outputs 	 base models with underlying assumptions and limitations (Cortignani et al., 2021) depending on the model: increased computing power economic dimension is prioritized (McNamara and Jackson, 2019b) fail to determine intangible factors, such as culture, rituality, spirituality,

Method	Strengths	Limitations
Quantitative: Econometric / L&D		etc (Mechler et al., 2020; Cortignani et al., 2021) not robust to a variety of socioeconomic and climate change scenarios
	Goal: identify limits to adaptation through mon	etarization

To sum up, there is a need for future-oriented, quantitative methods, that can cope effectively with uncertainty in order to identify under what conditions climate-related risks and limits to adaptation to climate change occur.

3.4. Complementary methods to identify limits to adaptation

The DMDU framework is commonly used to identify robust adaptation responses. Some studies have used this method to investigate adaptation measures to climate change, as demonstrated in the field of tourism at Swiss ski resorts (Vaghefi et al., 2021) or in water management in Peru (Muñoz et al., 2024b; Kalra et al., 2015) or in the US (Groves et al., 2013). The implementation of the DMDU framework is recommended when contextual uncertainties are deep, the possible policies are diverse and the system is complex, so experts' intuition is not sufficient (Lempert, 2019). Amongst others, *Robust Decision Making* (RDM) is a DMDU approach that prioritizes informed decisions over accurate predictions (Lempert, 2019). This approach shifts the focus to identifying potential solutions amongst a variety of scenarios rather than relying on precise forecasts (Carlsson Kanyama et al., 2019). RDM uses EMA to stress test future scenarios and thereby facilitates informed decision-making. Its advantages and disadvantages are listed in Table 3.

Table 3: Strengths and weaknesses of RDM to assess robust adaptation strategies.

Method	Strengths	Limitations
RDM	 decision-making process: bottom-up (Carlsson Kanyama et al., 2019) standardized, numerical output robust to uncertainty: fitting for a variety of socioeconomic and climate change scenarios. 	 base models with underlying assumptions and limitations depending on the model: increased computing power currently only applied to identify robust adaptation strategies. no application experience in identifying constraints or limits to adaptation local context is partially considered
	Goal: identify limits to adaptation that are robust to	o uncertainty about the future.

Based on the current state of knowledge, an attempt is made to apply EMA in a new context to build on the strengths of the method and to respond effectively to future scenarios. That is, to shift the focus from the robustness of adaptation measures success to situations of system failure. Specifically, the aim is to identify and quantify the critical factors and conditions that influence water scarcity.

3.5. Exploratory Modeling and Analysis (EMA)

RDM combines *Decision Analysis*, *Assumption-Based Planning*, scenarios, and *Exploratory Modeling* to stress test strategies over myriad plausible paths into the future, to then identify robust policies (Lempert, 2019). *Robust* in RDM is defined as "performing well over a wide range of futures" (Lempert, 2019). In the context of climate change data, calculated in different *Global Climate Models* (GCM), the policy debate was able to shift thanks to RDM from arguing over which GCM is the right one to identifying policies that give satisfactory results across different models (Bankes et al., 2013).

RDM is operationalized with EMA, which can be broken down into three steps: i) structuring the analysis, ii) modeling the future pathways by defining the uncertainty ranges, and iii) exploring the analysis by means of stress testing (Lempert 2019) (cf. Figure 6).

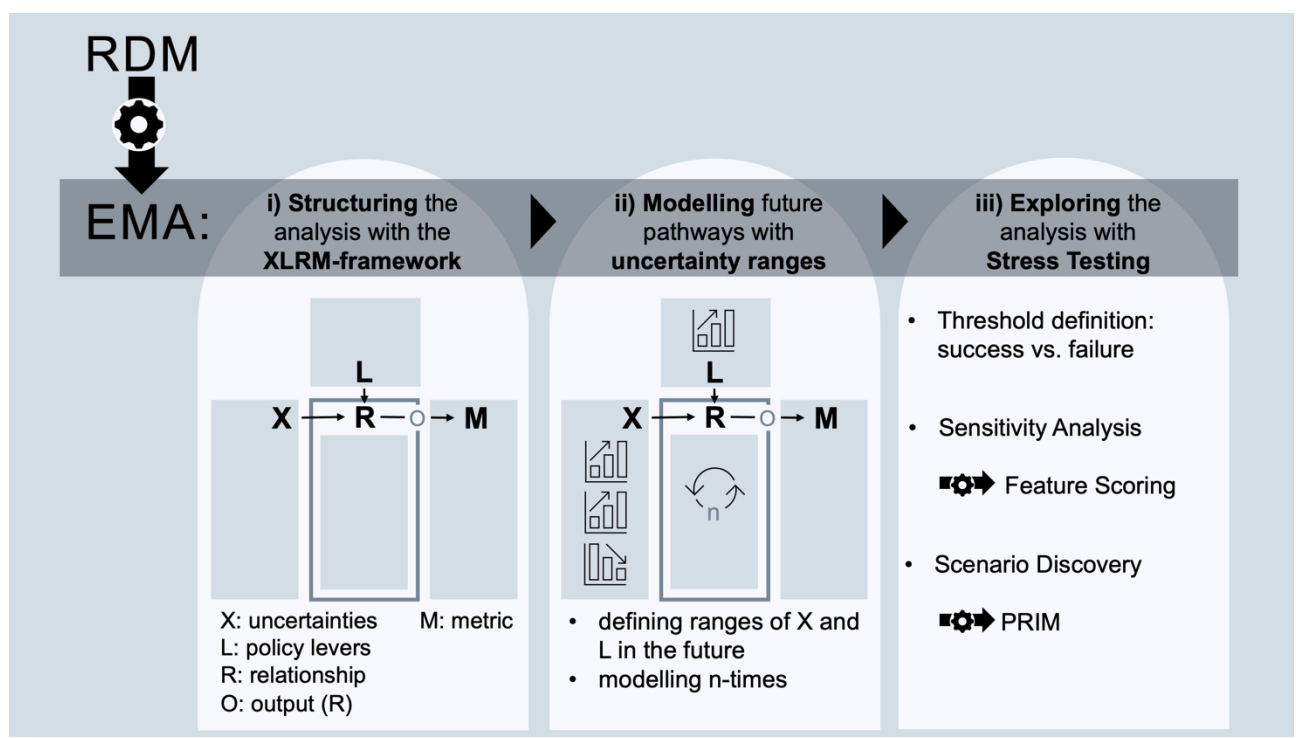


Figure 6: Schematic representation of the workflow to operationalize RDM (own illustration; based on Vaghefi et al., 2021; Muñoz et al., 2024b).

3.5.1. Structuring the analysis with the XLRM-framework

The first step starts with formulating the decision problem. An illustration of this from existing applications of the methods is as follows: Policymakers need to adopt appropriate strategies to avoid future water scarcity, as expressed by Muñoz et al. (2024b). To answer that question, it is recommended to group the elements of the analysis into four different groups, according to the XLRM-framework suggested by Lempert (2003) (cf. Figure 6, left box). Future exogenous uncertainties (X) and the mentioned strategies (L) have an impact on the success or failure of the system, i.e. water scarcity or no water scarcity. The relationship (R) can be understood as a function that changes with

the input parameters X and L. The output of the relationship function is ranked by the measure of performance (also called metric) according to its desirability (Bankes et al., 2013; Lempert, 2003; Lempert, 2019).

3.5.2. Modeling future pathways by defining ranges of uncertain variables

The second step (cf. Figure 6, middle box) is to define how the uncertain variables (X, L) may develop in the future. This is done by setting ranges that specify the upper and lower limits of the increase or decrease. Then, n simulations are run to model the different future situations.

In this thesis, the term *scenario* is employed to represent the significant uncertainty inherent in all external factors, as outlined by Lempert (2019). When applied to the context of climate change, a scenario can be interpreted as a specific set of possible future climate indicators. *Policy* is defined as a unique parameter setting for all policy levers (Vaghefi et al., 2021). Additionally, the term *experiment* is defined as the combination of a scenario and a policy.

3.5.3. Exploring the analysis with stress testing

The third step of EMA (cf. Figure 6), right box is done in an open exploration: Stress testing uses sensitivity analysis and scenario discovery to identify under what scenarios a strategy fails to achieve the objectives (Lempert, 2003; Bryant and Lempert, 2010; Moallemi and Malekpour, 2018).

Sensitivity Analysis operationalized with Feature Scoring

Feature scoring helps to identify the relative importance of various input variables for a certain outcome and represents a group of machine learning techniques (Guyon and Elisseeff, 2003). Each input variable is assigned a number that represents the importance of the factor on the outcome (metric). It is also possible to use binary classification to determine which input variables have the strongest influence on a particular outcome, such as e.g. a metric below a threshold (Kwakkel, 2017).

Scenario discovery operationalized with PRIM

The Patient Rule Induction Method (PRIM) is a data mining technique presented by Friedman and Fisher (1999) used for identifying and describing subgroups within a dataset that exhibit particular characteristics of behaviors. For EMA this means, its goal is to locate areas in the n-dimensional room originating from different experiments where the metric values are below or above a certain threshold. It does so by creating boxes, that encapsulate the regions of interest of similar metric outcomes by reducing the dimensions. The starting point of the iterative algorithm is the whole input space, meaning no variable is restricted. It then gradually "peels" away layers, thereby removing metric points of the experiments by reducing the input range of the X and L variables (Friedman and Fisher, 1999).

The boxes can be characterized by coverage and density:

$$Coverage = \frac{number\ of\ points\ with\ the\ metric\ outcome\ of\ interest\ in\ the\ box}{total\ number\ of\ points\ with\ the\ metric\ of\ interest\ in\ the\ dataset}$$

$$Density = \frac{number\ of\ points\ with\ the\ metric\ outcome\ of\ interest\ in\ the\ box}{total\ number\ of\ points\ in\ the\ box}$$

When the algorithm starts, the coverage equals one because it starts with the unrestricted full set of experiment outcomes. The trade-off between coverage and density can be understood as between false-positive and false-negative errors, therefore for further analysis, it is important to find a box with balanced coverage and density, or to be aware of the relationship between coverage and density of the selected box (Friedman and Fisher, 1999; Newman and Milkovits, 2021b).

PRIM employs a "patient" approach to rule induction, which means it explores the data thoroughly to search for significant patterns that lead to reliable subgroup identification. Another characteristic is its high user involvement which allows analysts to incorporate their expertise. Moreover, its results are readily understandable, making it suitable for analyses aimed at communicating results to stakeholders. One disadvantage is that this method can be very computationally intensive, depending on the number of experiments, and the statistical significance assessment must also be taken into account (Friedman and Fisher, 1999).

4. Method

This study applies EMA to identify and quantify the key drivers of future water scarcity within the social-ecological system of the Quillcay catchment. As EMA is used in a novel context – water scarcity and limits to adaptation – the method has been slightly modified to suit this application. With this method uncertainties from climate and socioeconomic projections by 2050 are considered. In the following chapters, the term *historical* is employed to denote the period from 1981 to 2014 and the term *future* refers to the period from 2015 to 2050.

4.1. Integration of the XLRM-framework in the case study

Policymakers and decision-makers in the Quillcay catchment need to know under what circumstances water scarcity will occur in the future and whether adaptation strategies can prevent it in order to take effective action. To answer this decision problem the different variables of the case study are organized with the help of the XLRM-framework:

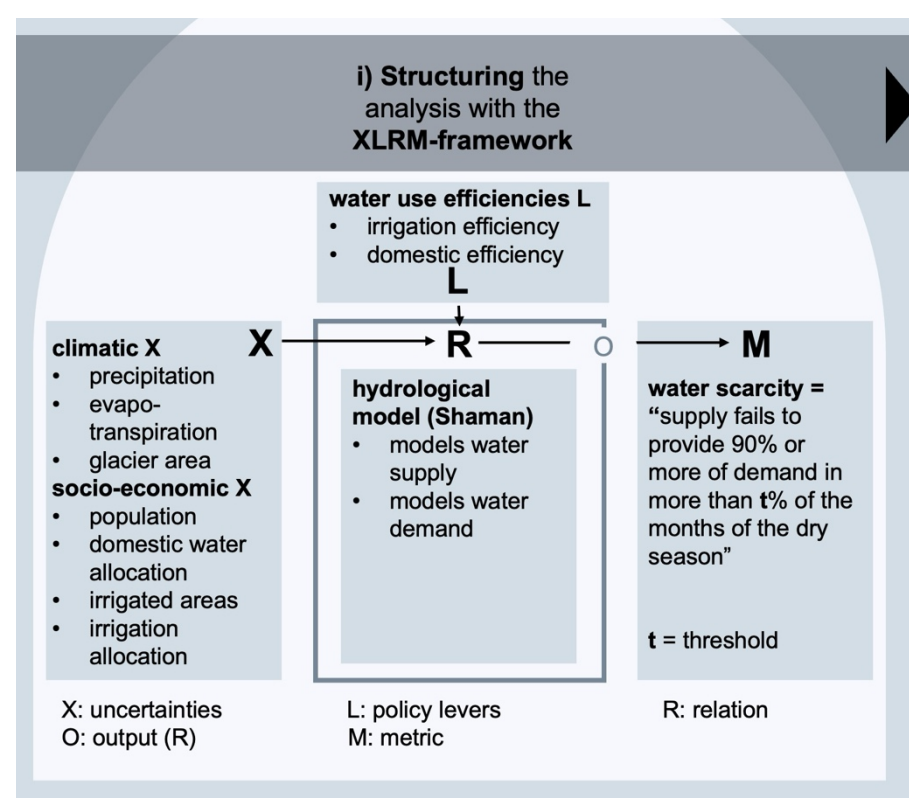


Figure 7: Schematic representation of step i) in the EMA workflow: the XLRM-framework set for the analysis of future water scarcity (own illustration; based on Vaghefi et al., 2021; Muñoz et al., 2024a).

The heart of the XLRM-matrix (cf. Figure 7) builds the hydrological model (R) that simulates water supply and water demand based on the input parameters. The input data to the hydrological model has been considered uncertain in the future. It is represented i) by climate scenario data, specifically by the future precipitation (x pp), future evapotranspiration (x eto), future glacier area (x area gla), and ii) by socioeconomic scenario data parametrized with future population (x pop), fu-

ture irrigated area (x_area_irr), future forest area (x_area_for), future domestic water allocation per person (x_alloc_dom) and agricultural water allocation (x_alloc_irr). Moreover, the one policy lever (L), the efficiency of irrigation systems (p_irreff), is included in the analysis. Alternatively, this policy

lever can be swapped to domestic efficiency (p_domeff). The hydrological model output will be turned into the metric that characterizes water scarcity in the dry months.

Future projections are always based on historical data used to calibrate a model or trend lines. This historical data as well as the individual elements of the XLRM matrix for the future projection are described in more detail, in particular, information on assumptions, data basis, and calculations are provided. More detailed information on the underlying data can be found in the appendix (cf. appendix 9.1.). Potential future developments (uncertainty ranges), cf. step ii) of EMA, are already justified, as this is an integral aspect of the description of future data. A summary of the XLRM-framework adapted to the case study is provided in Table 4. This table is followed by a detailed description of each component of the framework.

Table 4: Description of the uncertainties (X), policy levers (L), and the metric (M) and constants of the model (R) used in this study. The column "Data / Reference" gives an overview of the source of the defined ranges. More information about original data ("raw data") and modified data ("processed data") in appendix 9.1..

	Name	Description	Range	Data / Reference
X	Climate variables	uncertainty due to chang- ing climate parameters based on different GCM and scenarios	30 climate series: 3 climate scenarios (SSP1-2.6, SSP3-7.0, SSP5-8.5) each with 10 GCM	raw: BASD-CMIP6_PE. processed: datos_clim_1- 30
	<i>x_pp</i>	precipitation, [mm/month]	30 climate series	datos_pp_1-30
	x_eto	evapotranspiration, [mm/day]	30 climate series	datos_eto_1-30
	x_area_gla	glacier area, [km2]	30 climate series	datos_agla_1-30
	Socioeco- nomic varia- bles	uncertainty due to chang- ing socioeconomic pa- rameters		raw: iamc_db_x, pro- cessed: datos_socioec
	x_pop	change (2015 – 2050) [%] of the population in the catchment	based on 5 SSP scenarios range [%]: -8 - +36	raw: iamc_db_popula- tion_PER, processed: datos_socioec
	x_area_irr	change (2015 – 2050) [%] of irrigated areas in the catchment	based on 5 SSP scenarios range [%]: 4 - +37	raw: iamc_db_cropland_LAM, processed: datos_socioec
	x_area_for	change (2015 – 2050) [%] of forest area in the catchment	range [%]: -50 - +50	(Aide et al., 2019; Vázquez-Rowe et al., 2019)
	x_alloc_dom	change (2015 – 2050) [%] in domestic water allocation per person [l/day/capita]	current net domestic allocation: 120l/day/capita range [%]: -20 - +100 (or +50)	(Howard et al., 2020; Song and Jia, 2023; Muñoz et al., 2024b; Sedapal, 2022)
	x_alloc_irr	change (2015 – 2050) [%] in agricultural water allocation [m3/ha/d] for ir- rigation	current monthly net de- mand from (Quesquén Ru- miche, 2008) range [%]: -50 - +80 (or -25 - +40)	(Alemayehu et al., 2015; Esteve-Llorens et al., 2022; Taaime et al., 2023)
L	p_irreff	changing efficiency [%] of irrigation system	range [%]: 25 - 70	lower limit: 10% below current efficiency. upper limit: 70% (context realistic)

	Name	Description	Range	Data / Reference
L				(Quesquén Rumiche, 2008; Drenkhan et al., 2015, 2019; Muñoz et al., 2024a)
	p_domeff	changing domestic effi- ciency [%]	range [%]: 66 - 90	lower limit: current efficiency – 10%. (Rivas et al., 2014; PUB, 2023)
Con- stants of R (Shaman)	mf	melting factor (artificial factor calibrated to the model)	monthly variation	processed: datos_clim_1- 30
	qeco	environmental flow	monthly variation	processed: datos_clim_1- 30
	dom_back	backflows from domestic water withdrawals	50%	(Muñoz et al., 2024b)
	irr_back	backflows from agricul- tural water withdrawals	50%	(Muñoz et al., 2024b)
M	Metric for wa- ter scarcity	Supply fails to provide 90% or more of the de- mand in more than t% of the months in the dry season		(Kalra et al., 2015; Muñoz et al., 2024b; INEI, 2023)

4.1.1. Uncertainties X: climate scenario and socioeconomic data

The values of future climate projections are driven by Global Climate Models (GCM) and climate scenarios (SSP and RCP). Despite the omnipresence of the scenarios in climate change discourse, the choice of the GCM, meaning how the Earth's climate system is simulated, also has an impact on the projected climate variables. The Coupled Model Intercomparison Project (CMIP) is an initiative of the World Climate Research Program (WCRP) and seeks to compare and improve climate models (WCRP, 2024). It has become one of the foundational elements of climate science and serves as a critical resource of the IPCC (IPCC, 2022b). However, Fernandez-Palomino et al. (2024) noted that CMIP6 models are often too coarse for regional and local management decisions, especially when related to extreme hydrological conditions. Moreover, the data also shows substantial biases. In order to analyze water scarcity in the Quillcay catchment, the BASD-CMIP6-PE, a high-resolution (10km) climate dataset for Peru based on the bias-adjusted and statistically downscaled CMIP6 climate projections presented by Fernandez-Palomino et al. (2024) is used. It contains historical simulations and future projections of temperature and precipitation based on the SSP1-2.6, SSP3-7.0, and SSP5-8.5 scenarios and on ten different GCMs. In a performance assessment, they emphasize the reliability of this data in determining the impact of regional climate change on agriculture, water resources, and hydrological extremes (Fernandez-Palomino et al., 2024).

Given that the hydrological model will undergo calibration using *PISCOv1p1* discharge data (cf. section 4.1.3.), it is essential that the *BASD-CMIP6-PE* dataset exhibits comparable characteristics with the *PISCOv1p1* dataset. *PISCO* (SENAMHI, 2020) is built on the integration of satellite observations

(CHIRP) and ground-based data (Fernandez-Palomino et al., 2022). It is used for operational ends by SENAMHI in Peru for drought and flood monitoring and has been applied at catchment level (Llauca et al., 2021). By plotting the historical multiannual monthly average precipitation, it becomes evident that the BASD-CMIP6-PE precipitation data of all the GCMs is characterized by a shift in seasonality and a discrepancy in amplitude (cf. Figure 8). This consistent pattern across all GCMs justifies using their average for the historical period. It is important to note that model agreement is likely to result from their reliance on similar code and assumptions (Hakala Assendelft et al., 2020). Averaging GCM outputs does not necessarily improve data robustness. For this reason, the climate data (BASD-CMIP6-PE precipitation, minimum and maximum temperature) were approximated to the PISCOv1p1/v2p1 data by means of a bias-correction process, thus aligning them with observed historical data and improving the reliability of the climate projections. In R, this is operationalized with the multivariate bias-correction of climate model outputs (MBC) package, utilizing the MBCn (ndimensional) approach, which has the optimal ESS value across all combinations of scenarios and GCMs (0.75-0.9). Following the bias-correction of the climate data, the discrepancy in seasonality between the BASD-CMIP6-PE precipitation data and the PISCOv2p1 precipitation data persists (cf. Figure 8). However, the amplitude and, consequently, the total annual precipitation amount is more closely aligned with the PISCOv2p1 dataset (cf. Figure 8). On the right side of Figure 8, the plot indicates that the temperature data perfectly aligns with the PISCOv1p1 dataset.

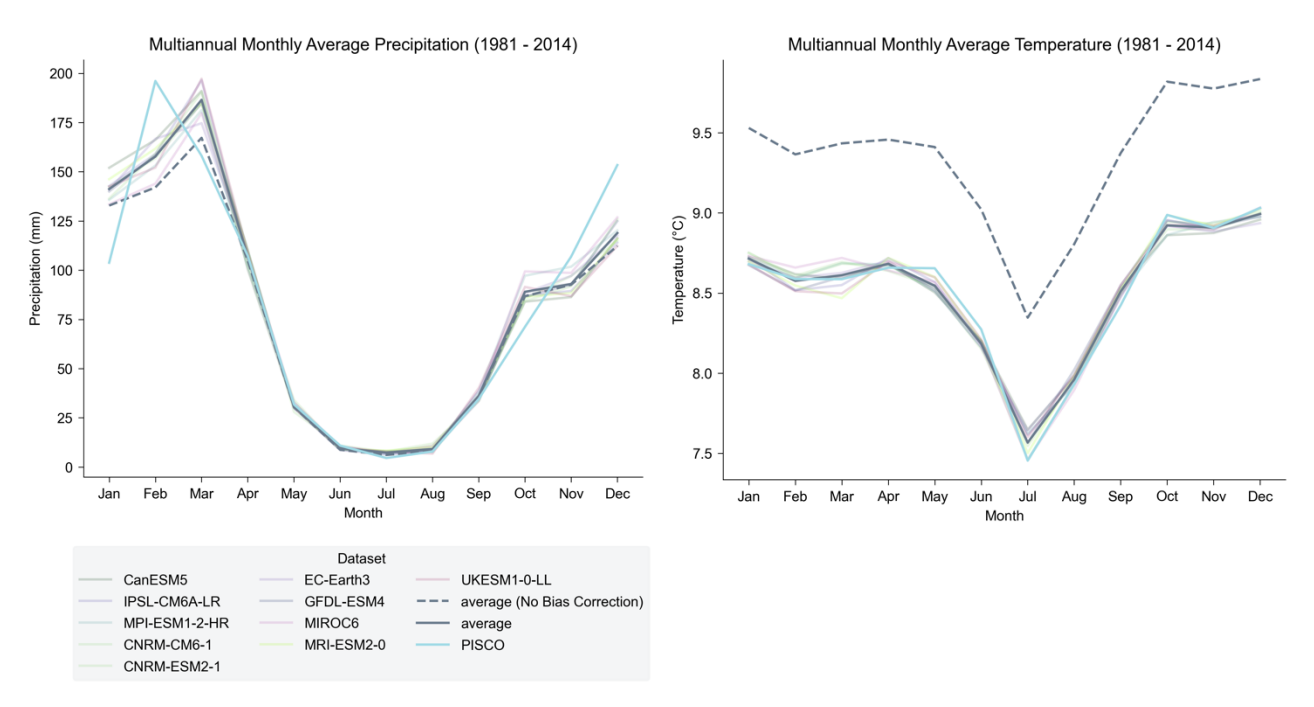


Figure 8: left: Effect of MBCn bias-correction on the average of the GCM compared to the multiannual monthly average precipitation of PISCOv2p1. right: Bias-corrected multiannual monthly average temperature data based on the average of the GCM (own illustration).

Based on bias-corrected climate data, precipitation, evapotranspiration, and glacier area are computed. The visualized climate scenario data is presented in this thesis in accordance with the IPCC and CMIP6 color palettes.

Precipitation (x1_pp_o)

The historical and future daily bias-corrected precipitation data (Fernandez-Palomino et al., 2023) are converted to cumulative monthly precipitation. As one expects, there is no clear trend for precipitation in the future (cf. Figure 9, 10). In general, a minimal increase can be assumed visually, which is also indicated by the change in the monthly average precipitation (cf. Figure 11). There is only one month in the catchment where the average of the future change is negative compared to the historical period. This occurs in May, the beginning of dry season. In addition, the box plots show a large range in the dry months, which may indicate future extreme events, i.e. periods of drought followed by wetter years, or uncertainty. Furthermore, the individual GCMs are also highly variable during the dry season, indicating a high degree of uncertainty in the GCMs for this seasonal phenomenon (cf. appendix 9.3.).

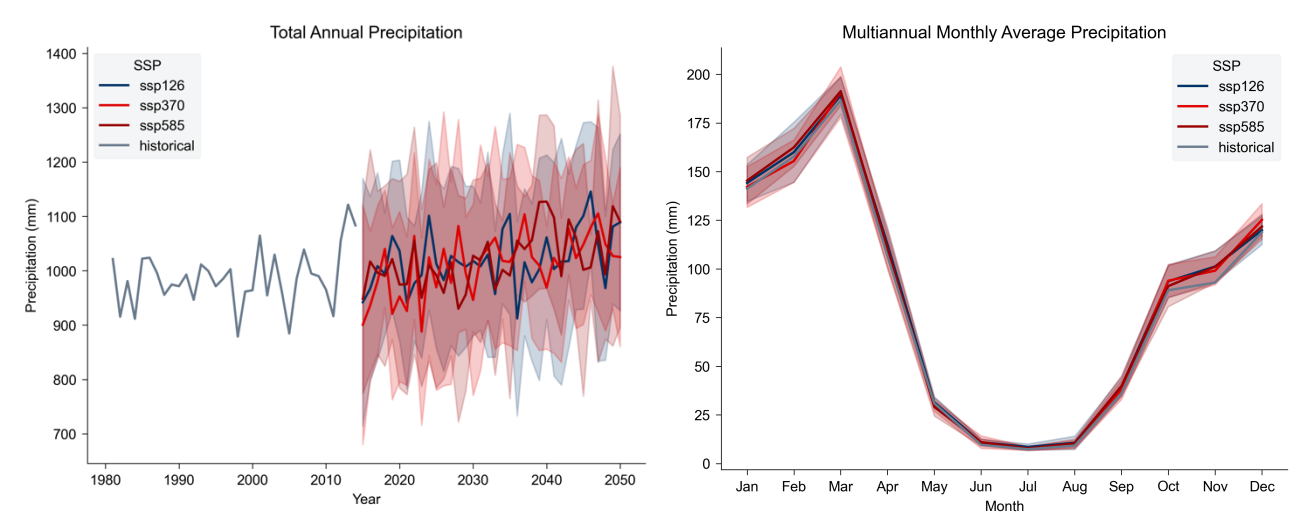


Figure 9: left: Historical and future total annual precipitation based on the three different climate scenarios. right: Multiannual monthly average precipitation based on the three different climate scenarios. The bold line represents the GCM average derived from the three climate scenarios (SSP1-2.6, SSP3-7.0, and SSP5-8.5), whilst the shaded areas illustrate the standard deviation from the climate models used for each climate scenario (own illustrations).

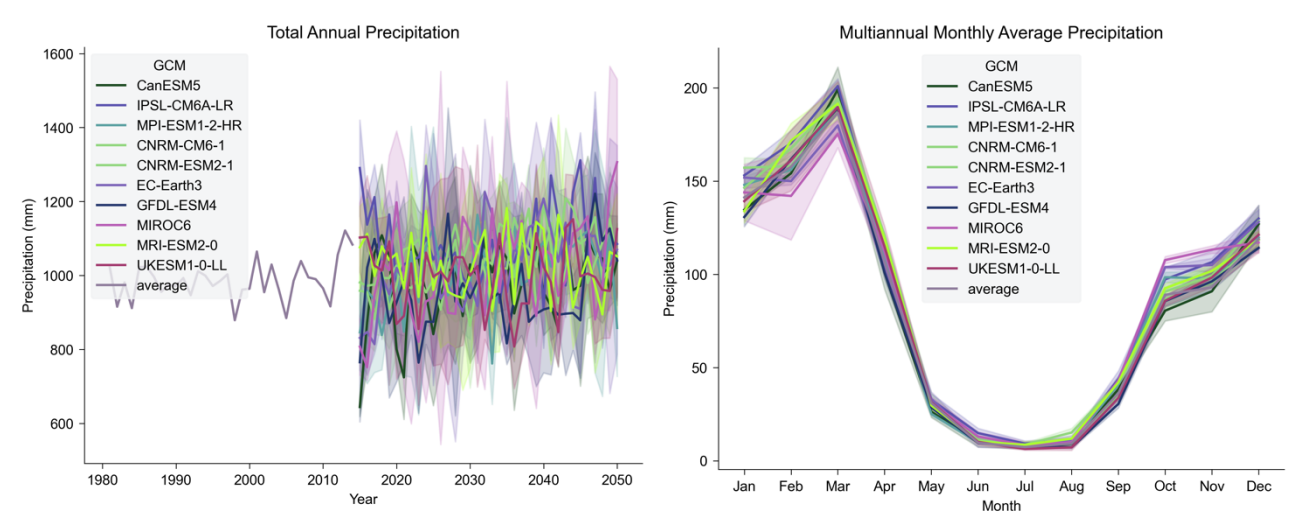


Figure 10: left: Historical and future total annual precipitation based on the different GCMs. right: Multiannual monthly average precipitation. The bold line represents the SSP average derived for each GCM, whilst the shaded areas illustrate the standard deviation from the climate models used for each climate scenario (own illustrations).

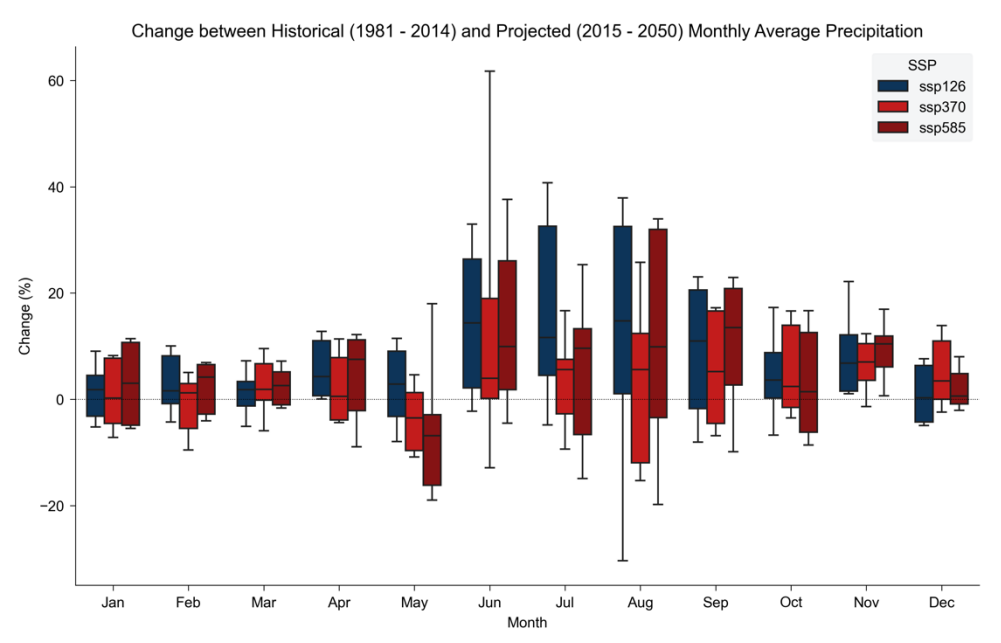


Figure 11: Comparison between historical and future precipitation patterns. The box groups 50% of the data equally around the median (horizontal line) and the whiskers extend to the 10% and 90% of the data respectively (own illustration).

The hypothesis that precipitation levels would increase in the future was confirmed by a statistical analysis. The analysis revealed no trend in historical annual precipitation, yet it did identify a statistically significant increase in future annual precipitation time series for all climate scenarios. A comparison of the historical and future scenarios reveals a moderately significant difference between the historical - SSP1-2.6 and historical - SSP5-8.5 time series (cf. appendix, 9.2.).

Evapotranspiration (x2_eto)

Given the challenges associated with the direct measurement of evapotranspiration in the field, it is commonly computed from weather data as the main factors affecting it are climatic parameters (Raes, 2009). Therefore, historical and future monthly reference evapotranspiration (ETo) are calculated using the *ETo package* in Python that is based on the FAO calculator. The Penman-Montheith-equation represents the rationale behind the FAO calculator. It allows a calculation procedure using limited meteorological parameters, namely minimum and maximum temperature, and assumptions for humidity, wind speed, and radiation based on the study site location. It is generally advised to avoid this ETo calculation with limited input data. However, as stated by Allen et al. (1998), it is still possible to obtain reasonable estimates with this limited dataset, when compared to alternative methods (Allen et al., 1998).

For the calculations the following assumptions serve as input data: i) mean elevation of the catchment (based on a GIS analysis) of 4467m.a.s.l., ii) latitude and longitude iii) light to moderate wind, and iv) a continental, semi-arid climate. In addition, the minimum and maximum temperature from bias-corrected *BASD-CMIP6* data (Fernandez-Palomino et al., 2023) have been used. Figure 12 illustrates that the historical multiannual monthly average evapotranspiration does not fully align with the pattern of the ETo from the *PISCOv1p1* dataset.

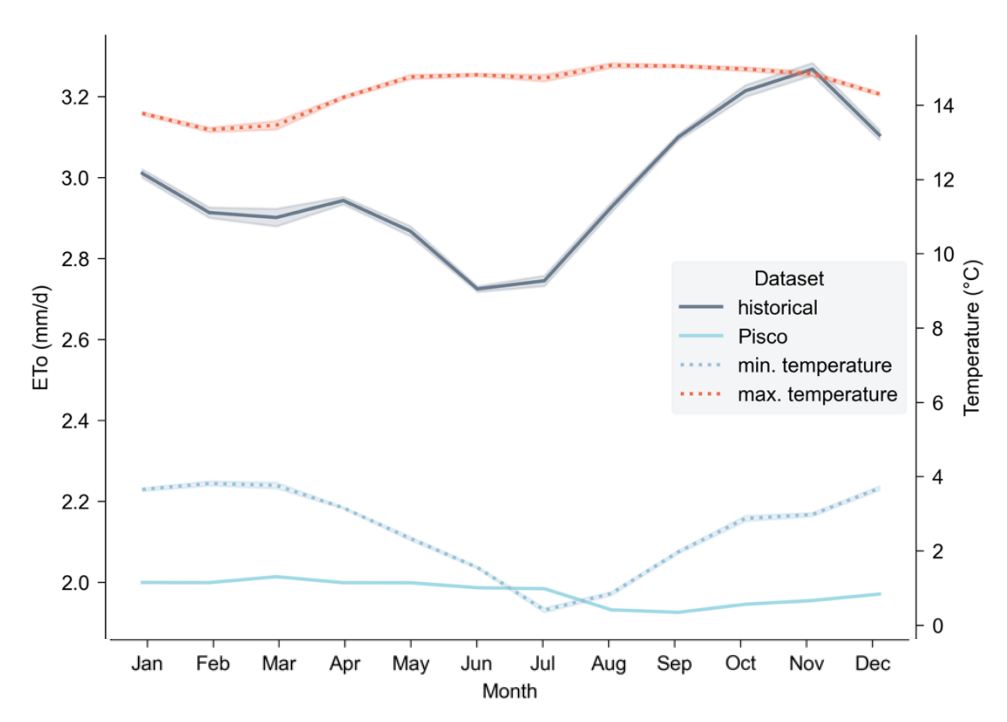


Figure 12: Bias-corrected multiannual monthly average evapotranspiration data based on the historical average of the GCM. The bold line represents the GCM average derived from the three climate scenarios (SSP1-2.6, SSP3-7.0, and SSP5-8.5), whilst the shaded areas illustrate the standard deviation from the climate models used for each climate scenario (own illustration).

It is evident that the pattern is not entirely, but to a noteworthy extent, influenced by the minimal temperature, which results in a minimum of ETo during the dry season. Therefore, the temperature data can explain a proportion of the discrepancy, indicating that the simplicity of the calculation method is not the sole contributing factor. However, the difference between the *PISCOv1p1* dataset and the FAO calculations, which is within the range of 1.2 mm/d, is negligible. According to the climate scenarios future ETo will increase in most of the months and decrease in March, April, and May. The use of constant climatic data (wind speed, humidity) to project future ETo represents a limitation of this approach, as these data may also be impacted by climate change.

Glacier area (x3 a gla)

The historical glacier surface is derived from Peruvian glacier inventories and from satellite imagery (ANA, 2014, 2018b).

For future glacier area calculation, the process begins with the 2016 glacier area shapefile from the Peruvian glacier inventory (ANA, 2018a), alongside a DEM (Jarvis et al., 2008) and temperature data from the *BASD-CMIP6* dataset (Fernandez-Palomino et al., 2023). Glacier retreat is then approximated by the relation between wet season *freezing level height* (FLH) and the total glacier area studied by Schauwecker et al. (2017). The FLH is defined as the "lowest altitude in the atmosphere, over a given location, at which the air temperature is 0°C" (American Meteorological Society, 2024). Schauwecker et al. (2017) found, that in the Cordillera Blanca, 17% of the total glacier area is below the wet season FLH. Moreover, the mean annual FLH is at an altitude of 4900m in this region. Hence, the total area can be approximately extrapolated, by assuming a constant lapse rate of 0.0065°C/m (Schauwecker et al., 2017).

As a limitation of this approach, they mention that the increase in FLH may even be higher, due to underestimations of mixed-phase cloud effects under a changing climate in the CMIP5 data (Schauwecker et al., 2017). Underestimations still occur in most of the GCMs in CMIP6 data (Hofer et al., 2024), which is used in this study. In addition to that, the FLH rise could be stronger than projected, if the El Niño Southern Oscillation (ENSO) variability is underestimated in climate data (Schauwecker et al., 2017). This is due to the fact that the FLH behavior is linked with ENSO in the tropics (Bradley et al., 2009). Although the approach has certain limitations, the combination of CMIP6 GCMs allows for the capture of a wide range of potential future ENSO behaviors, including intensification, no change, or even weakening (Heede and Fedorov, 2023). In addition, the DMDU method ensures that this uncertainty is effectively addressed. Consequently, these limitations do not significantly constrain the scope of this study. The delineation for recent years shows a generally acceptable approximation; for example, the difference between the INAIGEM estimate and the delineation for the year 2016 is 1.34 km². However, when compared with INAIGEM's historical corrected data (cf.

Figure 13), the rate of glacier area reduction is inconsistent, indicating differences in the trends of glacier retreat over time.

In line with the logic of the derivation, the area of glaciers is expected to decrease in the future in response to rising temperatures. This trend is illustrated in Figure 13, which uses climate data to project glacier area, showing a possible reduction from approximately 30 km² to 18 km² in 2050. The visual trend is confirmed by statistical analysis, which identifies an increase in the annual average temperature across both historical and future time series. Additionally, a significant difference is observed between the historical time series and the SSP1-2.6 and SSP5-8.5 scenarios (cf. appendix, 9.2.). The broad shaded areas in Figure 13 illustrate the significant uncertainty in glacier projections due to variability between GCMs (cf. appendix 9.3.), even when assuming the same climate scenario.

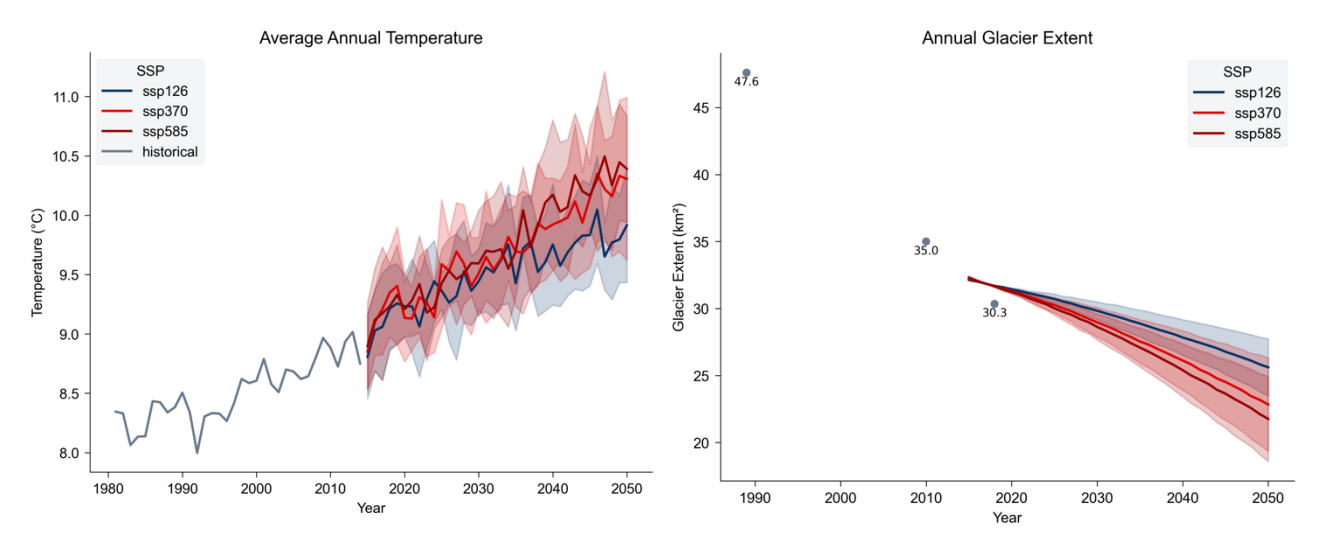


Figure 13: left: Average annual temperature. right: Glacier extent. In both figures, the bold line represents the GCM average derived from the three climate scenarios (SSP1-2.6, SSP3-7.0, and SSP5-8.5), whilst the shaded areas illustrate the standard deviation from the climate models used for each climate scenario (own illustration).

Unlike climatic data, historical socioeconomic data and its future uncertainty range are derived from historical datasets and extrapolated based on the parameter ranges defined by the five SSP scenarios (cf. sections 4.3.1. Population, 4.3.2. Irrigated area). For other variables, future projections are developed using assumptions supported by existing literature (cf. sections 4.3.3. Forest area, 4.3.4. Domestic water allocation, 4.3.5. Agricultural water allocation). This is the initial methodology for defining data ranges. Given the scarcity of data and the regional nature of the case study, certain data ranges are difficult to define. As a result, alternative potential ranges are presented for consideration.

Population (x pop)

Historical census population data at district level for Huaraz and Independencia can be downloaded from INEI's census and government projection (INEI, 2018). As the district level is not congruent with the catchment area, nor with the water distribution network, the data must be rescaled. Muñoz et al.

(2024b) who also dealt with a data-scarce study area, propose to use a function of the district fraction inside the catchment. However, this study suggests using the number of urban population in the districts as an approximation for the population in the study area: The census data of 2017 differentiates between the urban and the rural population and in that year it is obvious that most of the population lives in the only existing urban center of the districts of Huaraz and Independencia. As the main sources of water supply for the city of Huaraz are the Paria and Auqui river (Rivas et al., 2014) and the major urban settlement area of Huaraz is approximately consistent with the water distribution system of the city (cf. Figure 14, dashed rectangles), urban population can be used as an approximation. Yet, there are some settlements in the upper catchment above the city of Huaraz that are presumably not defined as urban. The resulting underestimation is compensated as not the entire urban area of the districts is included in the water distribution network of the city of Huaraz. The urban fraction is calculated by the mean of the fraction in the two districts and considered as constant in the entire historical period (1981, 1993, 2007), which of course is a rough approximation.

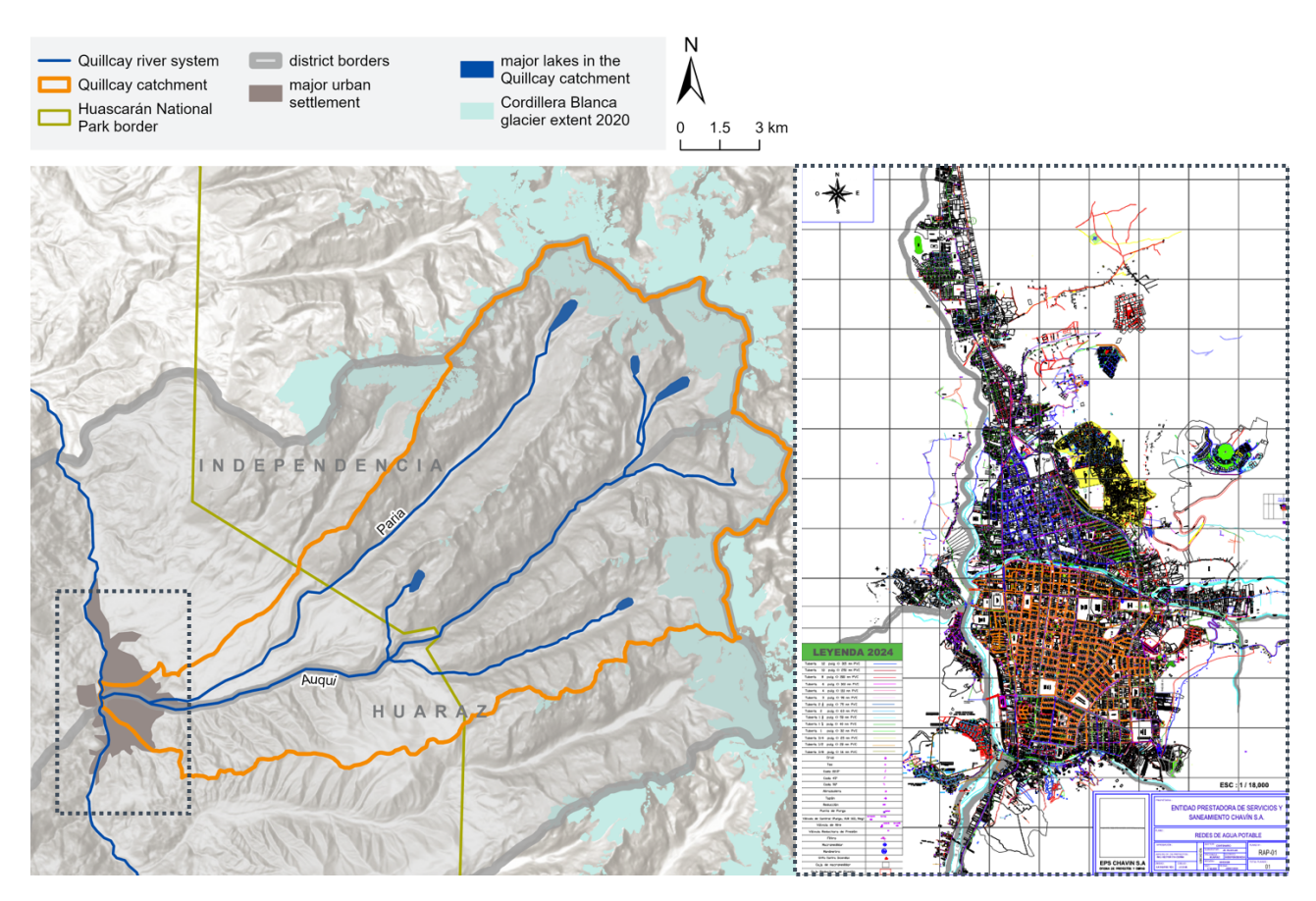


Figure 14: left: Quillcay catchment and its location within the political district borders and main urban settlement area (own illustration, data: delineation from Geo Perú "Ríos y Quebradas" and "Google Satelital" (2024), Quillcay catchment; Jarvis et al. (2008), Cordillera Blanca; ANA (2023), ESRI living atlas; Esri (n.d.). right: Drinking water network of the city of Huaraz in 2024 of Empresa Prestadora de Servicios de Saneamiento (EPS, Enterprise providing sanitation services) Chavín; EPS Chavín S.A. (2024).

For the future population, a range of change is defined based on the five SSP scenarios of the Peruvian population. This range, combined with current data, allows extrapolation with a polynomial (3rd order) function to obtain future annual population estimates.

Irrigated area (x_area_irr)

Data of historical agricultural area under irrigation from the national agricultural census (INEI, 2020) is rescaled from the district level as a function of the district fraction inside the catchment. Additionally, a local report from 2008 provides data on the proportion of irrigated land within the catchment area for that specific year (Quesquén Rumiche, 2008).

The future irrigated area is approximated based on the five SSP scenarios of cropland fractions in Latin America (Riahi et al., 2017; IIASA, 2018) resulting in a range of possible outcomes. The identified change of cropland is approximated to be the change in non-irrigated agricultural area since the share of non-irrigated agricultural land is negligibly small in the catchment area (Quesquén Rumiche, 2008). This range, combined with current data, allows extrapolation with a polynomial (3rd order) function to obtain future annual irrigated area estimates

Forest area (x area for)

Historical forest area data at an appropriate scale, provided by Peruvian institutions such as the *Catastro Forestal* (MIDAGRI) and *Geobosques* (MINAM), is limited to Amazonian regions. Therefore, historical forest cover must be calculated using the *MapBiomas Peru* remote sensing product (MapBiomas Peru, 2022), a land cover raster, clipped to the Quillcay watershed.

When looking at the range of change in forest area covered by the five SSP scenarios for Latin America (Riahi et al., 2017; IIASA, 2018), it becomes obvious that this range is highly biased by the Amazonian forest, as only deforestation (0 – 9% decrease) is suggested. However, spanning the future scenarios only with a decrease might be too simple to mirror the regional situation in the catchment. According to Pabón-Caicedo et al. (2020) several studies tried in the last decades to deepen the knowledge about land use and land cover change dynamics, including in the underresearched Andes region. A high spatial variability of transition trends in the Northern Andes (northern of the Quillcay catchment) has been observed (Rodríguez Eraso et al., 2013), which supports the problematic of using deforestation scenarios only. In addition, Aide et al. (2019) observed that in the Peruvian Andes above 2000 m.a.s.l., forest gain dominated in the period 2001-2014, again opposing the deforestation trend. Therefore, we suggest a regional change of forest area in a range between -50% – +50% to account for all possible scenarios, recognizing that such significant changes are feasible in small study areas, where dynamics can be more pronounced.

Domestic water allocation (x_alloc_dom)

Current net water demand is defined by a constant of 120 l/day/capita, reflecting average urban and rural water consumption in the Peruvian Andes (Drenkhan et al., 2019). The future range of domestic water allocation is determined by a lower limit defined by the *World Health Organization* (WHO)

declaration on optimal access to water as equivalent to more than 100 l/day/capita (Howard et al., 2020). The upper limit is set by the maximal observed value of 243 l/day/capita in some districts, such as Miraflores or San Isidro, in Peru's capital Lima (Sedapal, 2022). Given that the domestic water allocation is considered as uncertainty and not as a policy lever in this study, it is modeled as a gradual change, reflecting a continuous trend rather than an abrupt shift. Hence, it is extrapolated to 2050 using linear regression with a slope between -20% - +100%.

Nevertheless, the upper value defined in this context remains open to criticism on the basis that it reflects the maximum allocation of a highly inhomogeneous city. As an alternative to this, the mean observed value of 175 l/day/capita in Lima can be used as a basis for a more realistic upper limit (+45%) (Sedapal, 2022).

Agricultural water allocation (x alloc irr)

The current monthly net demand for irrigation was estimated for the Quillcay catchment in a report on the *Formalization of Water Rights and Extension to the National Water Registry* (PROFODUA) (Quesquén Rumiche, 2008), which serves as a basis for the agricultural water allocation in this study.

To account for future changes in agricultural practices, the net demand is multiplied by a factor that accounts for the crop water needs of the planted crop types. Using a constant factor is a simplistic approach and does not take into account changing growing seasons. At the lower end of the factor range, farmers would grow more crops that require less water than the current dominant crops, while at the upper end, farmers would grow more crops that require more water than the current dominant crops. This is consistent with the results presented in the study conducted by (Hagen et al., in review), which revealed that some farmers in the upper Santa catchment area have transitioned to the cultivation of commercially profitable, but water-intensive crops, commonly referred to as *cash crops*.

A shift to crops like amaranth and quinoa is used to calculate the lower limit: According to Alemayehu et al. (2015) the water requirement for growing amaranth is around 50% less than required for wheat. It is worth noting that the number originates from a study conducted in East Africa and cannot be directly applied to the tropical Andes. This is due to the fact that climatological factors play a significant role in determining crop water needs (Brower and Heibloem, 1986). Therefore, a second approximation is made with Quinoa. The lowest value crop water requirement value with reasonable harvest equals 300mm (Taaime et al., 2023). Comparing it with the mean of barley, wheat, and potato (550mm) (Allen et al., 1998), the present dominant corps, we note a reduction of water need of around 45%. The growing seasons are comparable to those of the reference crops, and for Quinoa, the growing season is even slightly shorter, which results in a lower water demand per month (Allen et al., 1998; Quesquén Rumiche, 2008). Thus, the lower limit is defined as -50%.

The upper limit is set by cash crops. Commercially profitable crops are currently mostly cultivated in the coastal areas, for example in plantations such as Chinecas or Chavimoc (Motschmann et al., 2020a). These crops include asparagus or avocado (Esteve-Llorens et al., 2022; Arias Montevechio et al., 2023). With higher temperatures in the future, it is possible that such crops will also be produced in the upper Santa catchment. Arias Montevechio et al. (2023) show in their study a shift to non-traditional crops, such as avocado in Abancay (department Apurímac). Obtaining reliable data on crop water requirements in Andean regions is a considerable challenge. Consequently, the estimated range was derived by comparing the average direct water volumes needed for irrigating avocado and asparagus cultivation on the Peruvian coast with the net irrigation requirement of the catchment, leading to an estimated 80% increase in water requirements. However, a key limitation of this approach is the aridity of the coastal region, which could result in overestimated irrigation requirements for the Andean region.

Similar to domestic water allocation, agricultural water allocation is considered as uncertainty and does not change abruptly in the period up to 2050 to illustrate a continuous shift in agriculture. Hence, it is extrapolated to 2050 using linear regression with a slope between -50% to +80%. It is important to note that the change in agricultural practices could also be seen as an adaptation measure.

As with the domestic water allocation, the upper and lower limits defined in this context are open to criticism on the basis that the entire agricultural area is assumed to change to more water-efficient crops or to commercial crops, respectively. An alternative range of -25% to +40% is therefore proposed. It considers the realistic progression of shifting agricultural practices, where up to 50% of the agricultural area will transition by 2050. This estimate accounts for the slow and limited nature of change due to factors such as the time required for adaptation, cultural beliefs, and soil properties.

4.1.2. Policy levers L: efficiencies

The current efficiency of irrigation systems used in the Quillcay catchment is at 35% (Rivas et al., 2014). In the studies conducted by Drenkhan et al. (2015; 2019) as well as by Muñoz et al. (2024b), a context-realistic upper value of 70% was selected. However, it should be noted that technically, an efficiency of 90% can be achieved with drip irrigation, as proposed in the bachelor's thesis of Dioses Noblecilla and Zapata Seminario (2017). This indicates the potential of technological development, to also improve water use efficiency in general. Given the credibility of the consulted sources, the range of agricultural water use efficiency of 25% – 70% is set.

The domestic water use efficiency is defined as the municipal system's efficiency measured at 76% (Quesquén Rumiche, 2008). For the sake of the exploration, the domestic water use efficiency is set between 66% and 90%. As in the agricultural sector, technical feasibility would allow very high efficiencies in the domestic sector. However, in practice, all water networks are subject to leakage and distribution losses. To illustrate a high efficiency in practice, Singapore's National Water Agency states to have a loss of approximately 8%, that is reached with rigorous leak management, which starts with thoughtful planning and ends with monitoring thanks to detection systems (PUB, 2023).

Thus, a context-specific upper value of 90% in water use efficiency appears theoretically achievable within the study area. However, this value is relatively high and may approach the upper bounds of realistic expectations.

4.1.3. Relation R: Shaman model

Glacio-hydrological simulation

The model that simulates water supply and demand must meet the requirements of the research objective, i.e. it must provide accurate discharge values, especially in the dry season, and perform well in the study area. Glacio-hydrological modeling in the tropical Andes is challenged by limited process understanding due to data scarcity and a gap in modeling approaches. With increasing data scarcity, the lumped Simple Hydrological Model for the Andes (Shaman model, presented by Muñoz et al., (2021)) provides more robust results than complex semi-distributed models and is therefore suitable for these challenges. It accounts for strong precipitation seasonality, year-round but still seasonal glacier melt, and only requires nine input parameters to calculate water supply (Muñoz et al., 2021). In summary, these parameters include precipitation, reference evaporation, glacier runoff - which is calculated based on glacier area and a melting factor - and five more parameters derived during the calibration process, as outlined by Muñoz et al. (2024b). Then, supply is calculated in a glacier module simulating glacier melt and a non-glacier module simulating groundwater (slow runoff) and superficial runoff (fast runoff) (cf. Figure 15) (Muñoz et al., 2024c). Domestic and irrigation water demand is subtracted from the simulated supply, while industrial demand is not considered, as industrial water withdrawal is neglectable in the Quillcay catchment (Quesquén Rumiche, 2008). The data and calculation methods described in sections 4.1.1. and 4.1.2. are used to define the model input parameters.

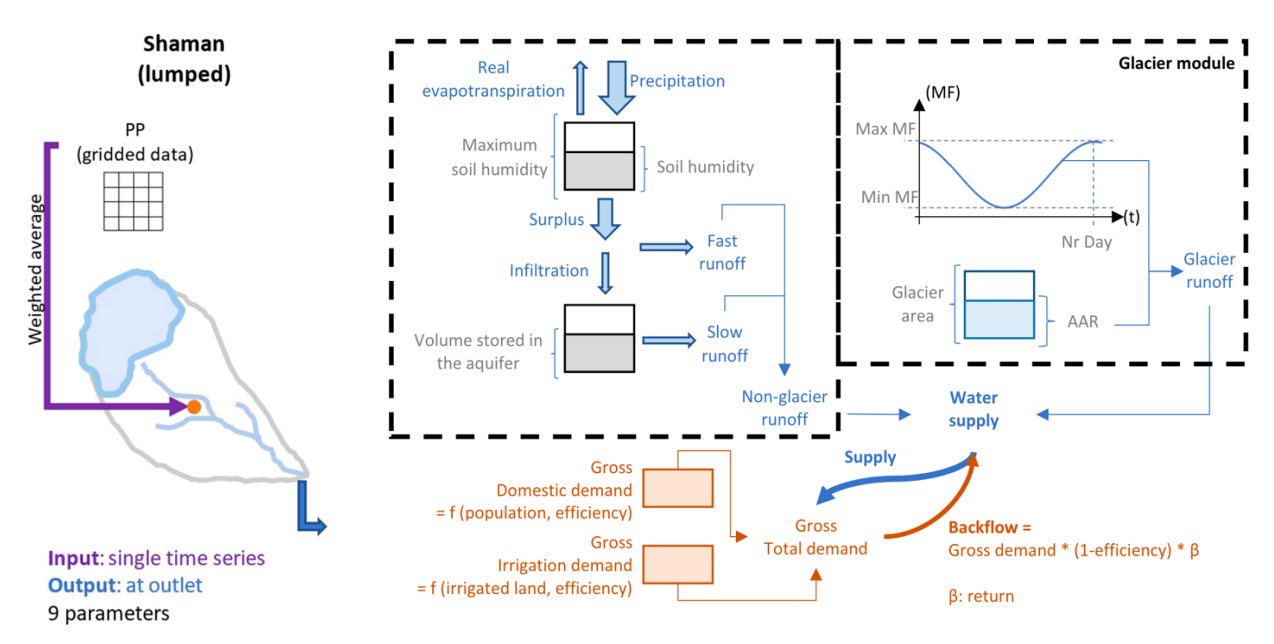


Figure 15: Schematic representation of Shaman model (Muñoz et al., 2021; Muñoz et al., 2024c).

The term *lumped* is used to describe the fact that spatial allocation of water is ignored in the Shaman model. Instead, it prioritizes sectoral demands, whereby water is first allocated to domestic use, then to irrigation, and finally to environmental needs (Muñoz et al., 2024b). This is consistent with the legal framework in the study area, where the *Ley de recursos hídricos ley Nº 29338* (Water Resources Law) specifies that domestic use takes priority over agricultural use (ANA, 2009). In conclusion, it can be stated that the Shaman model is an appropriate choice for achieving the objectives of the case study.

Constants in the glacio-hydrological simulation

Besides the input parameters of uncertainty and policy levers, the Shaman model requires additional input. A brief description of the constants that require further explanation is given in this subchapter.

The minimum environmental flow requirement can be estimated by different methods, depending on the amount of data required. However, no consensus exists on which method is the most reliable. According to the official methodology of the ANA, the minimum environmental flow requirement is defined as the flow with 95% persistence in cases where there is no data available for more detailed methods (ANA, 2016). This refers to the flow level that is exceeded 95% of the time over a period of at least 20 years (ANA, 2016). When historical discharge is unavailable, a hydrological model will be employed to generate the data (ANA, 2016). For the minimum environmental flow requirement in the Quillcay catchment, the period from 1981 to 2014 is studied and various flow percentiles are plotted (cf. Figure 16).

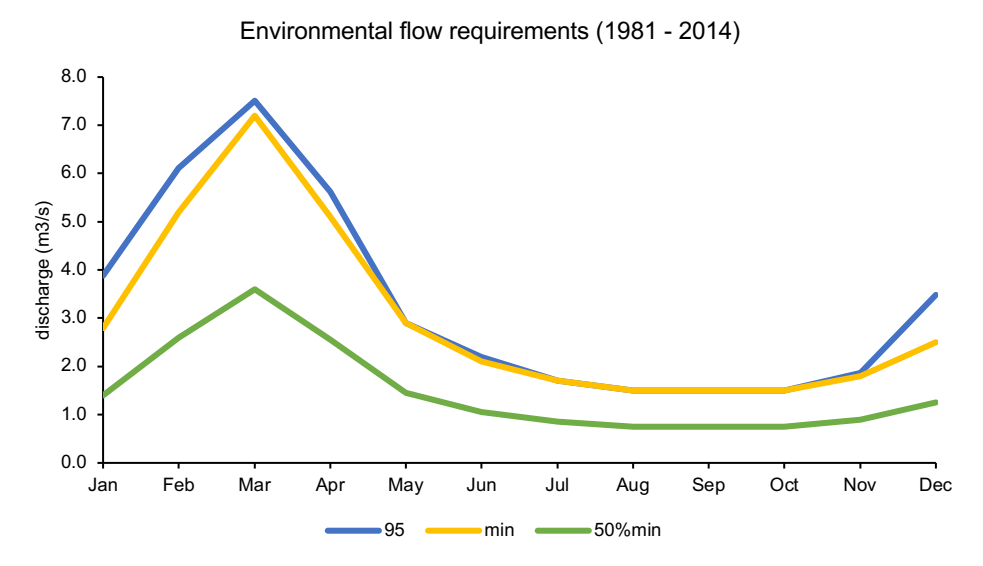


Figure 16: Environmental flow requirements (EFR) based on the observed runoff (1981 – 2014). The methods are persistence at 95% of total runoff used as environmental flow (95), minimal monthly average runoff (min), and 50% of the minimal monthly average runoff (50%min).

The problem with the 95% persistence method is that it is not meaningful for the catchment because the dry season values are too high compared to the available discharge, which is around 2m³/s in the dry season months. Therefore, the 50% of the minimal environmental flow requirement is used for the Shaman model. However, this approach has its limitations: it relies on a simple percentage and does not fully address the complex nature of the environmental flow requirement, which is a key factor in the water balance and strongly influence whether water availability is considered limited or sufficient. A more accurate estimation of the environmental flow would be ideal, but this falls beyond the scope of this thesis. This could serve as a potential objective for future studies. Alternatively, future research could explore treating the environmental flow as an uncertainty in water demand within the XLRM-framework.

In the Shaman model, a sinusoidal function is used to estimate glacier melt contributions (Muñoz et al., 2021). This approach considers glacier surface area, the proportion of the accumulation area, and a seasonal melting factor (Muñoz et al., 2021). While temperature is typically the primary driver of glacier melt, in the tropical Andes, additional factors such as precipitation and atmospheric humidity play significant roles, adding complexity to the modeling process (Vuille et al., 2008). To address the complexity, a melting factor used in Shaman is an artificial value calibrated specifically for the model, combining all relevant climate variables affecting glacier melt (Muñoz et al., 2021). For future projections, this calibrated factor is applied as a constant.

After accounting for losses in distribution systems, backflows are the fraction of water provided to end users that is returned to the system. To illustrate, in the domestic sector, backflows occur when a faucet is left running, allowing unused water to flow down the drain and re-enter the municipal system. In agriculture, this could occur through percolation of irrigation water into the groundwater. According to Song et al. (2020), uncertainty in backflows stems from their estimation, though it may

also result from variations in agricultural practices. Muñoz et al. (2024b) address this uncertainty in their case study by modeling backflows as a variable uncertainty (X) within their framework, with values ranging between 10% and 50%. In this study, the impact of changing backflow percentages on the EMA results was examined. Since the outcomes were found to be insensitive to variations in backflow percentages, the domestic and irrigation backflow rates were simplified and set to a fixed value of 50%.

Landcover fraction estimation for the calibration

In Shaman, the non-glacier module works with landcover differentiation. The surface runoff-to-infiltration ratio, or effective precipitation (Bos et al., 2009), varies across landcover classes, and this variability is accounted for by applying a unique c-factor to each individual module (Muñoz et al., 2024c). Therefore, the fractions of the land cover class *rock*, *forest*, *grassland*, *non-irrigated agriculture*, and *irrigated agriculture* must be defined.

To do so, existing land cover raster and vector data have been reclassified according to similar land cover properties of the four classes. More information about the data that was used, namely *COBER-TURAFIN1* (MINAM, 2009), *santa_cov* (MINAM, 2015), and *MapBiomas Cobertura y uso* (MapBiomas Peru, 2022), can be found in the appendix (cf. section 9.1.).

Table 5: Reclassification	logic for all existing	land cover classes in t	the original data

Reclassified land cover classes	Original classes (classification a)	Original classes (classification b)
Rock	urban area, high Andean area with sparse and no vegetation, scree/stony, rocky surface	urban area, high Andean area with sparse and no vegetation, scree/stony, rocky surface
Grassland	pasture, scrub, wetland	pasture, scrub (>4000 m.a.s.l.), wetland (>4000 m.a.s.l.)
Forest	plantation forest, high Andean relict forest, shrub thicket, native forest, introduced forest	plantation forest, high Andean relict forest, shrub thicket, native forest, introduced forest
Agriculture	coastal and Andean agriculture, agriculture	coastal and Andean agriculture, agriculture, scrub (<4000 m.a.s.l.), wetland (<4000 m.a.s.l)

The classification logic in Table 5 has been refined considering the borders of the Huascaran National Park (Esri, n.d.), whose borders are at around 4000 m.a.s.l.. According to (Motschmann et al., 2020a) agricultural area lies mostly between 3000 m.a.s.l. and the border of the National Park.

The differentiation between irrigated and non-irrigated areas is based on remote sensing data. Firstly, the *Normalized Difference Vegetation Index* (NDVI) is calculated to emphasize healthy vegetation (Jayakumar et al., 2018). The logic behind the analysis is that irrigated areas will not show a change in NDVI between the dry and wet seasons, whereas non-irrigated areas will show a decrease in NDVI. Irrigated agriculture is expected to have NDVI values between 0.4 and 0.7, in contrast to non-irrigated areas where NDVI values between 0.2 and 0.5 are expected in the dry season. For the

operationalization, Sentinel 2 data (ESA, 2023b, 2023a) (cf. appendix 9.1.) is chosen because of its suitable resolution for the relatively small catchment area. Two image sets are downloaded from the Sentinel Hub EO Browser, one for the dry season (August) and one for the wet season (March). A difference layer is subsequently calculated to identify potential declines in healthy vegetation from the wet season to the dry season. To avoid false detections of changes to other land cover classes, the data is clipped to agricultural areas, and negative values are ignored. A threshold of 0.3 for NDVI change is chosen as this value allows the detection of significant changes in NDVI while avoiding the detection of false positive irrigated areas. This results in approximately 9% of non-irrigated areas and 91% of irrigated areas.

In comparison to the findings of Rivas et al. (2014), which indicated that 96.2% of the agricultural area is irrigated, the value derived from the NDVI-change appears to be a realistic representation, while the threshold remains relatively non-restrictive in the non-irrigated areas. Nevertheless, this analysis is not without weaknesses. Firstly, the agricultural areas identified from the land cover data appear rather arbitrary when compared to satellite imagery. Secondly, the irrigated areas identified do not exhibit a similar pattern to that observed in the designated irrigation zones outlined by Stitelmann (2024).

Table 6: Comparison of different land cover fractions derived from analysis and reports.

	Raster (COE AFIN1, 2009		Raster (Map- Biomas, 2022)	Vector (santa_cov, 2013)	Historical data (cf. 4.1.1., 2015 / 2017)	Applied in Shaman ¹
Fraction of catchment [%]	Classification a [%]	Classification b [%]	[%]	[%]	[%]	[%]
Rock (+glac- ier)	51	53	45	55		48
Grassland	23	33	39	24		26
Forest	8	8	5	8	5	5
Agriculture	18	6	11	13		21
Irrigated					19.00	19 (91% of agric.)
Non-irri- gated						2 (9% of agric.)

As can be observed in Table 6, the proportion of land classified as rock and forest remains relatively consistent when different datasets and classification methods are employed. Given that there should be no discrepancy between the historical data employed for the socioeconomic scenarios and the land cover fractions used as a foundation for the Shaman model, the historical data (cf. Table 6, bold) has been set as a fixed value for the forest and irrigated area fractions in Shaman. Since the

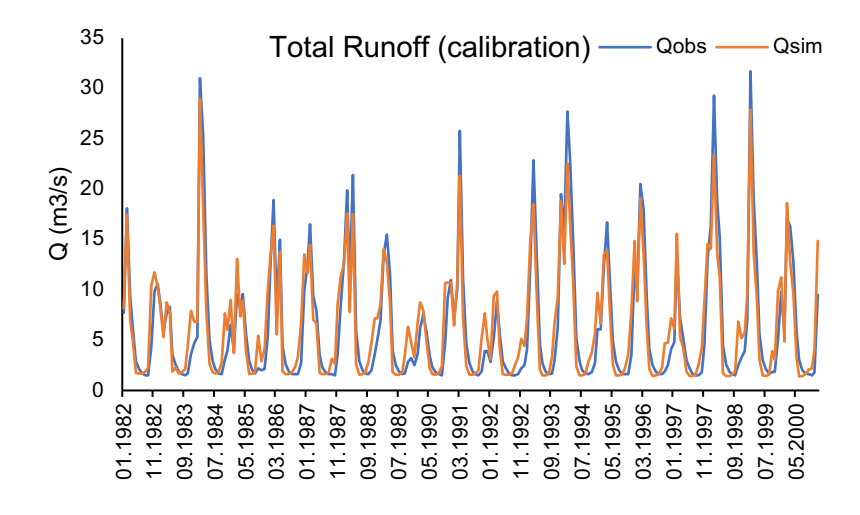
_

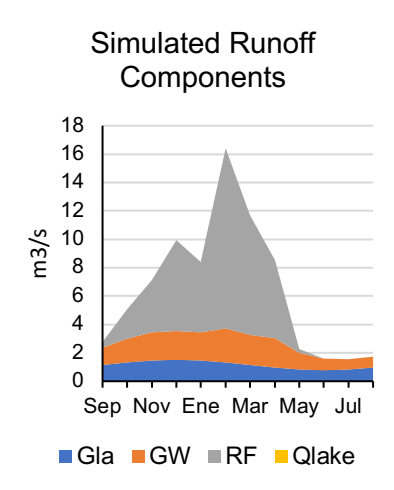
¹ rounded for readability.

distinction between the classes was already not entirely clear from the definitions of the original datasets, the resulting fractions are not precise. The average fractions of rock and grassland have been determined through an empirical adjustment process, thereby ensuring consistency within the broader dataset. To account for the observed increase in arable land between the historical and GIS data, adjustments were made by proportionally reducing the grassland coverage. While the methodology employed is grounded in heuristic adjustments, the resulting fractions align closely with the ranges provided by various datasets. It should be noted that considerable variation in the agricultural data is acknowledged; however, the reliability of these values is supported by the historical data, which is based on a local report that can be trusted.

Calibration strategy

With the identified land cover fractions, the model can be calibrated to assess its performance. A calibration period (1981 - 2000) and a validation period (2001 - 2014) are defined, where the simulated monthly runoff is compared to the measured stream flow from the *PISCOv1p1* dataset (SENAMHI, 2020) (cf. appendix 9.1.) following the calibration strategy according to Muñoz et al., 2021. The measures of model performance in Shaman that capture average, high, and low flows are respectively: the coefficient of determination (R²), the Nash-Sutcliffe efficiency (Nash), and the logarithmic Nash-Sutcliffe efficiency (Nash-In) (Muñoz et al., 2021). The proportion of glacier melt was compared with the findings of (Buytaert et al., 2017), which quantify the contribution of glacier melt to the total runoff volume.





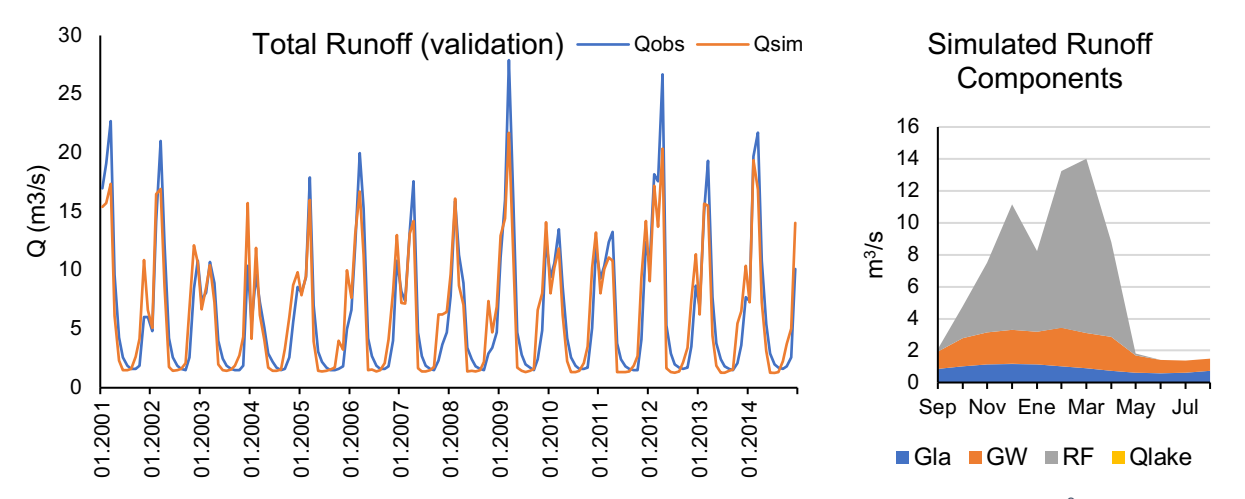


Figure 17: Total runoff and glacier contribution in the calibration and validation period. Calibration (R²: 0.93, Nash: 0.86, Nash-In: 0.76), validation (R²: 0.92, Nash: 0.84, Nash-In: 0.78).

Figure 17 shows that, overall, the model successfully simulates the runoff pattern in the Quillcay catchment. However, a visual assessment reveals a small shift in the timing of the low flows: the simulated flow decreases faster in the dry season than the observed flow. As the research focuses on water scarcity, the main goal of the calibration is to obtain a good representation of the low flows in the dry season (Muñoz et al., 2021). The measure for low flows (Nash-In) is the smallest of the three model performance indicators, nonetheless, Nash-In values of 0.76 and 0.78 are still acceptable.

4.1.4. Metric M: water scarcity indicator

In the XLRM-framework, the resulting output of the hydrological model, namely water supply and water demand, has to be transformed into a metric of water scarcity. Damkjaer and Taylor (2017) argue in favor of using threshold indicators instead of holistic metrics. One of the threshold indicators presented in their work is the freshwater Withdrawal-Availability ratio (WTA), which defines water scarcity as a percentage of total annual withdrawals across the agricultural, domestic, and industrial sectors, before applying a threshold to classify it as water stressed or not (Raskin et al., 1996). However, in the Peruvian Andes, interannual variability is crucial due to seasonal fluctuations that can lead to either floods or droughts. Moreover, the proportion of industrial demand is insignificant in the Quillcay catchment (Quesquén Rumiche, 2008). This metric is therefore rejected as it fails to reflect the main local factors influencing water scarcity.

To account for interannual variability, the metric used by Kalra et al. (2015) and by Muñoz et al. (2024b) was adapted to the current local context of water availability in the catchment area: Water scarcity throughout the study period is defined as a situation where supply fails to provide 90% or more of the demand in more than t% of the months of the dry season. The 90% represents the current situation, documented in water access reports, where not all water needs can be met (INEI, 2023). The t% represents the threshold: e.g. in a study conducted with local authorities in Lima, a

threshold of 10% was used (Kalra et al., 2015). However, taking into account the high subjectivity of what is considered intolerable, the threshold could be lower or higher than 10%. The threshold is defined in step iii) of the EMA, here we simply note that the definition of the threshold is crucial for the results.

4.2. Integration of uncertainty ranges in the case study

A notable challenge in the integration of EMA is the definition of strict ranges for uncertain variables. For instance, future trends in domestic water allocation and irrigation allocation are not clearly defined as outlined in section 4.1.1. and 4.1.2. because of the distinction between 'technically possible' and 'contextually feasible. To address this challenge, three different range definitions are introduced to be used in (iii) stress testing. This approach not only helps to assess how effectively EMA can be used to identify and quantify key drivers of future water scarcity but is also consistent with the documentation of the TMIP-EMAT workbench: Newman and Milkovits (2021a) point out that altering the range of input parameters in the experimental setup affects the model results. Since the methodologies utilized by the TMIP-EMAT workbench align with those employed in this research, this can be directly applied to this context. The implementation of three different range scenarios (cf. Figure 18, 19) also helps to understand how different stakeholder perspectives would translate into EMA and how this affects the outcome.

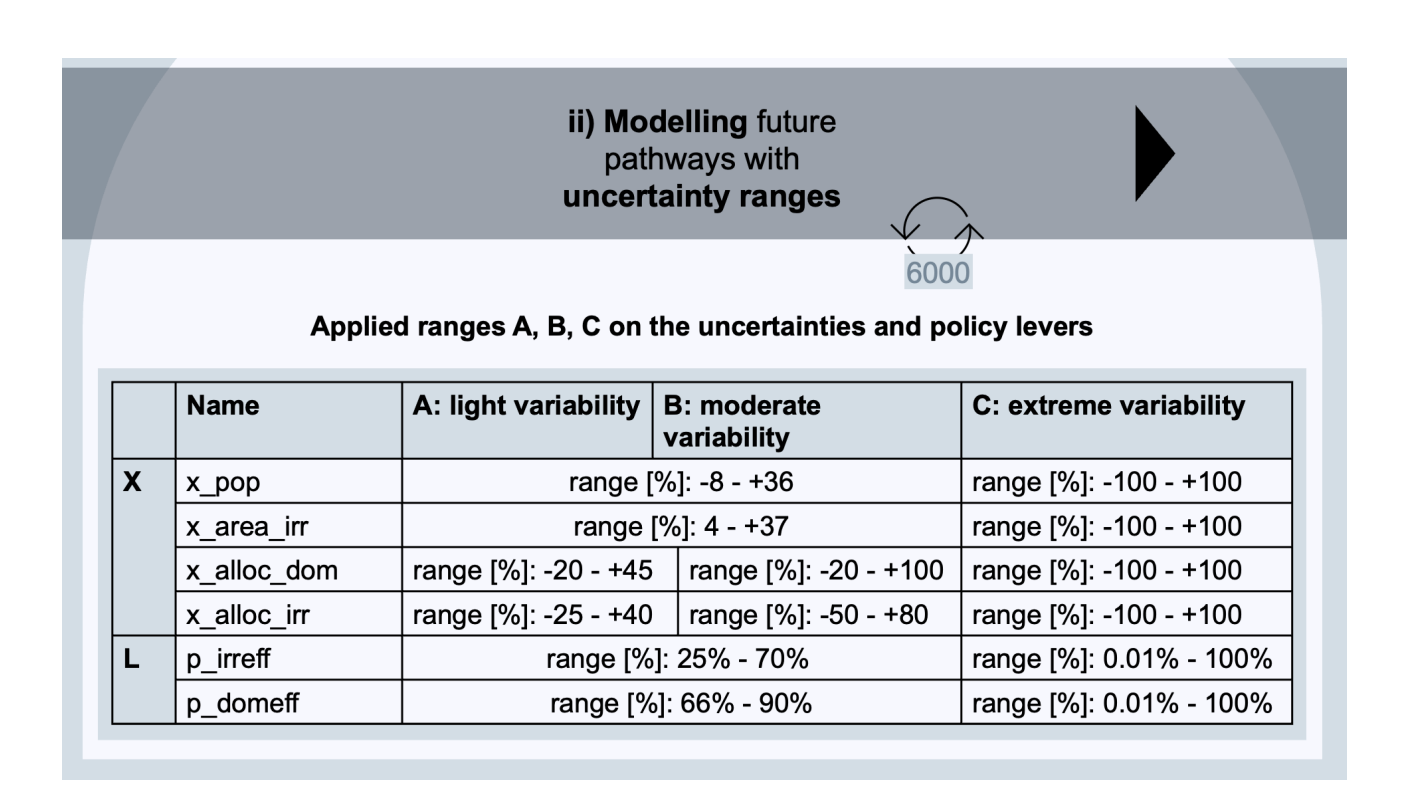


Figure 18: Schematic representation of step ii) in the EMA workflow: applied range definitions A, B, and C on the uncertainties and policy levers. Variables (X, L) that are not listed are not subject to different range scenarios.

The baseline definition, represented by the *B: moderate variability* range, is theoretically possible, though arguably less realistic given the context of the study area. In contrast, the *A: light variability* range definition represents a realistic definition for the context by adapting the ranges of the domestic and irrigation water allocation. The *C: extreme variability* range definition represents extreme variability, setting the ranges for all uncertainties and policy levers affecting water demand to an extreme value. This scenario builds on EMA's ability to deal with a wide range of future uncertainties and aims to explore the complete range of possible outcomes by fully utilizing this capability. However, it is acknowledged that these ranges might not align with realistic expectations. The results of the *C: extreme variability* range definition need to be checked in the iii) stress testing to ensure that they are realistic. To summarize it is important to note, that with changing the range definitions, only socioeconomic ranges are affected, whereas climatic ranges do not change.

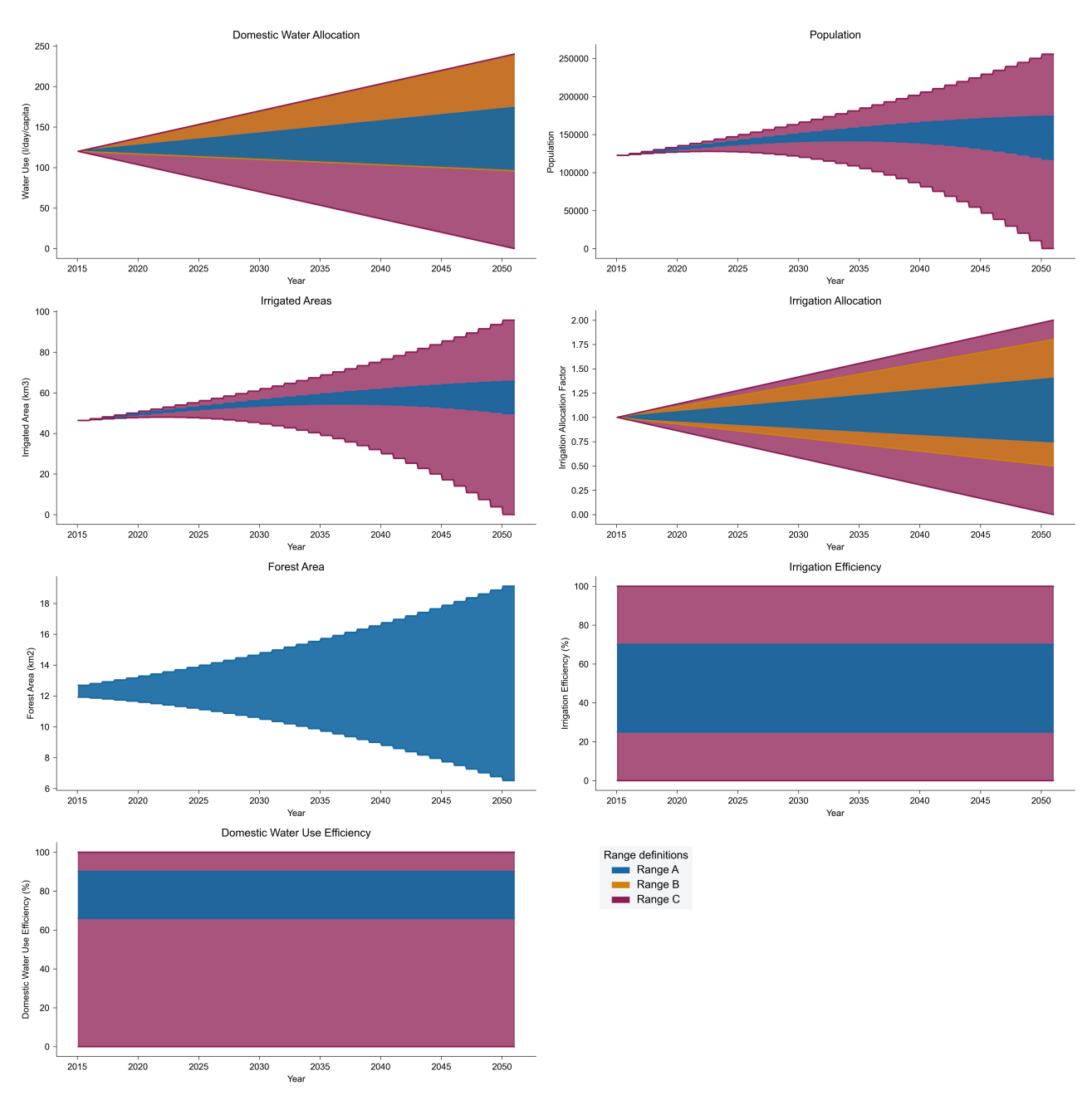


Figure 19: Applied range definitions of the uncertain variables in part ii) of EMA.

4.3. Integration of stress testing in the case study

The calibrated Shaman model is implemented in the open-source software EMA Workbench (Kwakkel, 2017) using Python to run simulations from 2015 to 2050, whereby the first five years are used as model initialization according to Muñoz et al. (2021). As shown in Figure 18, each run consists of 6000 experiments by the Shaman model, of which 300 scenarios and 20 policies are used as inputs. The number of scenarios and policies is determined by the number of simulations needed to representatively span the range of uncertain variables. Since the number of uncertainties exceeds the number of policy levers, this number is also higher. The final number of experiments is validated through an iterative sensitivity analysis of the Feature Scoring results.

Several runs are conducted to gain insight into the effect of varying the parameters. First, the different range definitions require multiple runs. Second, only one policy is used as an input policy lever (L) at a time. The policy is either the change in household efficiency or the change in irrigation system efficiency. Third, the goal is to assess the importance of individual climatic factors on water scarcity. Therefore, two scripts are used: In the first option, climate variables are combined through their respective climate scenarios and GCMs. In the second, variables such as precipitation, glacier area, and evapotranspiration are treated independently and can be linked across scenarios and GCMs in EMA simulations. For example, precipitation may be taken from the SSP1-2.6 scenario, while glacier area is derived from SSP8-5.8. Although such specific combinations may not occur in the future, this method allows for exploring how different variable interactions contribute to system failure.

4.3.1. Threshold setting

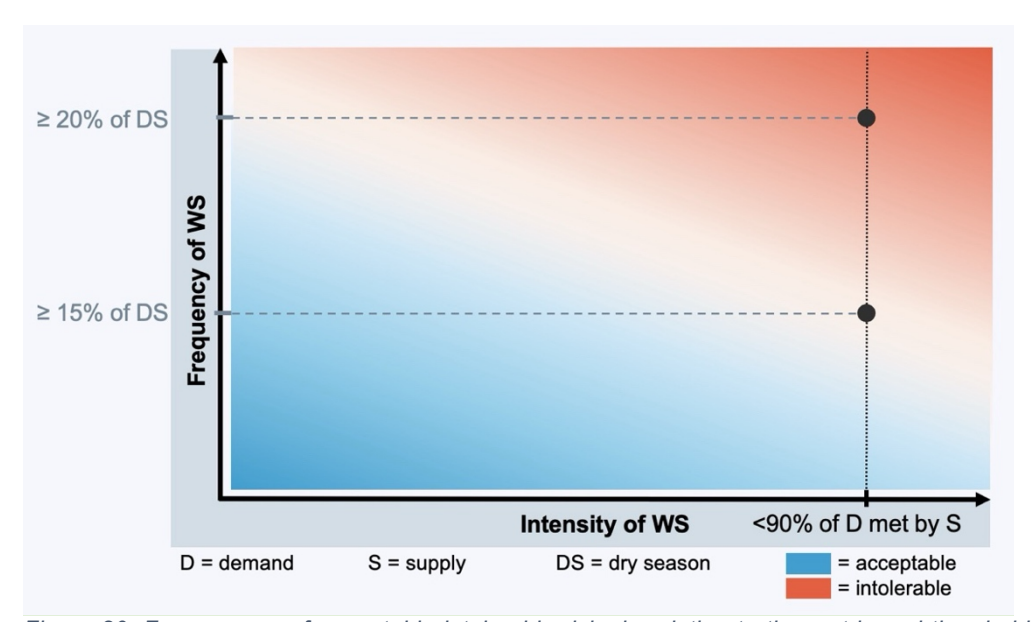


Figure 20: Fuzzy space of acceptable intolerable risks in relation to the metric and threshold setting operationalized in EMA, adapted from Dow et al. (2013) (based on Klinke and Renn (2012)). In the way EMA has been adapted, the frequency of water scarcity (WS) can be changed by varying the threshold, thus the analyzed black point can be moved on the black dotted line. The continuous color gradient of acceptable and intolerable risks represents the gradual change in perception from acceptable to tolerable to intolerable risk and illustrates the concept rather than the exact manifestations.

Defining the metric and its threshold is essential for identifying situations of intolerable water scarcity. The metric is composed of the intensity and the frequency of water scarcity: water scarcity equals the situation when supply fails to provide 90% (intensity) or more of the demand in more than t% of the months of the dry season (frequency) (cf. Figure 20). This can be understood as one specific point in the risk space. By adjusting the threshold, it is possible to scale the frequency on a vertical axis in the risk space (cf. Figure 20, black dotted line). As a result, the way EMA is implemented in this study can identify the driving factors that lead to the specific location in the risk space.

It is important to consider that the threshold setting directly affects the number of experiments classified as water-scarce, potentially resulting in either none or all experiments being identified as such. When applying EMA, this makes a sensitivity analysis or scenario discovery impossible, thus limiting

the ability to generate meaningful insights. Therefore, selecting thresholds that enable valuable insights is a critical step in the operationalization process. However, individual perceptions of acceptability vary, making the choice of thresholds inherently subjective. This subjectivity will be further explored in section 5.2.2., with a focus on how the analyzed thresholds can be understood in a social-ecological system.

4.3.2. Sensitivity Analysis operationalized with Feature Scoring

In the sensitivity analysis, Feature Scoring is used once to analyze the outcomes of all metric values, then Feature Scoring is applied with a threshold of $t \ge 0.2$ and $t \ge 0.15$ for both, irrigation efficiency and domestic water use efficiency (L).

4.3.3. Scenario Discovery operationalized with PRIM

The PRIM algorithm output is visualized in the form of pair scatter, accompanied by figures illustrating the non-operational ranges. These figures demonstrate, under the specified coverage and density conditions, the restricted ranges in which water scarcity occurs. Pair scatter includes density functions, contour plots, and scatter plots. The latter breaks down the 9-dimensional space (8 uncertainties, 1 policy) and visualizes it as a 2-dimensional representation (Muñoz et al., 2024b). In addition to the scatter plots, contour plots are analogous to topographic maps, with lines indicating regions where the density of data points is similar. This demonstrates the overlaps between the two distinct categories of cases, namely the successful and unsuccessful ones. The red rectangle shows the operational ranges in the plots. Moreover, density functions show trends for successful and unsuccessful experiments of each factor, depending on its value. In this case study, the term *successful* is counterintuitive and refers to scenarios with similar metric outcomes that the study focuses on — in this analysis, those above the threshold indicating water scarcity. To sum up, the pair scatter shows the specific combination of factors that have been restricted to say that in this specific range, they drive water scarcity.

5. Results

The results lead chronologically through the steps according to the method and show at the same time the insights from the case study about water scarcity in the Quillcay catchment (cf. Research question 2), alongside iterative decisions and lessons learned during the operationalization (cf. Research question 1).

5.1. Discharge modeling

From the 6000 simulation runs in range B, where variables for discharge calculation remain constant and the choice of range is therefore inconsequential, monthly discharge simulations were retrieved. Figure 21 illustrates the comparison between historical observation data and historical simulated data. The left plot highlights differences between historical observed and future data. This discrepancy could be attributed to the selected input dataset, namely the precipitation data, which demonstrates a seasonal shift when compared to the observational data. This shift is partly reflected in the simulated discharge. Furthermore, residual differences after calibration and bias-correction are also visible. However, part of this shift can be attributed to climate change, as melting glaciers and the loss of their storage function lead to a seasonal discharge pattern increasingly resembling precipitation (Vilímek et al., 2024). For the purpose of visual and statistical analyses, the focus is on changes driven by climate warming, excluding biases from dataset and calibration differences. Therefore, in future analyses, historical simulated data will be used.

A visual analysis of the historical simulated data and the future projections reveals the key characteristics of projected climate warming impacts on hydrological patterns. First, Figure 21 shows more extreme monthly average discharges: reduced flows during the dry season and higher peak flows during the wet season. The watershed flow regime becomes more dependent on precipitation seasonality, with a more pronounced dry season (Vilímek et al., 2024). Second, although the annual average discharge is stable, the annual average dry season discharge decreases and has been declining since the historical period (cf. Figure 22, 23), an observation aligning with interviews conducted in the Cordillera Blanca (Bury et al., 2011). When considering projections of moderately increased future precipitation, the Quillcay catchment is evidently in a post-peak water context. Peak water refers to the point at which glacial melt runoff reaches its maximum due to an initial increase in melt, followed by a decline as glacial ice reserves decrease over time (Baraer, 2012) (cf. Figure 24). In this context, ice volume loss exerts a greater influence on dry season discharge compared to annual discharge (Vilímek et al., 2024), as illustrated in Figure 22. Conversely, wet season discharge exhibits an increase (cf. Figure 21), while annual discharge variability, anticipated to rise due to the loss of glacier buffering (Vilímek et al., 2024), remains undetectable in the annual average. Yet, Huss and Hock (2018) project a 21–59% decrease in dry season glacier runoff in the Santa River basin

by 2090, and Baraer et al. (2012) noted a decade ago that the Santa River had already passed peak water, supporting the assumption that the study area faces similar challenges and has already passed this stage. Third, Figure 22 (right) displays an outlier in the 2047 dry season average discharge, attributable to highly variable dry season precipitation under the SSP1-2.6 scenario. This variability is not reflected in the annual average precipitation and may be indicative of extreme events, as outlined in the Sixth Assessment Report of the IPCC, which states that increasing global warming leads to more pronounced changes in extremes (IPCC, 2023). The high discharge values originate from the GCM MIROC6 (cf. appendix, 9.3).

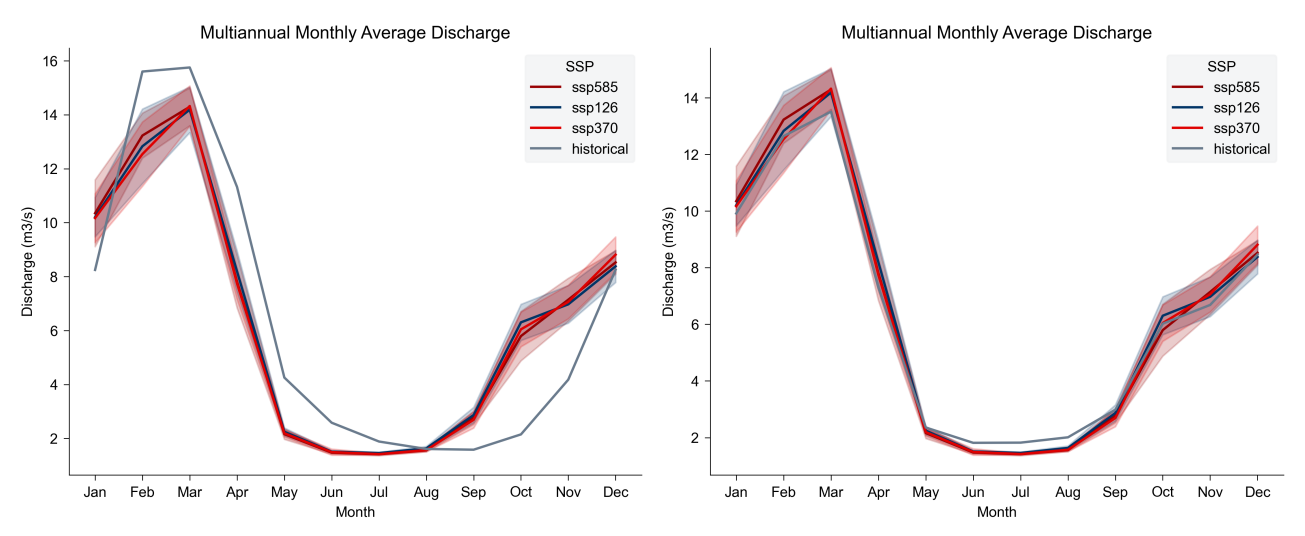


Figure 21: Multiannual monthly average discharge colored based on the three different climate scenarios. left: Historical PISCO data. right: Simulated historical data. The bold line represents the GCM average derived from the three climate scenarios (SSP1-2.6, SSP3-7.0, and SSP5-8.5), whilst the shaded areas illustrate the standard deviation from the climate models used for each climate scenario (own illustrations).

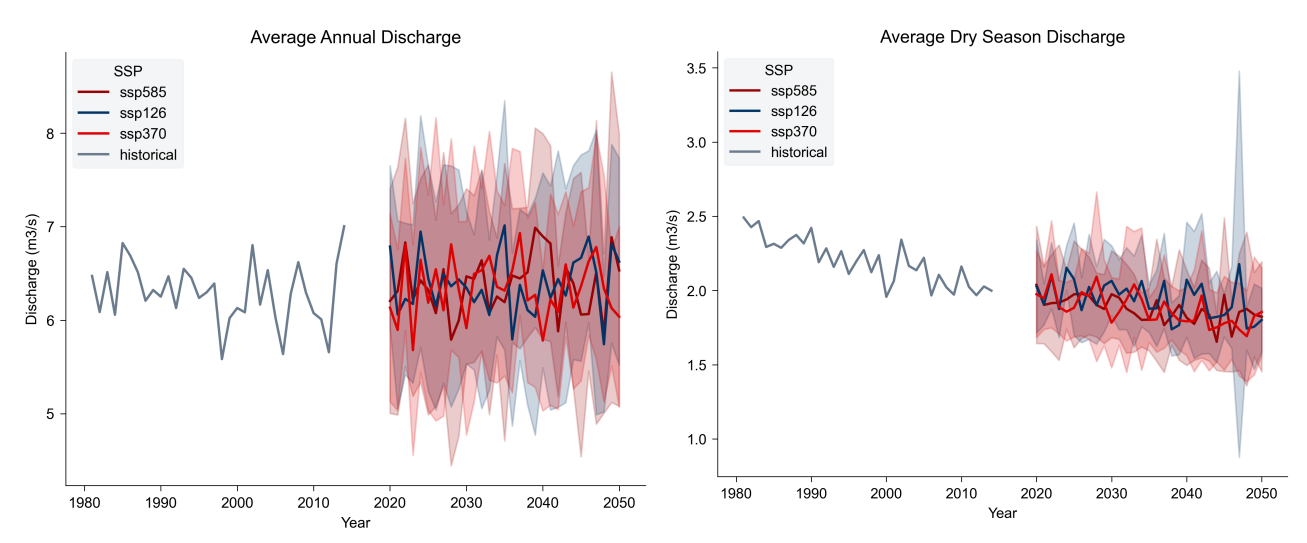


Figure 22: left: Average annual discharge. right: Average dry season discharge. Both datasets are based on the three different climate scenarios and simulated historical data. The bold line represents the GCM average derived from the three climate scenarios (SSP1-2.6, SSP3-7.0, and SSP5-8.5), whilst the shaded areas illustrate the standard deviation from the climate models used for each climate scenario (own illustrations).

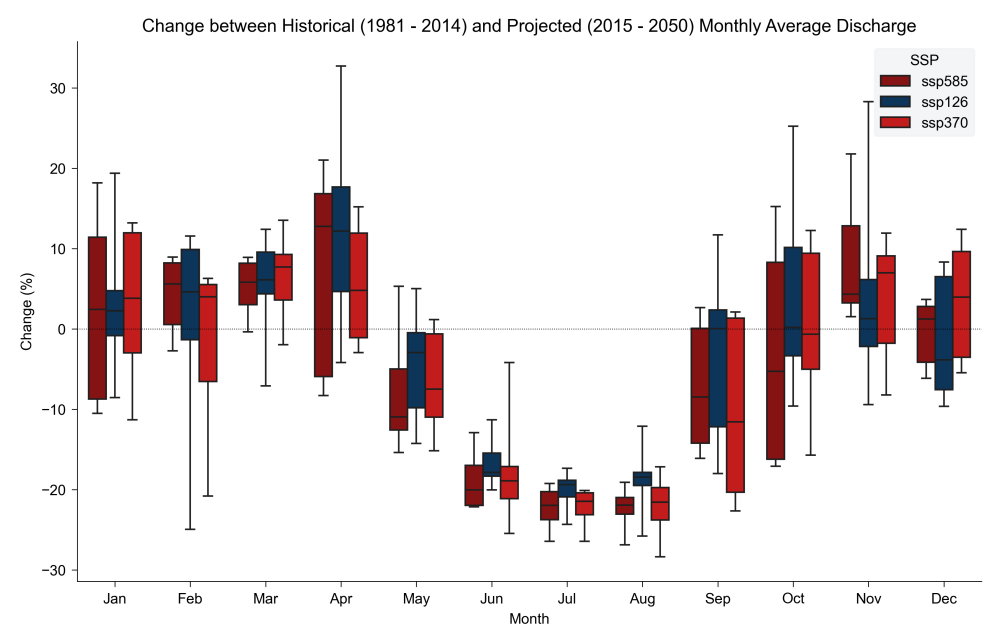


Figure 23: Comparison between historical and future discharge patterns. The box groups 50% of the data equally around the median (horizontal line) and the whiskers extend to the 10% and 90% of the data respectively (own illustration).

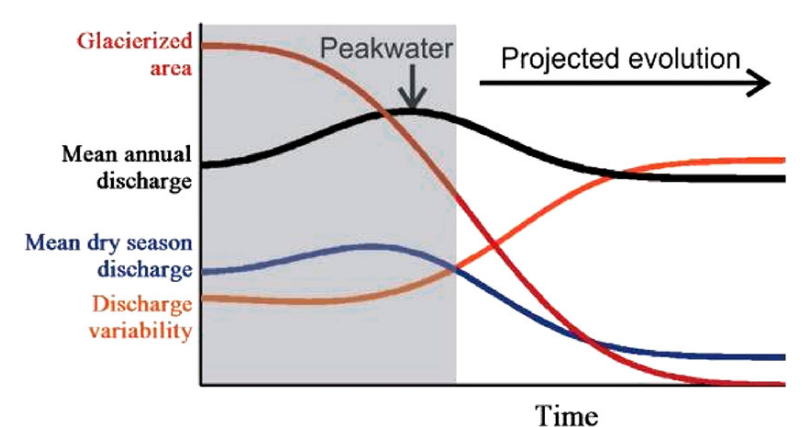


Figure 24: Concept of peak water. The gray-shaded area represents the evolution until 2020 for an analysis in the upper Santa river (Guittard et al., 2020; based on Baraer et al., 2012).

The hypothesis, based on visual assessment, that the average dry discharge will decrease in the future and that the average annual discharge shows no trend is confirmed by statistical analysis (cf. Table 7). A comparison of the historical and future scenarios reveals a significant difference between the historical and future average dry season discharge (cf. Table 8).

Table 7: P-values from the Mann-Kendall test (α = 0.05) applied to historic (1981-2014) and average scenario (2015 - 2050, 2020 – 2050 for simulated discharge) time series. Simulated historical runoff data were used to isolate the contributions of climate scenarios from discrepancies between simulated and observed data.

Climate variable	historical	SSP 1-2.6	SSP 3-7.0	SSP5-8.5
Annual average discharge (m³/s)	p-value: 0.98 trend: no trend	p-value: 0.36 trend: no trend	p-value:0.95 trend: no trend	p-value: 0.36 trend: no trend
Dry season average discharge (m³/s)	p-value: 2.2e-05 trend: decreasing	p-value: 0.02 trend: decreasing	p-value: 1.07e-03 trend: decreasing	p-value: 5.96e-04 trend: decreasing

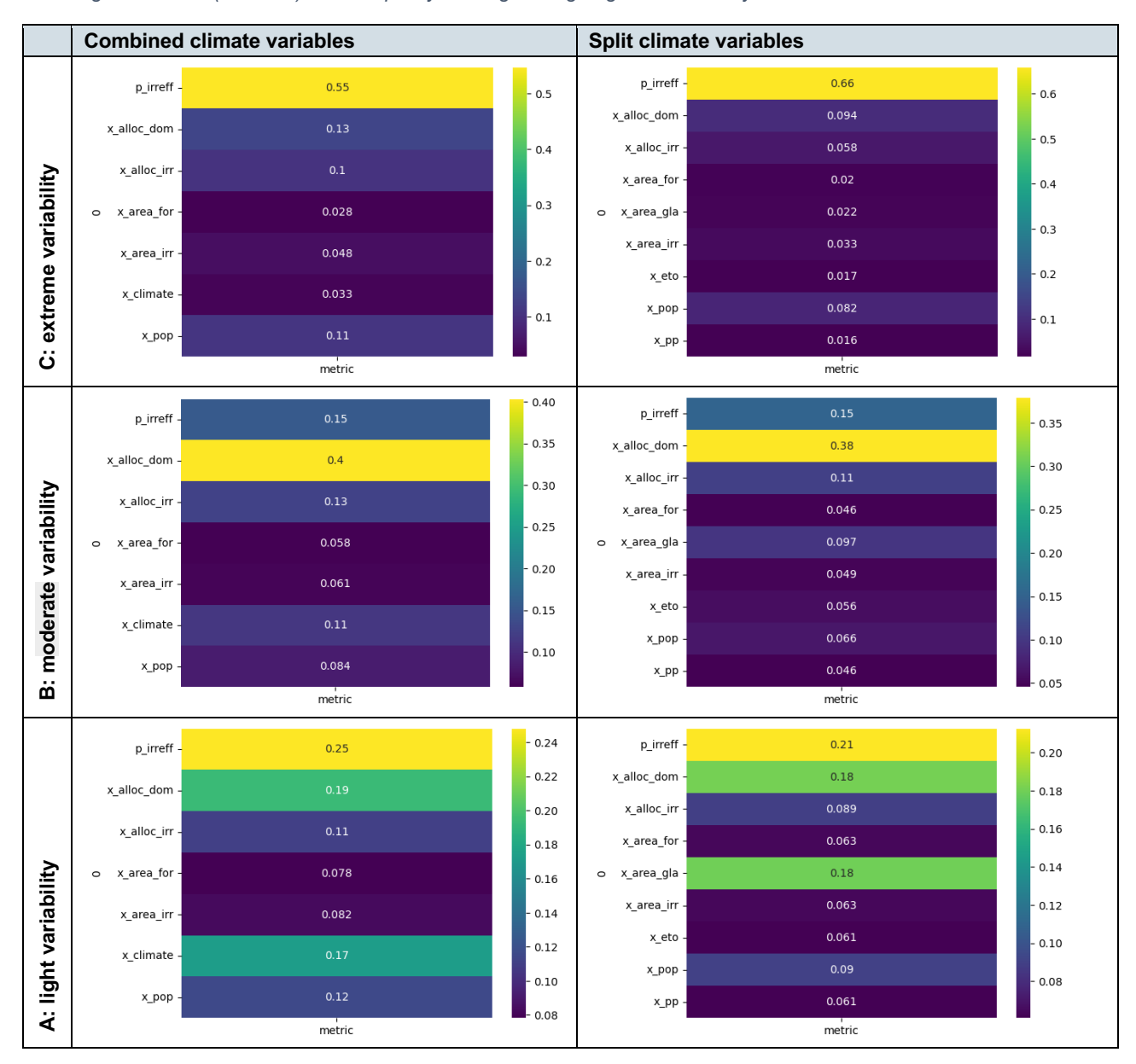
Table 8: P-values for testing statistical significance and post hoc test results are reported for significant findings, with a significance level of $\alpha = 0.05$ for all tests.

Climate variable	Statistical difference?	Post-hoc test	
Annual average discharge (m³/s)	Welch's ANOVA p-value: 0.98 significant difference: NO	-	-
Dry season average discharge (m³/s)	Welch's ANOVA p-value: 4.46e-26 significant difference: YES	Games-Howell Historical – SSP 1-2.6: Historical – SSP 3-7.0: Historical – SSP 5-8.5:	significant p-value 5.14e-10 6.58e-12 8.12e-12

5.2. Stress testing: Sensitivity Analysis operationalized with Feature Scoring

5.2.1. Impacts of irrigation efficiency and uncertainty variables on the water balance

Table 9: Results from Feature Scoring according to the applied script (combined climate variables / split climate variables) and range scenarios (A / B / C) with the policy leverage being irrigation efficiency.



The heatmaps in Table 9 rank the uncertainty and policy factors according to their influence on all metrics across the 6000 simulations. Comparing the left and right columns, it can be said that the two different ways of handling the climate data – either as aggregated climate scenarios (differentiated in the script by scenario-GCM combination) or as split components (glacier area, evapotranspiration, precipitation), which can be linked together in the EMA simulations regardless of their scenario-GCM affiliation – have little to no impact on the ranking of the factors. For this reason, the differentiation is not shown in the further results, and the split version is preferred as it shows the main influencing component of climate uncertainty. It should be noted that the overall influence of climate results from the interaction of the three variables, i.e. the interaction of the three Feature Scoring values.

Moreover, Table 9 confirms that the ranges of uncertain variables, as outlined in the TMIP-EMA documentation (Newman and Milkovits, 2021a), influence the Feature Scoring outcome. Specifically, irrigation efficiency significantly impacts the metric in range definitions A and C, while domestic allocation notably affects the metric in range definition B. As this does not give insights into key drivers of water scarcity in specific, another Feature Scoring has been conducted to specifically focus on experiments that are defined as situations of water scarcity.

5.2.2. Impacts of irrigation efficiency and uncertainty variables on water scarcity

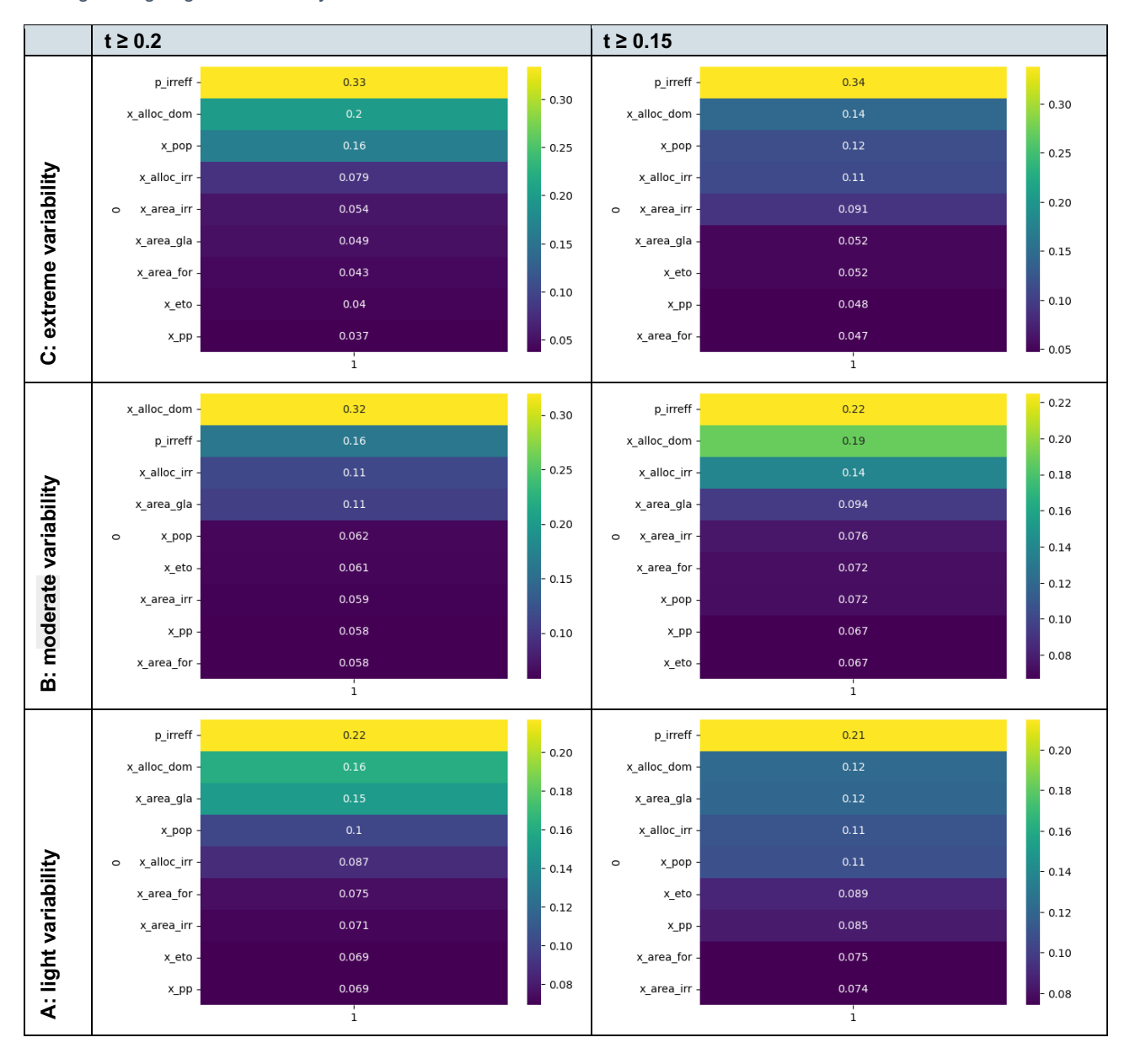
As stated in 5.2.1., only the results of the split climate variables are shown henceforth. In contrast to 5.2.1., a binary classification can be introduced in the Feature Scoring by a threshold value to divide the metric values into those indicating water scarcity and water availability. The current Feature Scoring value in this subchapter thus shows the most influential input parameters on the metric values that are equal to or higher than the threshold. To clarify, a threshold \geq 0.2 means that 20% or more of the time, supply does not meet 90% or more of the demand. For the interpretation, it is also important to mention that the threshold of \geq 0.15 represents a more stringent definition of water scarcity.

Table 10 demonstrates that the threshold value proposed by Kalra et al. (2015) (\geq 0.1) is not applicable to the local context. This is because almost all experiments in range definitions A and B would be classified as water-scarce with this threshold, which impedes the Feature Scoring algorithm from providing insights. Therefore, it is necessary to select a threshold that avoids universal system failure. Consequently, thresholds of \geq 0.2 and \geq 0.15 will be applied comparatively in subsequent analyses. However, it is important to note that these thresholds do not necessarily represent acceptable water supply situations, as they have not been chosen based on stakeholder perceptions or analysis of societal preferences. Instead, they represent artificially defined thresholds for the purposes of this study.

Table 10: Number and share of experiments considered as water-scarce depending on threshold setting and range setting.

	t ≥ 0.2	t ≥ 0.15	t ≥ 0.1
# experiments considered water scarce	C: 2447, 41%	C: 4018, 67%	C: 5641, 94%
	B: 4387, 73%	B: 5718, 95%	B: 5995, 100%
	A: 3434, 57%	A: 5547, 92%	A: 6000, 100%

Table 11: Results from Feature Scoring with $t \ge 0.2$ and $t \ge 0.15$ according to the range scenarios (A / B / C) with the policy leverage being irrigation efficiency.



When trying to identify the factors within the social-ecological system of the Quillcay catchment that drive water scarcity based on the results in Table 11, two things are striking. First, irrigation efficiency is the most influential factor on water scarcity time series in all threshold-range definition combinations, except for 0.2-B (threshold ≥ 0.2 , range definition = B) where domestic allocation becomes more important. Second, it is found that the climate scenarios become more important as the adaptation options and the potential evolution of uncertainties become narrower. In particular, the glacier

area has the greatest influence on water availability. A more detailed analysis of the hydrological model provides insights into the underlying factors explaining these observations.

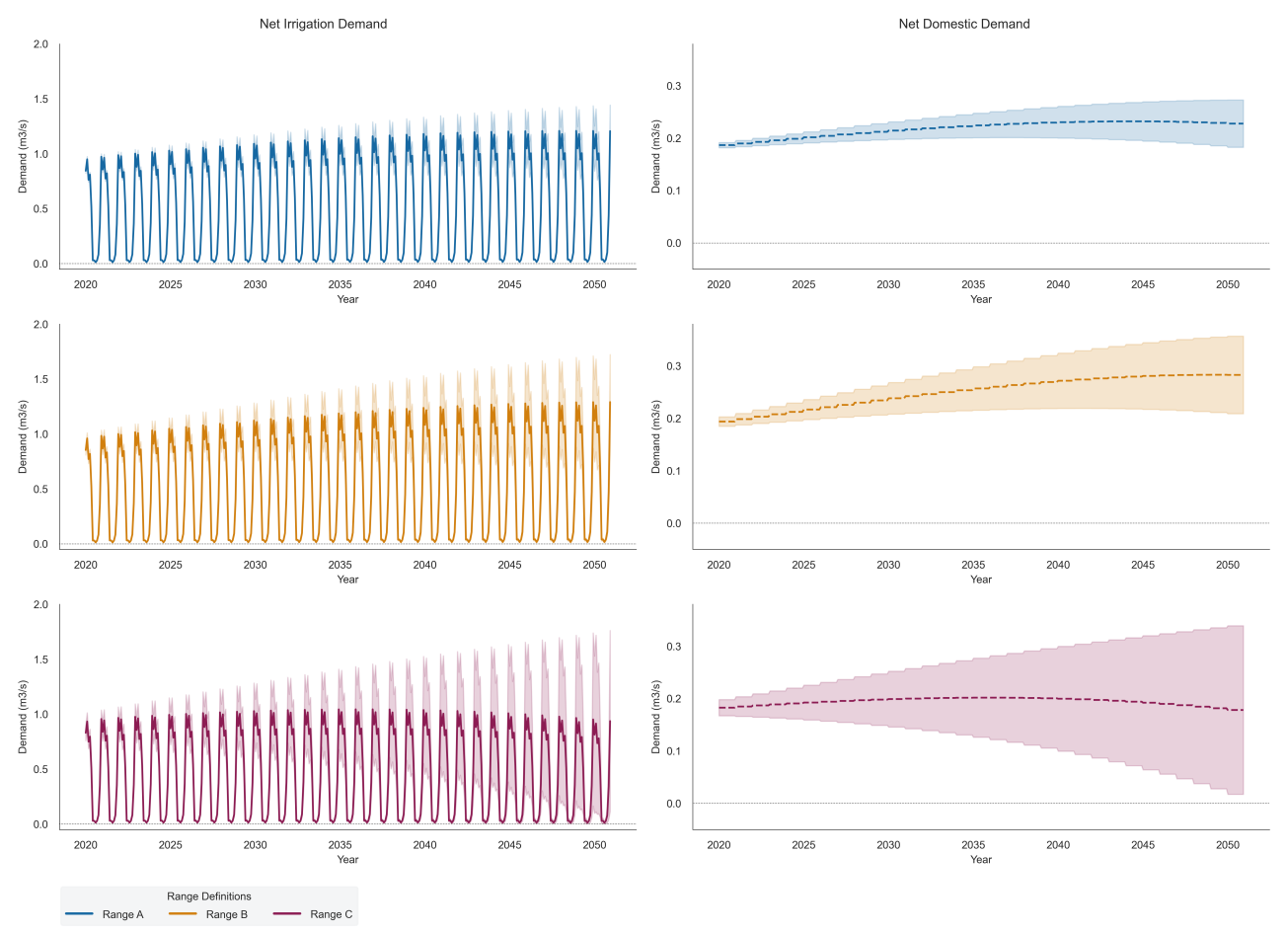


Figure 25: Comparison of water demand based on sectors from 2020 to 2050 (L = irrigation efficiency). The bold line represents the average of all monthly simulations, whilst the shaded areas illustrate the standard deviation.

Based on the input data, the domestic water demand remains constant on a seasonal basis but increases or decreases annually depending on the applied range definition. In contrast, irrigation demand shows a clear seasonal variation, with higher demand during the rainy season, when more crops are typically grown, compared to the dry season (Quesquén Rumiche, 2008). This pattern is evident in Figure 25, where irrigation demand decreases significantly during the dry season. When comparing net irrigation demand to net domestic demand, irrigation demand during its peak months can be up to five times higher than domestic water demand. However, between June and October, this proportion drops drastically, making net domestic demand more significant than net irrigation demand (cf. Figure 26). The concerned months with a more important domestic demand are the same for the entire study period and in all the range scenarios analyzed. Considering the metric logic, four out of the five months that contribute to the metric are dominated by net domestic demand. As a result, at a higher threshold (≥ 0.2), water scarcity is more likely to result from unmet domestic demand. Conversely, with a lower threshold, which reduces the frequency of unmet demand required to be classified as water scarce, even a small deficit – such as one caused by irrigation during

its single dominant month — can lead to water scarcity. This in turn increases the Feature Scoring value of irrigation demand. This dynamic explains why, in Table 11, domestic water allocation becomes less important under range definition B when water scarcity definition is more stringent (horizontal axis). On the vertical axis ($t \ge 0.2$) of Table 9, when changing the range definition from B to A, irrigation efficiency emerges as the most significant factor. This occurs because the upper limit of the domestic water allocation range is reduced, while the lower limit remains unchanged. In contrast, for the agricultural allocation range, both the upper and lower limits are narrowed, e.g., agricultural practices may shift to either less water-efficient or less water-intensive crops compared to Range B. These adjustments affect water availability in different ways. For domestic water allocation, narrowing only the upper bound favors water availability. However, for agricultural water allocation, reducing both limits has mixed effects: it can improve water availability in some cases, but also cause water scarcity in others. As a result, irrigation efficiency plays a critical role in offsetting these changes in agricultural allocation, making it the most important factor influencing water scarcity in range definition A (see Table 10). This change to range definition A also results in less cases of system fails (cf. Table 10).

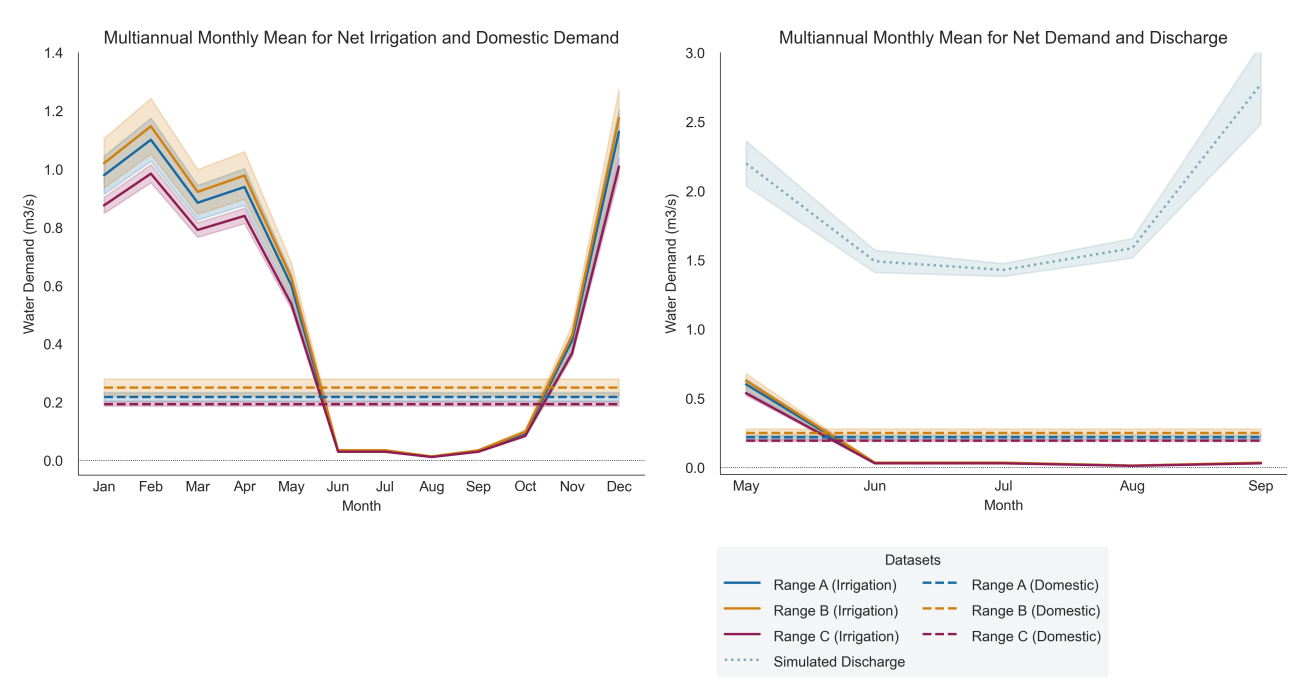


Figure 26: Comparison of water demand (multiannual monthly mean) based on sectors of all simulations from 2020 – 2050. The bold line represents the average of all simulations, whilst the shaded areas illustrate the standard deviation.

The second observation highlights the importance of glacier area in contributing to water scarcity as the range definitions of socioeconomic factors become less extreme, indicating that the potential for socioeconomic change is narrowing. Given that the climate scenarios are the same in range definitions A, B, and C, it makes sense that the weight of glacier area increases. It is important, however, to clarify: Out of the three climatic variables – evapotranspiration, precipitation, and glacier area – the latter is clearly the dominant factor. Since glacier area is delineated based on temperature data,

this not only suggests that future temperature scenarios contribute to a decrease in glacier area, but also that glacier area becomes a critical driver of water scarcity. However, this approach does not provide information on the relative contributions of precipitation- and temperature-induced melting and thus on the contribution of these climatic factors to water scarcity. A comparison of precipitation and temperature data shows a clear positive trend in temperature, while precipitation exhibits only a minor increase (cf. Figure 27, cf. 9.2.). The presence of a clear temperature trend leading to a reduction in glacier area, combined with the consistently high contribution of glacier meltwater to total dry season runoff, highlights the critical role of glacier area as a key driver of water scarcity.

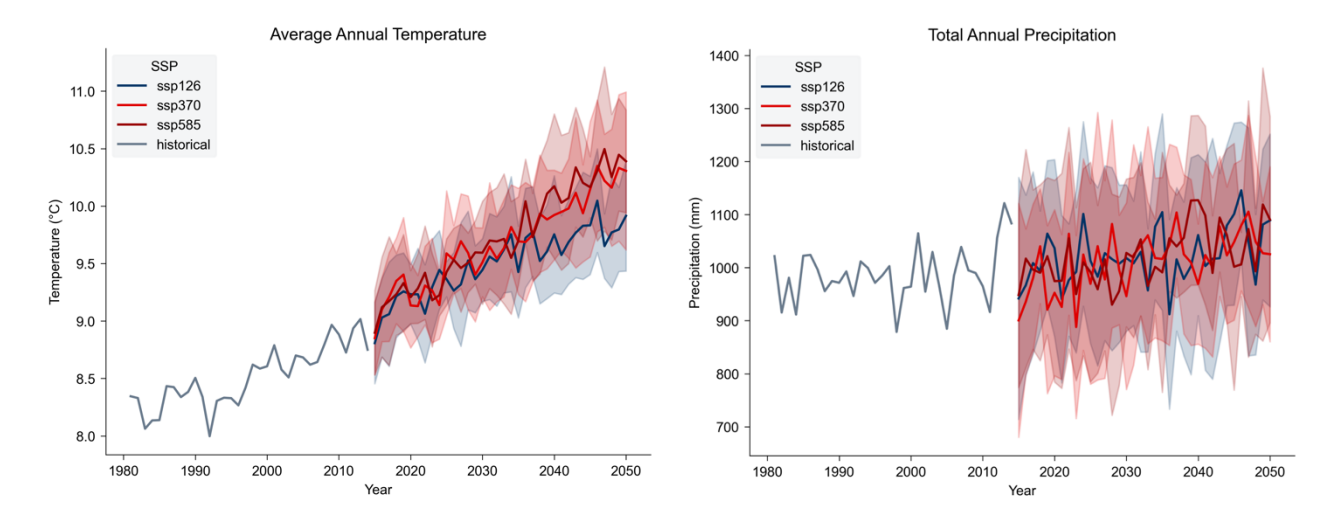


Figure 27: Historical and future total annual temperature, precipitation based on the three different climate scenarios. In both figures, the bold line represents the GCM average derived from the three climate scenarios (SSP1-2.6, SSP3-7.0, and SSP5-8.5), whilst the shaded areas illustrate the standard deviation from the climate models used for each climate scenario (own illustration).

5.2.3. Impacts of domestic efficiency and uncertainty variables on water scarcity

Table 12: Number and share of experiments considered as water-scarce depending on threshold setting and range setting.

	t ≥ 0.2	t ≥ 0.15	t ≥ 0.1
# experiments considered as water scarcity	C: 4061, 68%	C: 5395, 90%	C: 5966, 99.4%
	B: 5100, 85%	B: 5958, 99.3%	B: 100%
	A: 4447, 74%	A: 5988, 99.9%	A: 100%

t ≥ 0.2 t ≥ 0.15 p domeff 0.44 p domeff 0.22 0.40 x alloc dom x alloc irr 0.35 0.18 0.087 x pop x alloc dom 0.30 Extreme variability 0.16 0.067 x alloc irr x area irr 0.25 0.14 0.086 x area irr 0.053 x eto 0.20 x area gla 0.045 x_pop 0.12 0.15 x_area_for 0.038 x_area_gla 0.067 0.10 0.037 x_eto x_pp 0.061 0.08 x_pp 0.035 x_area_for 0.059 0.05 ن i i x alloc dom p domeff 0.18 0.250 x_alloc_irr x_alloc_dom 0.16 0.225 x_alloc_irr x_area_gla Moderate variability 0.14 p_domeff x area for 0.089 0.175 0.078 o x area gla x pp 0.12 x area for 0.078 0.150 х рр 0.096 0.10 x_area_irr x_eto 0.125 0.08 0.069 x pop gog x 0.100 0.068 0.055 x area irr x eto 0.075 0.06 ä i í x_alloc_dom 0.19 p_domeff 0.24 0.18 0.225 0.200 x alloc irr x alloc irr 0.175 x_pp 0.14 Light variability 0.150 x_pop x_area_gla x_eto x_alloc_dom 0.12 0.125 x_pop x_pp 0.100 0.10 x area in x_area_irr 0.075 x_area_for ä

Table 13: Results from Feature Scoring with $t \ge 0.2$ and $t \ge 0.15$ according to the range scenarios (A / B / C) with the policy leverage being domestic efficiency.

When changing the policy lever from irrigation efficiency to domestic efficiency, the same pattern in the share of unmet water demand across all experiments is observed (cf. Table 12). For a threshold of $t \ge 0.15$ in the range definitions A and B, more than 99% of the experiments have a metric exceeding the threshold. Therefore, these results should be interpreted with caution as they may not be meaningful.

In examining domestic efficiency, it becomes evident that it can be an important contributor to water scarcity (cf. Table 13). This is particularly evident when no threshold is set, where it can be identified as a pivotal driver of both water scarcity and availability. But it also holds true for a part of runs with a threshold. Given that current domestic efficiency is already high at 76%, the potential for change, whether positive or negative, is relatively limited in ranges definitions A and B. Consequently, this policy lever is relatively unimportant in these cases, and domestic water allocation, for example,

compensates with its broad range and hence becomes more significant. Therefore, the effectiveness of the adaptation measure is relatively low. This insight also motivates a prioritized focus on irrigation efficiency, as there is limited room for improvement in domestic efficiency.

5.3. Stress testing: Scenario Discovery operationalized with PRIM

In this section, the experiments are examined to derive insights from the analysis. As discussed in section 5.2.2., the chosen ranges and the threshold for distinguishing between intolerable and acceptable conditions are crucial. Therefore, it is assumed here, that the thresholds and ranges have already been intentionally selected. However, the large number of different runs, characterized by varying adaptation policies and different ranges of uncertain variables, results in a diverse set of outcomes that fail to provide a clear or consistent understanding of the conditions under which water scarcity occurs in the Quillcay catchment. This section consists of findings that are consistent with existing knowledge and examples that suggest areas for further investigation.

5.3.1. Threshold sensitivity shaping non-operational ranges

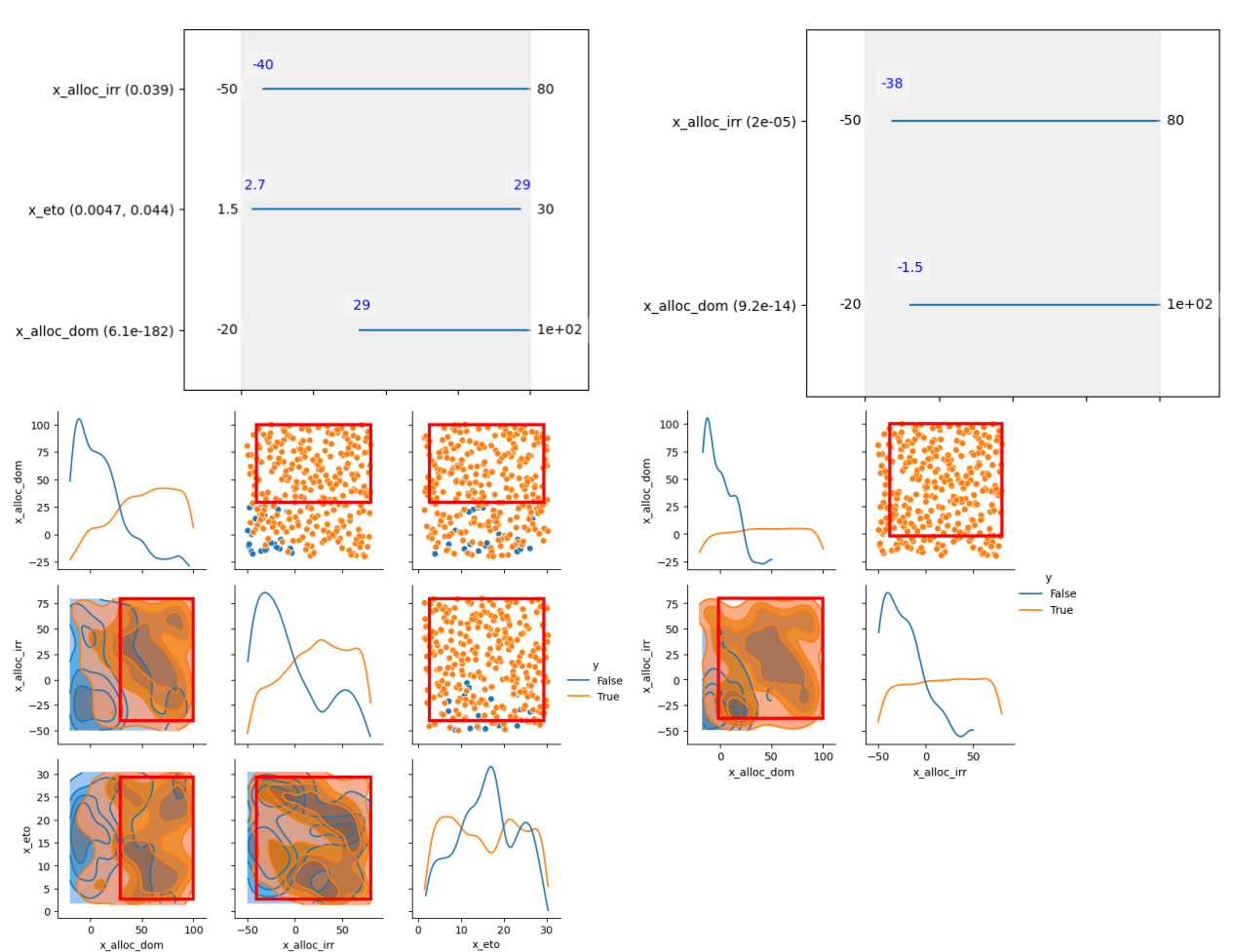


Figure 28: Scenario discovery outputs showing non-operational ranges on the upper horizon and pair scatter (range scenario B. left: $t \ge 0.2$ with coverage = 0.648 and density = 0.947; right: $t \ge 0.15$ with coverage = 0.79 and density = 0.982). The term True is counterintuitive, meaning successful or metric outcomes above the threshold.

When the definition of water scarcity is applied more stringently with a lower threshold value (cf. Figure 28, left), the non-operational range widens. In the figure for non-operational ranges, it is evident that the non-operational range of domestic water allocation is most sensitive to changes in the threshold. When water scarcity is defined more restrictively, water scarcity consistently occurs when domestic water allocation increases. At the same time, irrigation allocation can vary between -38% and 80%. Under this more restrictive threshold, almost 80% of all experiments classified as water scarce are explained by a non-operational range for domestic water allocation from -1.5% to +100% and irrigation allocation from -38% to 80%. For these restricted experiments, 98% were classified as water scarce.

In the non-operational range on the left (cf. Figure 28), the uncertainty variable of evapotranspiration is minimally restricted. This suggests that, in some cases, there are no informative results for a specific variable, as is the case here for evapotranspiration.

5.3.2. The lack of informative results

An example of this can be observed in the irrigation allocation and evapotranspiration variables (cf. Figure 28), which are minimally restricted, suggesting that they are not significant drivers of water availability or water scarcity. However, the scatter plot still indicates that, for evapotranspiration from the SSP3-7.0 scenario, a substantial number of cases of water availability are recorded. Furthermore, it is noteworthy that, the introduction of a fourth restricted variable leads to the loss of statistical significance. Therefore, it is crucial to select the box based on the variables and their informativeness and statistical significance to ensure that the analysis provides meaningful and reliable results.

5.3.3. Unrealistic operational ranges

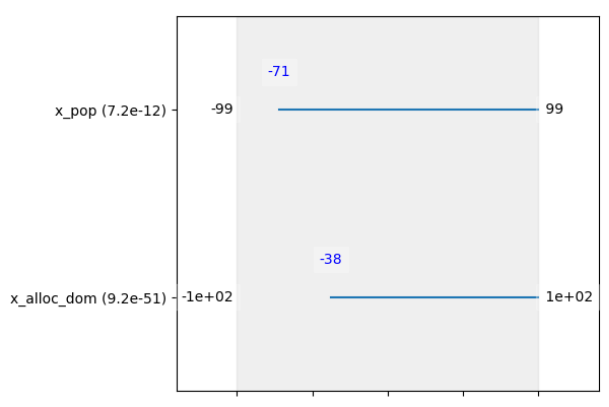


Figure 29: Scenario discovery outputs showing non-operational ranges (range scenario C, $t \ge 0.2$ with coverage = 0.819 and density = 0.588).

This specific box (cf. Figure 29) exhibits non-operational ranges for population growth between -71% and 99%, and for domestic allocation between -38% and 100%. Given the comparison with SSP population projections for Peru (IIASA, 2018), the value of -71% is clearly outside the realm of possibility, and a 38% reduction in water consumption is unlikely, as it falls below the WHO's declaration

value for optimal access to water (Howard et al., 2020). Consequently, these socioeconomic uncertainties can be regarded as key drivers of water scarcity, which are also likely to represent limits to adaptation due to their unrealistic ranges within this box. However, it is also necessary to take into consideration the density of the area, which reveals that, within the restricted space of the box, only 59% of the experiments indicate water scarcity, while 41% show water availability.

5.3.4. Interactions between adaptation measures and socioeconomic uncertainties

In contrast to Figure 29, a different box is analyzed in Figure 30, with different coverage and density. In addition to the socioeconomic uncertainties, which are unlikely to transition into the operational range, the adaptation measure of irrigation efficiency now becomes more important. In 60% of the experiments where the system fails, low irrigation efficiency combined with a relatively wide range of population and domestic allocation changes explains the outcome. The non-operational range for the socioeconomic uncertainties remains within the ranges defined in A and B and is therefore likely to be reached in the future. Consequently, it can be concluded that water scarcity in the catchment is likely to occur under numerous socioeconomic and climatic scenarios unless irrigation efficiency increases from the current 35% to 62%. According to the simulations, there is a 76% probability that water scarcity will occur under these conditions.

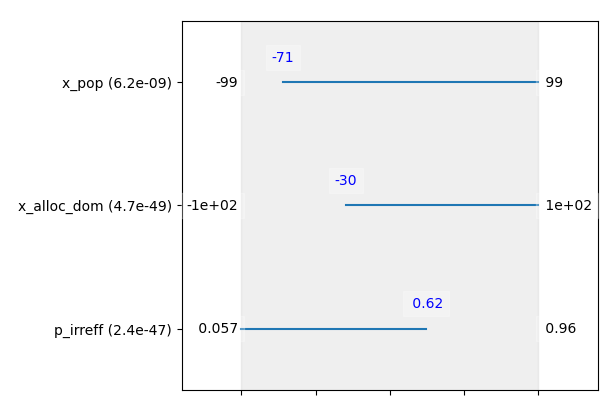


Figure 30: Scenario discovery outputs showing non-operational ranges (range scenario C, $t \ge 0.2$ with coverage = 0.603 and density = 0.76).

The scatter plot (cf. Figure 31) clearly shows in the density plots that as irrigation efficiency increases, the number of cases of water scarcity ("True") decreases. In contrast to that, with a more positive growth of population and domestic allocation the cases of water scarcity increase.

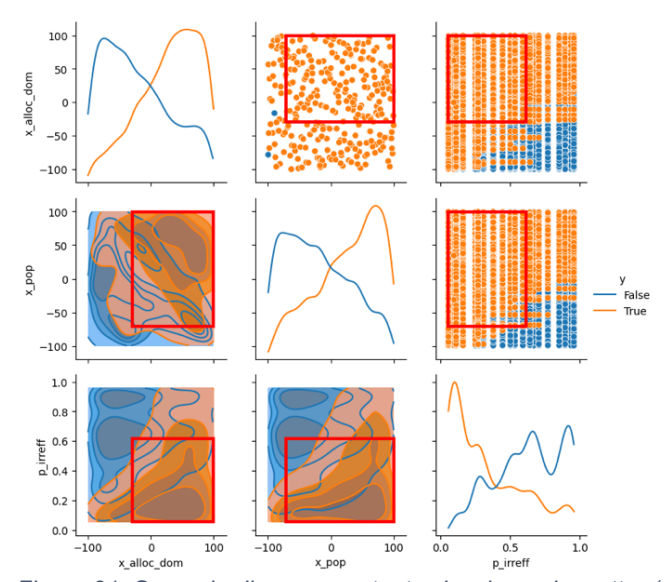


Figure 31: Scenario discovery outputs showing pair scatter (range scenario C, $t \ge 0.2$). The term True is counterintuitive, meaning successful or metric outcomes above the threshold.

5.3.5. Interactions between adaptation measures and climatic uncertainties

In Figure 32 and 33, climate scenarios become significant, which is consistent with the findings in section 5.2.2., when the ranges are defined based on range definition A. It is important to note that the values for glacier area in the graph in Figure 33 do not directly correspond to the actual glacier area but instead represent the file number associated with the combination of climate scenario and GCM. Specifically, SSP1-2.6 is represented by values 1-10, SSP3-7.0 by values 11-20, and SSP5-8.5 by values 21-30. Thus, it can be concluded that within the non-operational range of SSP3.70 to 5.85 and an irrigation efficiency below 50%, water scarcity is likely to occur. However, the coverage and density analysis show that not all cases within these conditions lead to water scarcity, as only 63% of the experiments in this box have a metric indicating water scarcity. Interestingly, a restricted glacier area variable does not appear with a smaller threshold than the one chosen here. Understanding the reasons for this would require further research.

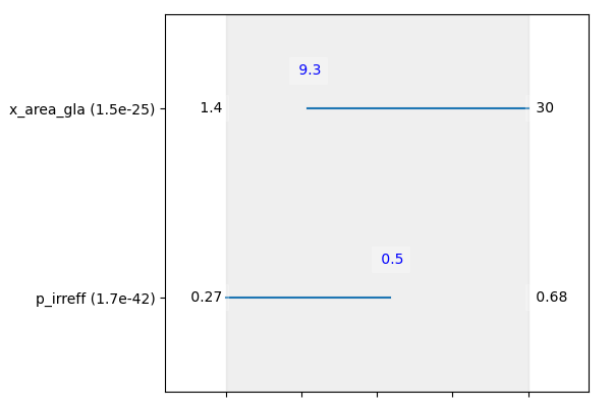


Figure 32: Scenario discovery outputs showing non-operational ranges and pair scatter (range scenario A, $t \ge 0.22$ with coverage = 0.630 and density = 0.634).

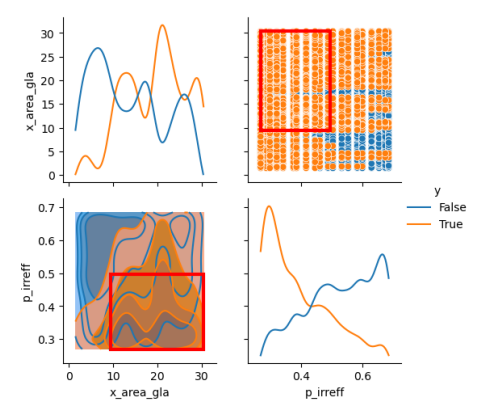


Figure 33: Scenario discovery outputs showing pair scatter (range scenario A, $t \ge 0.22$). The term True is counterintuitive, meaning successful or metric outcomes above the threshold.

6. Discussion

The discussion builds on the findings from the case study in the Quillcay catchment, as well as from the iterative learnings from the operationalization and is presented in a structured manner, aligning with the thematic focus of the research questions. Specifically, it examines the identified key drivers of future water scarcity in the case study (sections 6.1.1., 6.1.2.), the limitations of EMA's operationalization in the case study (section 6.2.1.) and its implications for EMA's general boundaries derived from the case study (section 6.2.2.). Finally, it addresses the broader conceptual question of advancing adaptation limit and risk assessment using EMA (section 6.3).

6.1. Factors driving water scarcity and potential adaptation limits in the Quillcay catchment

6.1.1. Insights from the Sensitivity Analysis

The identified stressors driving water scarcity in the study area change with different range definitions of the uncertain variables and with varying thresholds. Yet, the impact of the adaptation measure, whether it is improving domestic water use efficiency or irrigation efficiency combined with domestic water allocation, consistently proved to be of undeniable importance (cf. section 5.2.1. -5.2.3.). The dynamic interplay between adaptation measure and domestic water allocation is explained in section 5.2.2., emphasizing how it is shaped by two key elements: the definition of the range and the threshold for determining when the frequency of water shortages becomes intolerable. Moreover, as the socioeconomic uncertainty ranges become narrower (e.g. range definition A), climatic factors, particularly glacier area, become more important (cf. section 5.2.2.). This finding aligns with the conclusions of Buytaert and Bièvre (2012), who found that glacier retreat may have a relatively limited impact on water supply compared to other factors, like demographic changes. However, their analysis focused on a downstream region, specifically the city of Lima, which is different from the conditions analyzed in the Quillcay catchment. In general, as Hock et al. (2019) have indicated, future increases in water demand due to population growth and other socioeconomic factors are foreseen to outweigh the effects of climate change-induced alterations on water accessibility. Nevertheless, the results provided by the Feature Scoring allow to relativize this: Population growth is not the primary driver. Instead, water use efficiency, domestic and irrigation allocations also have a significant impact. The influence of climate should not be underestimated, as more realistic socioeconomic scenarios are narrower (range definitions A and B) and, in these cases, the glacier area represents one of the dominant driving factors.

6.1.2. Insights from the Scenario Discovery

In the scenario discovery in section 5.3.4 (range definition C) it is noted that the adaptation measure irrigation efficiency plays an important role in overcoming or causing water scarcity. The PRIM analysis cannot identify specific constraints that hinder improvements in irrigation efficiency. However, these constraints could potentially include financial limitations, cultural barriers, or a lack of information. Such factors may impede adaptation efforts and could quickly evolve into significant limitations. Furthermore, other socioeconomic uncertainties that are identified to be decisive factors in non-operational scenarios, i.e. restricted in PRIM, must be considered. For example, as discussed in section 5.3.4., domestic allocation has the potential to outweigh adaptation efforts. Even with irrigation efficiency improved to 62% compared to current levels, water scarcity still occurs in 72% of these experiments due to simulated population growth and domestic water allocation. In the scenario discovery in section 5.3.5. (range definition A), it is found that in the majority of experiments where irrigation efficiency was below 50%, more pessimistic climate scenarios lead to system failure. In such cases, it can again be assumed that constraints restrict the adaptation of irrigation efficiency to below 50%, which leads to a limit to adaptation if it cannot be overcome. In addition, based on the scenario discovery results, climate uncertainties contribute to water scarcity and may offset some of the benefits of adaptation measures.

The comparison between domestic efficiency and irrigation efficiency revealed that climate scenarios become more important as the ranges of uncertainties that have a positive impact on water availability narrow and the room for adaptation decreases. E.g. for the domestic sector, where current efficiency is already high (76%), there is limited potential for further improvement, which reduces the effectiveness of this policy: increases in domestic water allocation cannot be mitigated by efficiency improvements. In both cases – irrigation efficiency and domestic water use efficiency – the importance of climatic factors becomes more pronounced, which explains why climate scenarios, more specifically glacier area is a restricted variable in section 5.3.5.

6.2. Limitations of integrating EMA to identify key drivers of water scarcity

6.2.1. Adapting EMA to the Quillcay catchment: assumptions and their limitations

Assumptions and limitations in the input data

In general, data scarcity is responsible for the uncertainty of the input data or input range. First, the aggregation or collection of data on a large scale can obscure regional trends. For the Quillcay catchment, SSP scenarios were derived from datasets containing population data at the national scale (Peru) and cropland data at the continental scale (Latin America). The impact of small-scale developments, such as rural-urban migration or abandonment of farmland, are not considered. In contrast, an attempt has been made to adapt the SSP scenarios to possible regional change

scenarios in the case of forest area. However, this was not done for population and cropland, which may have resulted to different ranges of future scenarios. Similarly, the historical socioeconomic data downscaled from the district level to the catchment level is equally subject to limitations in precision. Some additional efforts have been made to uncover the regional trends, e.g. with the statistically downscaled CMIP6 climate projections, which bridge the gap between coarse GCM resolutions and finer regional requirements. Nevertheless, they also show a small shift in seasonality from the observed data in the PISCO dataset. Second, as the study area is in a region with limited data availability, it was required to consider data from different regions, such as different climate zones, as was the case with the uncertainty of the transition to commercial crops. In terms of the Quillcay catchment, it is unclear what the impact on water demand will be, and it is also unclear how intensive the trend of transition to commercial crops will prevail in the region. Third, certain components of the hydrological model were approximated using formulas and calculations. In some cases, the approximations may not be significant, for instance, in the case of evapotranspiration, which is not a primary factor influencing discharge. In other cases, the approximations could be improved by further refining the input data. In general, however, if realistic ranges are appropriately defined, the EMA method effectively minimizes the impact of uncertainty associated with the input parameters X and L.

Possible modifications of the input data

For the defined inputs, several potential modifications or extensions could enhance future research. First, environmental flow requirements could be integrated into the analysis as part of water demand, varying as an uncertainty depending on different estimation methods. Although evaluating the suitability of these estimation methods lies beyond the scope of this thesis, incorporating them in future studies could provide a more comprehensive perspective. Second, defining input parameters within the XLRM-framework poses challenges, particularly when classifying them as either uncertainties or levers. For instance, socioeconomic variables such as forest area, agricultural water allocation based on crop types, and domestic water allocation could also be framed as policy levers. In this study, however, only one parameter is treated as a policy to maintain focus on identifying adaptation limits. Third, agricultural water demand, depending on agricultural practices could be refined by accounting for the growing seasons of dominant crops. Last, the implementation time of publicly funded policy projects and its impact on the water balance is not currently captured in the input parameters. Including implementation times, either as uncertainties or levers, could significantly improve the model's representativeness and applicability. These considerations highlight avenues for improving the foundation of the catchment-specific framework.

Implications of the chosen hydrological model

Another key factor in structuring the analysis is the choice of the hydrological model, as it defines spatial and temporal characteristics of the modeled discharge. The used lumped model in the case

study provides insights into monthly runoff while disregarding spatial distribution. On the one hand, neglecting the spatial dimension creates a blind spot for understanding spatial patterns inside of the catchment. For instance, if there are informal settlements that often have no access to public water distribution (Drenkhan et al., 2015), this could lead to a higher vulnerability of this marginalized group, which is often affected by maladaptation (IPCC, 2022a). As a result, an increase in domestic water efficiency alongside an overall increase in allocations may fail to address informal settlements, leaving their populations vulnerable, and such potentially intolerable risks may go undetected due to insufficient spatial resolution of the model. Furthermore, the spatial distribution of irrigation points may also be of importance, to avoid maladaptation and contribute to climate justice. However, due to the low number of required input parameters in the context of data-scarce mountain regions, this model still represents a viable choice for the relationship (R). On the other hand, the crops' susceptibility to water stress fluctuates significantly depending on the specific growth stages they are in (Terán-Chaves et al., 2023), hence the temporal dimension is also important. Since the Shaman only models monthly discharge, the resulting metric cannot capture these critical periods in detail, potentially overlooking important short-term drought impacts on crop growth. In addition to spatial and temporal characteristics, the prioritization of human water uses and management in the applied model deserves attention: Scott et al. (2021) suggest the use of a more holistic model that integrates societal and ecological dimensions of water security to reduce the trade-off between human and environmental water needs. In this case study, this would entail placing greater emphasis on environmental flow requirements, as outlined in the discussion on modifications to input data. This integrated approach promotes equitable water management and highlights synergies, such as ecosystem services, that benefit both people and the environment (Scott et al., 2021). Moreover, Muñoz et al. (2024b) consider the use of socio-hydrological models to integrate a more expansive array of socioeconomic factors, thus allowing, for instance, the assessment of governance strategies. In conclusion, while the lumped hydrological model serves as a practical tool for data-scarce regions, the integration of more spatially and temporally detailed approaches, along with the consideration of environmental and socioeconomic factors, would provide a more comprehensive and equitable assessment of water security challenges.

Limitations of the metric and thresholds

The manner in which water availability is quantified, that is to say, the definition of the metric, is of significant consequence in the context of EMA (Kwakkel and Pruyt, 2013; Marchau et al., 2019). The following limitations of the metrics applied in the case study have been identified: One such limitation lies in the definition of the dry season from May to September, which is at this point static. However, as highlighted by Giráldez et al. (2020) the onset of the rainy season is the most decisive factor in the rainfed agriculture in the study area of Mantaro river basin (Ayacucho), a pattern that can similarly be assumed for the study area due to comparable climatic and agricultural conditions. Since the

determination of dry and rainy season is quite complex, this has not been implemented. A further challenge is to take local realities into account to create meaningful outputs. Another limitation lies in the way the severity of water scarcity was defined. This assumes that at least 90% of the water deficit must be saturated, based on a recent report on public water access. However, this threshold does not necessarily reflect what is acceptable. The dimension of social justice should also be taken into account and integrated into the metric (Juhola et al., 2024). Finally, the metric currently only accounts for water availability. Yet, according to interviews with locals and practitioners, one of their main concerns regarding secure water access is water quality (Hagen et al., in review; Singer et al., 2017). Lakes and rivers of the regions are contaminated through heavy metals mainly due to acid rock drainage that is caused by glacier retreat (Burns et al., 2011; Santofimia et al., 2017; Garcia et al., 2023). Lake Palcacocha is already showing the first signs of acidification, which could lead to a severe supply shortage for the city of Huaraz in the short term (Hagen et al., in review). Moreover, water quality is also affected by extreme rainfall events that cause turbid water, according to the residents interviewed (Hagen et al., in review). Therefore, it is crucial to create a metric for water quality as well as to assess limits to adaptation in the Quillcay catchment.

Another critical aspect is the creation of an inclusive and context-specific thresholds. For example, Kalra et al. (2015) defined a threshold of 10% developed in collaboration with local authorities in Lima. Conversely, in the case study of the Peruvian Andes, some simulation runs showed that there is no experiment where water demand can be met 90% of the time, highlighting the need for context-specific thresholds and the involvement of local stakeholders.

Implications of using different range definitions

The implementation of three different range definitions provides valuable insights into how different stakeholder perspectives are translated into EMA. As discussed in sections 5.2.1. to 5.2.3. range definitions considerably affect the identified driving factors, a result that deserves further consideration. Muñoz et al. (2024b) highlight that the strength of EMA lies in its ability to utilize broad ranges, making it a viable and realistic option for data-scarce regions like the Peruvian Andes. Extending ranges to extreme values can be beneficial for understanding the full spectrum of operational and non-operational ranges. However, when interpreting the results, it is essential to consider what ranges are achievable or realistic to obtain meaningful insights into drivers and potential limits to adaptation in the future. Furthermore, it should be noted that the importance of the five driving factors (efficiency, domestic and irrigation allocation, population, and glacier area) changes with different ranges, influencing the non-operational spaces that can be explored. Therefore, setting realistic ranges wherever possible is essential to gain accurate and actionable insights.

Limitations in the integration of stress testing

During the integration of stress testing the benefit of adding a threshold to the Feature Scoring has become evident due to two reasons. To begin with, when the standard Feature Scoring approach is applied, the results highlight the driving factors that influence the metric in general. However, when a threshold is introduced, as outlined in section 5.2.2., the results focus specifically on the driving factors within the social-ecological system of the Quillcay watershed that directly contribute to water scarcity. In addition, the application of different thresholds reveals the dynamic interplay between sectoral demands and their dominance over net water demand, which shapes the drivers of water scarcity. For example, as shown in the same section, the temporal aspect of the threshold, i.e. the frequency of water scarcity, highlights in range definition B a shift in dominance from the domestic water sector to the agricultural sector. Finally, it is important to note that the introduction of a threshold inherently requires assumptions about what constitutes an intolerable level of water unavailability, an issue that will be explored further in the discussion.

Another approach to adapting EMA would be to use the density measure (output of the PRIM algorithm), which is the percentage of successful or unsuccessful experiments, to capture the non-binary nature of risk space. This accounts for the gradual transition from acceptable to tolerable to intolerable risks. Further research could explore the effective implementation and analysis of the density measure.

6.2.2. Boundaries of EMA in the case study: analytical capabilities and constraints

The role of factor selection in shaping EMA's insights and blind spots

Using EMA, researchers must select the factors included in the analysis of water scarcity, which creates the first limitation in its operationalization. The adapted framework is only able to capture water availability, mainly due to the choice of the model and input parameters. However, crucial factors such as water quality are not accounted for in the current framework and might have been overlooked without the local knowledge summarized in the qualitative research by Hagen et al. (in review). Similarly, cultural aspects of water (Drenkhan et al., 2015), as well as the economic and social feasibility of adaptation measures, are excluded from both the model and its associated metrics. Nevertheless, certain challenges, such as the economic feasibility of adaptation measures, have already been addressed in other EMA studies. For instance, Kalra et al. (2015) incorporated economic considerations by including a budget in their analysis and they also propose that water quality should be incorporated into future studies. Moreover, the choice of the adaptation measure also has an impact. As noted by Muñoz et al. (2024b), the implementation of infrastructure measures is easier to assess in hydrological models, whereas others, for example, governance, call for new approaches. Therefore, the inclusion of novel factors in the EMA framework requires collaboration between scientists and decision-makers, which in turn highlights a central aspect of effective water

management (Scott et al., 2021; Muñoz et al., 2024b), but also the need for interdisciplinary collaboration in academia (Berkhout and Dow, 2022).

Finally, it is imperative for the scientific community to exercise caution when proposing predefined adaptation measures that align predominantly with socio-culturally embedded paradigms, such as focusing solely on technical solutions like improving water use efficiency. It is also crucial that marginalized groups, such as smallholder farmers, are given an active role in research processes. Participatory methods should ensure that their voices are heard and that their experiential knowledge and specific needs are incorporated into scientific research and decision-making (Neuburger and Singer, 2016).

Conceptualization of the water scarcity

One boundary of the analytical capabilities of EMA, as applied in this case study, lies in the way the risk of water scarcity is conceptualized. Figure 20 in section 4.3.1. illustrates the logic used in the case study to define intolerable water scarcity. The figure reflects that there is no sharp boundary between acceptable, tolerable and intolerable water scarcity. However, adaptation limits are subjective for different actors (Barnett et al., 2015) and therefore adaptation limits visualized in a schema would take various shapes. Hence, there are no lines added to the figure to indicate limits to adaptation, unlike Figure 3 in section 3.2.1. It is undoubtedly a one-sided and simplified scheme, e.g. when compared to the risk propeller described in section 3.2.2., which emphasizes the interplay between the magnitude of climate hazards, exposure and vulnerability in shaping key risks (O'Neill et al., 2022). Yet, it highlights the boundaries of EMA's adaptation in the context of this study: The black dotted line, representing the possible thresholds, defines the only space, spanned by frequency and intensity, where insights can be gained. Specifically, analysis is limited to the locations of the black dots for a given threshold, despite the risk space being more complex. To summarize, the definition of water scarcity is crucial to the outcome of EMA; thus, it is worth questioning how water scarcity is conceptualized as loris (2012) and Scott et al. (2021) suggest.

Transferability to other fields or regions

Finally, the transfer to fields or regions other than mountain water management involves a re-evaluation, mainly the first step of EMA i) Structuring the analysis with the XLRM-framework; thus, it cannot be directly applied one-to-one. On the one hand, transferability to other fields is possible in principle, but components of the XLRM-framework need to be adapted: uncertainties are defined based on the context of the new field, policy levers depend on feasible adaptation measures considered by policymakers, and the model needs to be able to simulate the relevant process. Similarly, the metric and threshold need to be adapted. In conclusion, while EMA can be transferred to identify key drivers of other climate-related risks and adaptation limits, the general challenges and limitations of the method remain. On the other hand, transferability to other regions to identify key drivers of water

scarcity is given but again requires different adjustments. Due to the variability of hydrological characteristics, researchers must select an appropriate hydrological model, taking also into account the available input data. Different regions present unique modeling challenges, such as data scarcity in mountainous areas. For example, hydrological models for cold regions often do not adequately account for characteristic hydrological processes (Wheater et al., 2022). Similarly, the development of appropriate models for semi-arid and arid regions remains underdeveloped (Daneshmand et al., 2019). Therefore, regional hydrological deficits need to be identified and addressed before transferring this method to another region, as the performance of hydrological models plays a critical role in predicting hydrological changes (Vetter et al., 2017). As in other cases, metrics and thresholds need to be adapted to the specific context. However, before applying EMA to other regions, it would be beneficial to first apply it in a similar approach to another mountainous region, such as the Alps, where more data are available. This would facilitate the setting of ranges and require only one run of the simulations, resulting in a better understanding of the potential of the EMA results and the key drivers derived. In conclusion, the transfer of this method to other regions or fields could enhance understanding of its potential for identifying key drivers of climate-related risks and limits to adaptation. However, despite its numerical output, comparisons across regions or sectors remain infeasible due to the required context-specificity of the analysis.

6.3. Advancing adaptation and risk assessments with EMA: insights and recommendations

Contextualizing EMA findings with local collaboration

A key question that arises is how to contextualize the findings from EMA. By means of the case study, it was found that EMA can identify key drivers of climate-related risks, its non-operational ranges and illustrate situations where adaptation measures interact with climatic or socioeconomic uncertainties, potentially outweighing each other's influence. However, constraints to adaptation cannot be directly identified by the adapted EMA. EMA serves as a tool to explore potential future scenarios, and in collaboration with local researchers and affected stakeholders, it can help identify future constraints that may hinder adaptation, thereby revealing the limits to adaptation. This approach could also help to address skepticism about applying RDM, and thus EMA, in data-scarce countries (Bhave et al., 2016), as robustness can be assessed in a less data-intensive manner by incorporating stakeholder perceptions and expert judgment (Bhave et al., 2014). Therefore, collaboration with local policymakers and researchers is essential to make EMA a valuable tool.

Challenges of limited theory in quantifying adaptation limits with EMA

The integration of EMA with existing adaptation and risk assessment frameworks holds the potential for advancing the understanding and quantification of limits to adaptation. However, the current body

of theory regarding limits to adaptation challenges the development of systematic methods for their quantification. Primarily, the imprecise definition and use of the term "limit to adaptation" complicates its differentiation from a constraint, as it is frequently used interchangeably with "tipping point" or "barrier" in literature (Dow et al., 2013; Barnett et al., 2015; Leal Filho et al., 2021). The IPCC definition is insufficient for the systematic quantification of limits to adaptation, as it lacks a robust framework to systematically address the inherent subjectivity in determining acceptable versus intolerable risks and identifying for whom these judgments apply (Juhola et al., 2024). Second, there is a limited number of case studies on limits to adaptation. For instance, Thomas et al. (2021) found that from their sample of 1682 papers about limits and constraints in social systems, only one percent of the papers included detailed information about limits to adaptation. The existence of a substantial number of qualitative case studies could offer valuable insights and provide a foundational orientation for the subsequent numerical quantification of social factors. The foundational dependency lies in the need for qualitative research on limits to adaptation to provide the necessary context, which is essential for enabling its quantification and the development of a comprehensive, bottom-up methodological approach. In terms of methodology, Juhola et al. (2024) support this observation and state that there is a need for assessment frameworks, methods, and models for adaptation limits to be empirically applied in general. This means that there is also little guidance on good and bad practice for the quantitative approach. This situation, however, should encourage scholars to collaborate across disciplines and initiate the development and refinement of the necessary tools.

Complementing EMA with existing frameworks

Juhola et al. (2024) is one of the few studies that established a framework for assessing limits to adaptation, with potential for integration with EMA. The operationalization of EMA in the case study is characterized by alignment with the framework, while also highlighting areas where further adaptation and risk assessments could fill gaps or provide complementary insights. As demonstrated, EMA has the capacity to link biophysical and socioeconomic data to create quantitative metrics, as suggested by Juhola et al. (2024). Moreover, actors' basic needs can be covered, e.g. in the case study with the aspect of water availability and scarcity respectively. Finally, it can be argued that well-being, an aspect that according to Hagen et al. (in review) must be considered when identifying limits to adaptation, can be included in EMA by a threshold set by the involved population. As discussed in section 6.2.1., the dimension of Juhola et al.'s governance system, but also basic ecosystem functions are largely neglected in the case study and should be implemented in further studies (2024). For instance, the environmental flow requirement was not included as a focus within the EMA framework. Also, the interplay of water availability and water quality, basic ecosystem function as well as actors' basic needs remains a blind spot in this study. In general, EMA would have the ability to incorporate these lacking dimensions.

When developing the EMA framework, researchers must define a context-specific and inclusive threshold, which requires society to engage in discussions about what constitutes intolerable risks. It is particularly important to involve local populations and other stakeholders that are affected by or engaging in the process of adaptation (Juhola et al., 2024), as constraints and limits to adaptation vary between actors (Dow, Berkhout, Preston, et al., 2013; Barnett et al., 2015; Warner, 2016). The different individual perceptions of limits to adaptation cannot yet be fully captured by EMA. As shown in the case study, the use of a single threshold is intended to analyze water scarcity as a risk at the community level (cf. Figure 34)).

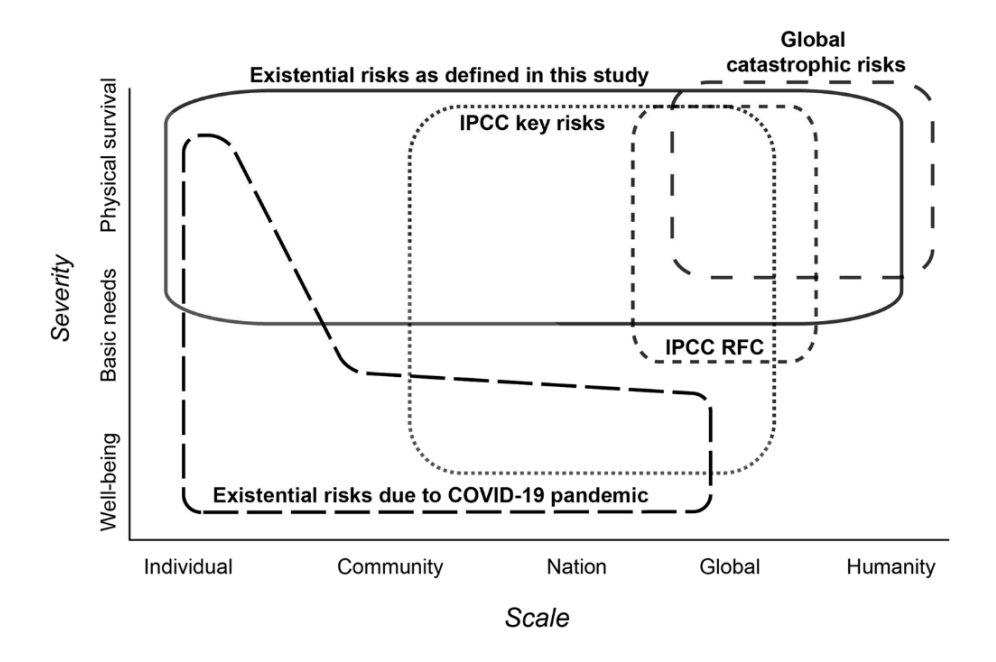


Figure 34: Different risk definition that have an implication of the scaling of the threshold. They are spanned between an axis of scale from individual to global and humanity and an axis of the the severity of how the subjects are impacted by Huggel et al. (2022)

However, EMA is operationalized to assess only one specific point in the risk space. If the threshold were constructed differently, it might be possible to cover the scale from individual to community, or in other cases even extend the range to a larger entity. The sufficiency scale proposed by Juhola et al. (2024) could, in a simplified way, be reflected in the vertical dotted threshold line (cf. Figure 20 in section 4.3.1.). Another potential approach to operationalize the scale is by treating the threshold as an uncertainty, similar to the method used by Weibel (2022), where the uncertainty range varies along the sufficiency scale. Translating stakeholders' needs and societal goals into distinct thresholds and mapping them onto the vertical threshold line or the uncertainty range – representing the sufficiency scale – remains an essential step. While this translation has not yet been undertaken, future research should explore it to also enable a clear distinction between actor-level objectives and system-level objectives. Moreover, Juhola et al. (2024) even suggest setting thresholds based on an ethical perspective considering social justice. Defining what is intolerable then allows societies to set strategic directions, with the EMA providing valuable insights.

Another solution is to complement EMA with an even more individual insight, e.g. gained through a *Sustainable Livelihood Framework* (SLF) approach, to assess an individual's capacity to respond to change (McNamara et al., 2017). This example invites further reflection on the potential synergies between qualitative studies and EMA, depending on their strengths and weaknesses and vice versa. In conclusion, collaborative efforts are essential to fully understand the complex interactions between society, individuals, nature, and the economy.

Synergies between qualitative studies and EMA in decision making

A comparison of the quantitative EMA approach with qualitative methods reveals their distinct strengths and limitations in supporting complex decisions under uncertainty. On the one hand, EMA provides a standardized, numerical output that is representative of a wide range of socioeconomic and climate change scenarios. In addition, it not only identifies key drivers of climate-related risk but also provides insights into the underlying interdependencies. For example, the case study found that the importance of variables such as irrigation efficiency and household allocation vary depending on the threshold set. This variation depends on factors such as the dry season and monthly sectoral water demand. Such insights would typically require qualitative approaches, such as expert interviews, to uncover. On the other hand, EMA cannot fully capture the contextual and subjective insights that are integral to qualitative approaches. While contextual factors, such as the need to include water quality in the case study, can be incorporated, this can only be done by providing a local perspective. In addition, climate-related risks that are analyzed with only one threshold in EMA fail to analyze the entire spanned risk space composed of individual perceptions. Furthermore, it is difficult to address non-quantifiable factors with EMA, as it must be translated into the XLRM-framework which represents an important challenge. For instance, to incorporate the acceptability of an adaptation measure it must be converted into a quantitative metric (Muñoz et al., 2024a). However, translating socio-cultural factors into numerical values remains challenging and is still best assessed through qualitative methods, such as SLF analysis. For example, this approach enabled McNamara et al. (2017) to find that an adaptation limit for relocation was constructed by both sense of place and economic factors, which would have hardly been detectable using EMA as it has been implemented to date. Finally, while qualitative approaches are inherently participatory as they base e.g. on interviews, EMA could theoretically be conducted without involving stakeholders, but this makes its results less valuable. To conclude, while EMA is defined as a bottom-up approach (Carlsson Kanyama et al., 2019), meaning that the models and analysis are designed to reflect the real-world concerns, uncertainties, and preferences of those directly impacted by the decisions. This is a crucial characteristic that should not be neglected, as it is what makes the method meaningful.

Advancing quantitative methods within and beyond the EMA

Within EMA, there are other options that could also be suited for the quantification of key drivers and limits to adaptation of climate-related risks. The approaches within EMA can be separated into open exploration, that includes stress testing to explore how the system might respond to different possible future scenarios and their potential impacts and directed search that includes worst-case-scenario discovery and many-objective optimization (Moallemi et al., 2020). It is important to note that stress testing is just one application of EMA, and the effectiveness of other techniques could be explored in future research. Within DMDU there is the promising approach of Dynamic Adaptive Policy Pathways (DAPP) developed by Haasnoot et al. (2019). As the name suggests it takes into account that decisions are made over time in dynamic interaction with the social-ecological system (Haasnoot et al., 2019) and has already been applied in studies about the adaptation to climate-related risks (Kalra et al., 2015), but, like EMA, not for adaptation limits. Its design purpose was not to identify limits to adaptation, but it shows path dependencies explicitly, by mapping adaptive strategies and their robustness under varying conditions (Marchau et al., 2019). It identifies points in time at which pathways fail due to constraints, such as financial constraints, or due to the ineffectiveness of adaptation measures, thus highlighting potential limits to adaptation (Kalra et al., 2015). It would then be necessary to determine whether the constraints can be addressed. Another promising avenue for further exploration, involves Tipping Point Analysis (TPA) (Berkhout et al., 2014; Haasnoot et al., 2019). When integrated with DAPP, TPA could offer enhanced insights into the timeframe in which adaptation is required or when irreversible changes become inevitable (Haasnoot et al., 2019). This approach also accounts for uncertainty in the future, but its effective implementation, similar to EMA, requires further study. Beyond EMA, there is not another method that is significantly more suited and developed to assess limits to adaptation quantitatively: Juhola et al. (2024) have expressed criticism regarding the fact that the major strands of research such as Integrated Assessment Modeling (IAM), do not consider limits to adaptation at all, or only in a very generic way. Another example they mention is Planetary Boundaries, which primarily analyzes the environmental dimension and does so on a planetary scale (Juhola et al., 2024). This makes it unsuitable for regional analyses of adaptation limits (Juhola et al., 2024). Another example is L&D, which is suitable for localizing vulnerabilities to intolerable risks, but provides no profound insights into adaptation limits (Surminski and Lopez, 2015; Huggel et al., 2018; McNamara and Jackson, 2019b; Mechler et al., 2020; Motschmann et al., 2020a). Moreover, current L&D publications are considered to be insufficiently critical, with a strong emphasis on the economic dimension that hinders understanding of the broader socioeconomic context (McNamara and Jackson, 2019a).

Recommendations for enhancing adaptation limits assessments with EMA

In light of the preceding considerations, the following recommendation outlines the use of EMA in the study of limits to adaptation. To effectively integrate EMA, it is crucial and recommended to consider the local context and actors and to complement this novel approach with existing frameworks. Scholars must carefully select relevant variables, as a large set can be computationally intensive (Muñoz et al., 2024b). It is also important to identify policy levers based on their potential, as some adaptation measures may have almost reached their maximum capacity. While EMA's strength lies in handling uncertainty, local knowledge is essential for defining meaningful ranges of uncertain variables. When applying EMA locally, thresholds and metrics must be carefully constructed. Therefore, it is essential to determine which actors' needs and basic ecosystem functions are most relevant to the phenomenon under study. Involving local stakeholders helps avoid blind spots inherent in traditional hydrological models that focus mainly on physical rather than human aspects. Involving the public in decision making on how to respond to climate change has the advantage of not only making the EMA results more meaningful but also increasing public acceptance of adaptation measures that are later selected (Steg, 2023; Kalra et al., 2015). This can also be transferred to limits to adaptation. While some audiences favor qualitative insights, others are persuaded by the perceived objectivity of quantitative findings. Importantly, the quantification of factors within a social system cannot be entirely detached from qualitative research, as both approaches complement and enhance one another. In climate change communication, combining insights from EMA with approaches like DAPP can convincingly illustrate the potential pathways of measures and their limitations while also incorporating qualitative narrative. A future-oriented strategy should therefore prioritize integrated solutions, leveraging the strengths of both qualitative and quantitative methods to address diverse audience preferences and foster more effective communication and decisionmaking. In conclusion, the novel method EMA offers insights into climate-related risks and its limits within climate adaptation, particularly when combined with qualitative fieldwork to address both the technical and socio-cultural dimensions of the issue.

7. Conclusion

Climate change threatens social-ecological systems, among others, in areas dependent on glacial meltwater, like the tropical Andes. Given its reliance on glacial meltwater, the Quillcay catchment is a key region for studying the limits to adaptation to water scarcity. Understanding these limits and their constraints is critical for making informed decisions and avoiding maladaptation. This study examined how EMA can be adapted to new contexts to better address future climate-related challenges. It first addressed the adaption of the EMA framework to analyze the critical factors and conditions leading to future water supply failures and potential limits to adaptation within the socialecological system of the Quillcay catchment. In the first part of EMA, step i), the case study variables were organized within the XLRM-framework: the hydrological model Shaman (R) was used to simulate water supply and demand, while uncertainties (X) about future climatic and socioeconomic developments were represented by selected input parameters. Adaptation measures (L) were modeled as changes in water use efficiency. Key findings regarding the integration of EMA from steps ii) and iii) highlight the challenges of defining ranges for uncertain variables in this data-scarce region. To address this, three range definitions were applied, resulting in diverse stress test results for key drivers of water scarcity. Overall, future water scarcity in the Quillcay catchment is primarily influenced by socioeconomic factors. The available policy levers include domestic, and irrigation water use efficiency, both of which play a critical role alongside future domestic water allocation. Furthermore, as the range of socioeconomic uncertainty narrows, the importance of climatic factors, namely the reducing glacier area, increases. This finding indicates that socioeconomic factors must be considered in the development of policies related to climate-induced changes in water availability in the Andes, nevertheless, climatic factors should not be underestimated, especially when there are challenges in defining the range of socioeconomic uncertainties.

For nuanced interpretation of results and meaningful use of EMA, it is critical to understand the limitations of EMA implementation. To begin with, the choice of input data determines which critical factors driving water scarcity are captured. In addition, the choice of the model (R) and the resulting metric (M) significantly influences the analysis, determining the relationships and drivers that can be identified. Another limitation is the choice of ranges and thresholds that has a significant impact on the results. Ranges need to reflect realistically feasible changes in uncertain variables in the local context, which can be challenging. In the adapted EMA framework implemented in this case study, thresholds were found to be useful for identifying system failures within stress testing. However, for meaningful results, an inclusive and context-specific threshold must be established by incorporating the perspectives of those directly affected in the Quillcay catchment. Lastly, the transferability of EMA to fields or regions other than mountain water management is possible, however it requires adjustments mainly in structuring the XLRM-framework.

Building on the case study findings, this thesis expanded to explore in a broader context how EMA can integrate or complement existing frameworks, methods or theories to assess limits to adaptation to climate related risks and constraints. EMA has proven valuable for linking biophysical and socioeconomic data, providing insights into interactions between adaptation measures and uncertainties. It is relatively robust to uncertainty and provides standardized numerical outputs. However, it was not possible to identify constraints that lead to limits to adaptation. This highlights the need, to complement EMA with both methods and frameworks for a comprehensive analysis of the social-ecological system. First, both theoretical and practical advances are needed to better understand limits to adaptation. Second, future collaborative interfaces are essential to enhance the effectiveness of EMA. Engagement with local stakeholders is critical to contextualize EMA findings. Building partnerships with local researchers and policymakers increases the robustness of EMA by incorporating local perceptions and expert judgments, especially in data-poor regions. For instance, it is beneficial to involve those directly affected or involved in the adaptation process in the design of metrics and thresholds. In addition, collaboration with qualitative researchers is essential to address the limitations of EMA and to broaden the methodological approach, for example by integrating qualitative approaches to leverage its strengths. It is particularly important to develop methods for translating both actor-level and system-level objectives into different thresholds and meaningful metrics. Finally, combining promising methods from DMDU, such as DAPP, with EMA offers further potential.

In conclusion, addressing these research directions and the fostering of collaborative intersections will maximize the value of EMA. For policy and decision-makers in regions like the Quillcay catchment, EMA can provide valuable insights into the conditions under which future climate-related risks may occur and deepen the understanding of individual and community capacities to adapt to them. This approach can play a critical role in shaping adaptation policies, reducing future risks, and ensuring more effective decision-making.

8. References

- Acevedo-Osorio, Á. et al. (2017) Sustentabilidad y variabilidad climática: acciones agroecológicas participativas de adaptación y resiliencia socioecológica en la región alto-andina colombiana. *Luna Azul.* [Online] (44), 06–26.
- Adger, W. N. et al. (2009) Are there social limits to adaptation to climate change? *Climatic Change*. [Online] 93 (3–4), 335–354.
- Aggarwal, A. et al. (2022) Adaptation to climate change induced water stress in major glacierized mountain regions. *Climate and Development*. [Online] 14 (7), 665–677.
- Aide, T. M. et al. (2019) Woody vegetation dynamics in the tropical and subtropical Andes from 2001 to 2014: satellite image interpretation and expert validation. *Global Change Biology*. [Online] 25 (6), 2112–2126.
- Alemayehu, F. R. et al. (2015) The potential for utilizing the seed crop amaranth (Amaranthus spp.) in East Africa as an alternative crop to support food security and climate change mitigation. *Journal of Agronomy and Crop Science*. [Online] 201 (5), 321–329.
- Allen, R. et al. (1998) Crop evapotranspiration Guidelines for computing crop water requirements. *FAO Irrigation and drainage paper*. 56.
- American Meteorological Society (2024) *Freezing level* [online]. Available from: https://glossary.ametsoc.org/wiki/Freezing level (Accessed 19 September 2024).
- ANA (2015) Evaluación de recursos hídricos en la cuenca Santa. [online]. Available from: https://repositorio.ana.gob.pe/handle/20.500.12543/23 (Accessed 16 April 2024).
- ANA (2014) Inventario nacional de glaciares del Perú (2010).
- ANA (2018a) *Inventario nacional de glaciares del Perú (2016*). [online]. Available from: https://www.arcgis.com/home/item.html?id=c38451dc61a64a3287f5511fc8b5cbcb (Accessed 16 April 2024).
- ANA (2023) *Inventario nacional de glaciares del Perú (2020*). [online]. Available from: https://www.arcgis.com/home/item.html?id=ea055f40a9084e05b2fc7fd0544468fc (Accessed 16 April 2024).
- ANA (2009) Ley de recursos hídricos. ley N° 29338 p.11–143. [online]. Available from: https://repositorio.ana.gob.pe/handle/20.500.12543/228 (Accessed 17 April 2024).
- ANA (2018b) Reanálisis del primer inventario nacional de glaciares del Perú (1989). [online]. Available from:

 https://www.arcgis.com/home/item.html?id=a5980a767581450db5f5d00c2d0b9000 (Accessed 6 January 2024).
- ANA (2016) *R.J. N°098-2016-ANA*. [online]. Available from: https://www.ana.gob.pe/normatividad/rj-no-098-2016-ana-0.
- Arias Montevechio, E. et al. (2023) Traditional crops and climate change adaptation: insights from the Andean agricultural sector. *Climate and Development*. [Online] 15 (9), 723–737.
- Bankes, S. et al. (2013) 'Exploratory Modeling and Analysis', in Saul I. Gass & Michael C. Fu (eds.) *Encyclopedia of Operations Research and Management Science*. [Online]. Boston,

- MA: Springer US. pp. 532–537. [online]. Available from: https://doi.org/10.1007/978-1-4419-1153-7 314 (Accessed 23 February 2024).
- Baraer, M. et al. (2012) Glacier recession and water resources in Peru's Cordillera Blanca. *Journal of Glaciology*. [Online] 58 (207), 134–150.
- Barnett, J. et al. (2015) From barriers to limits to climate change adaptation: path dependency and the speed of change. *Ecology and Society*. [Online] 20 (3). Available from: https://www.ecologyandsociety.org/vol20/iss3/art5/ (Accessed 8 March 2024).
- Berkhout, F. et al. (2014) Framing climate uncertainty: Socio-economic and climate scenarios in vulnerability and adaptation assessments. *Regional Environmental Change*. [Online] 14.
- Berkhout, F. & Dow, K. (2022) Limits to adaptation: building an integrated research agenda. *WIREs Climate Change*. [Online] 14 (3), 12.
- Bezner Kerr, R. et al. (2022) Interplays between changing biophysical and social dynamics under climate change: Implications for limits to sustainable adaptation in food systems. *Global change biology*. [Online] 28 (11), 3580–3604.
- Bhave, A. G. et al. (2014) A combined bottom-up and top-down approach for assessment of climate change adaptation options. *Journal of Hydrology*. [Online] 518, 150–161.
- Bhave, A. G. et al. (2016) Barriers and opportunities for robust decision making approaches to support climate change adaptation in the developing world. *Climate Risk Management*. [Online] 14, 1–10.
- Bos, M. G. et al. (eds.) (2009) 'Effective precipitation', in *Water requirements for irrigation and the environment*. [Online]. Dordrecht: Springer Netherlands. pp. 81–101. [online]. Available from: https://doi.org/10.1007/978-1-4020-8948-0_3 (Accessed 28 December 2024).
- Bradley, R. S. et al. (2009) Recent changes in freezing level heights in the Tropics with implications for the deglacierization of high mountain regions. *Geophysical Research Letters*. [Online] 36 (17). Available from: https://onlinelibrary.wiley.com/doi/abs/10.1029/2009GL037712 (Accessed 20 September 2024).
- Brower, C. & Heibloem, H. (1986) 'Chapter 2: Crop water needs', in *Part II Determination of irrigation water needs*. Training manual. Available from: https://www.fao.org/4/s2022e/s2022e02.htm#chapter%202:%20crop%20water%20needs (Accessed 12 July 2024).
- Bryant, B. P. & Lempert, R. J. (2010) Thinking inside the box: A participatory, computer-assisted approach to scenario discovery. *Technological Forecasting and Social Change*. [Online] 77 (1), 34–49.
- Burns, P. et al. (2011) A multi-parameter hydrochemical characterization of proglacial runoff, Cordillera Blanca, Peru. *The Cryosphere Discussions*. [Online] 5, 2483–2521.
- Bury, J. T. et al. (2011) Glacier recession and human vulnerability in the Yanamarey watershed of the Cordillera Blanca, Peru. *Climatic Change*. [Online] 105 (1–2), 179–206.
- Buytaert, W. et al. (2017) Glacial melt content of water use in the tropical Andes. *Environmental Research Letters*. [Online] 12 (11), 114014.
- Buytaert, W. & Bièvre, B. (2012) Water for cities: the impact of climate change and demographic growth in the tropical Andes. *Water Resources Research*. 48.

- Calvin, K. et al. (2023) IPCC, 2023: Climate Change 2023: Synthesis Report. Contribution of Working Groups I, II and III to the Sixth Assessment Report of the Intergovernmental Panel on Climate Change [Core Writing Team, H. Lee and J. Romero (eds.)]. IPCC, Geneva, Switzerland. [online]. Available from: https://www.ipcc.ch/report/ar6/syr/ (Accessed 10 November 2024).
- Carlsson Kanyama, A. et al. (2019) "We want to know where the line is": comparing current planning for future sea-level rise with three core principles of robust decision support approaches. *Journal of Environmental Planning and Management*. [Online] 62 (8), 1339–1358.
- Cortignani, R. et al. (2021) Paths of adaptation to climate change in major Italian agricultural areas: Effectiveness and limits in supporting the profitability of farms. *Agricultural Water Management*. [Online] 244.
- Damkjaer, S. & Taylor, R. (2017) The measurement of water scarcity: defining a meaningful indicator. *Ambio*. [Online] 46 (5), 513–531.
- Daneshmand, H. et al. (2019) Water and salt balance modelling of intermittent catchments using a physically-based integrated model. *Journal of Hydrology*. [Online] 568, 1017–1030.
- Dioses Noblecilla, F. F. & Zapata Seminario, R. E. (2017) Sistema de riego tecnificado por goteo para cultivo de Quinua, financiado por fondo contravalor Peru-Francia; en el distrito Tauripampa, provincia Yauyo. Trujillo: Universidad Privada Antenor Orrego. [online]. Available from:

 https://repositorio.upao.edu.pe/bitstream/handle/20.500.12759/5741/REP_ING.CIVIL_FER NANDO.DIOSES_RAUL.ZAPATA_SISTEMA.RIEGO.TECNIFICADO.GOTEO.CULTIVO.Q UINUA.FINANCIADO.FONDO.CONTRAVALOR.PERU.FRANCIA.DISTRITO.TAURIPAMP A.PROVINCIA.YAUYOS.LIMA.2017.pdf?sequence=1&isAllowed=y (Accessed 21 October 2024).
- Dow, K., Berkhout, F., Preston, B. L., et al. (2013) Limits to adaptation. *Nature Climate Change*. [Online] 3 (4), 305–307.
- Dow, K., et al. (2013) Limits to adaptation to climate change: a risk approach. *Current Opinion in Environmental Sustainability*. [Online] 5 (3–4), 384–391.
- Drenkhan, F. et al. (2019) Managing risks and future options from new lakes in the deglaciating Andes of Peru: The example of the Vilcanota-Urubamba basin. *Science of The Total Environment*. [Online] 665, 465–483.
- Drenkhan, F. et al. (2015) The changing water cycle: climatic and socioeconomic drivers of water-related changes in the Andes of Peru. *WIREs Water*. [Online] 2 (6), 715–733.
- EPS Chavín S.A. (2024) *Mapas catastrales* [online]. Available from: https://www.epschavin.com/mapas-catastrales/ (Accessed 1 August 2024).
- ESA (2023a) 2023_03_04_Sentinel-2_L2A_B04/08. [online]. Available from: https://apps.sentinel-hub.com/eo-browser/?zoom=10&lat=41.9&lng=12.5&themeId=DEFAULT-THEME&to-Time=2024-07-09T08%3A02%3A13.682Z (Accessed 23 June 2024).
- ESA (2023b) 2023_08_21_Sentinel-2_L2A_B04/08. [online]. Available from: https://apps.sentinel-hub.com/eo-browser/?zoom=10&lat=41.9&lng=12.5&themeId=DEFAULT-THEME&to-Time=2024-07-09T08%3A02%3A13.682Z (Accessed 23 June 2024).

- Esri (n.d.) *ArcGIS Online Living Atlas of the World*. [online]. Available from: https://livingatlas.arcgis.com.
- Esteve-Llorens, X. et al. (2022) Environmental footprint of critical agro-export products in the Peruvian hyper-arid coast: A case study for green asparagus and avocado. *Science of The Total Environment*. [Online] 8, 1815–1686.
- Fernandez-Palomino, C. et al. (2023) BASD-CMIP6-PE: bias-adjusted and statistically downscaled CMIP6 projections over Peru and Ecuador. [online]. Available from: https://dataservices.gfz-potsdam.de/pik/showshort.php?id=473f27a6-86dd-11ed-95b8-f851ad6d1e4b (Accessed 25 July 2024).
- Fernandez-Palomino, C. A. et al. (2022) A novel high-resolution gridded precipitation dataset for Peruvian and Ecuadorian watersheds: development and hydrological evaluation. *Journal of Hydrometeorology*. [Online] 23 (3), 309–336.
- Fernandez-Palomino, C. A. et al. (2024) High-resolution climate projection dataset based on CMIP6 for Peru and Ecuador: BASD-CMIP6-PE. *Scientific Data*. [Online] 11 (1), 34.
- Friedman, J. H. & Fisher, N. I. (1999) Bump hunting in high-dimensional data. *Statistics and Computing*. [Online] 9 (2), 123–143.
- Garcia, J. L. et al. (2023) *Identifying acid lakes and associated rock exposure in glacial retreat zones in the Peruvian Andes using Landsat 8 imagery*. [online]. Available from: https://www.researchsquare.com/article/rs-3059034/v1 (Accessed 7 June 2024).
- Gerlicz, A. et al. (2019) Use and perceptions of alternative economic activities among smallholder coffee farmers in Huehuetenango and El Quiché departments in Guatemala. *Agroecology and Sustainable Food Systems*. [Online] 43 (3), 310–328.
- Giráldez, L. et al. (2020) Change of the rainfall seasonality over central Peruvian Andes: onset, end, duration and its relationship with large-scale atmospheric circulation. *Climate*. [Online] 8 (2), 23.
- Groves, D. G. et al. (2013) Adapting to a changing Colorado River: making future water deliveries more reliable through robust management strategies. [online]. Available from: https://www.rand.org/pubs/research_reports/RR242.html (Accessed 15 November 2024).
- Grupo Banco Mundial (2023) *Perú acciones estratégicas para la seguridad hídrica*. [online]. Available from: https://www.bancomundial.org/es/topic/water/publication/peru-strategic-actions-toward-water-security (Accessed 25 January 2024).
- Guyon, I. & Elisseeff, A. (2003) An introduction to variable and feature selection Leslie Pack Kaelbling (ed.). *Journal of Machine Learning Research*. [Online] 3 (7–8), 1157–1182.
- Haasnoot, M. et al. (2019) 'Chapter 4 Dynamic Adaptive Policy Pathways (DAPP)', in Vincent A. W. J. Marchau et al. (eds.) *Decision Making under Deep Uncertainty: From Theory to Practice*. [Online]. Cham (CH): Springer International Publishing. Available from: http://link.springer.com/10.1007/978-3-030-05252-2 (Accessed 10 December 2023).
- Hagen, I. et al. (in review) *Identifying constraints and limits to adaptation to climate-related risks in the Peruvian Andes.*
- Hakala Assendelft, K. et al. (2020) Hydrological Modeling of Climate Change Impacts. *Encyclopedia of Water: Science, Technology, and Society.* Hoboken (USA): Wiley, 1-20.

- Harvey, C. A. et al. (2014) Extreme vulnerability of smallholder farmers to agricultural risks and climate change in Madagascar. *Philosophical Transactions of the Royal Society B: Biological Sciences*. [Online] 369, 20130089.
- Heede, U. K. & Fedorov, A. V. (2023) Towards understanding the robust strengthening of ENSO and more frequent extreme El Niño events in CMIP6 global warming simulations. *Climate Dynamics*. [Online] 61 (5), 3047–3060.
- Heikkinen, A. (2017) Climate Change in the Peruvian Andes: A Case Study on Small-Scale Farmers' Vulnerability in the Quillcay River Basin. *Iberoamericana Nordic Journal of Latin American and Caribbean Studies*. [Online] 46 (1). Available from: https://iberoamericana.se/articles/10.16993/iberoamericana.211 (Accessed 13 November 2024).
- Herrador-Valencia, D. & Paredes, M. (2016) Cambio climático y agricultura de pequeña escala en los Andes ecuatorianos: un estudio sobre percepciones locales y estrategias de adaptación. *Journal of Latin American Geography*. [Online] 15 (2), 101–121.
- Hock, R. et al. (2019) 'High mountain areas', in H.- O. Pörtner et al. (eds.) *IPCC Special Report on the Ocean and Cryosphere in a Changing Climate*. in press: Intergovernmental Panel on Climate Change.
- Hofer, S. et al. (2024) Realistic representation of mixed-phase clouds increases projected climate warming. *Communications Earth & Environment*. [Online] 5 (1), 1–12.
- Howard, G. et al. (2020) Domestic water quantity, service level and health.
- Huggel, C. et al. (2018) Loss and Damage in the mountain cryosphere. *Regional Environmental Change*. [Online] 19 (5), 1387–1399.
- Huggel, C. et al. (2022) The existential risk space of climate change. *Climatic Change*. [Online] 174 (1–2).
- Huss, M. & Hock, R. (2018) Global-scale hydrological response to future glacier mass loss. Supplementary information. *Nature Climate Change*. [Online] 8 (2), 135–140.
- IIASA (2018) *IAM Scenarios*. [online]. Available from: https://tntcat.iiasa.ac.at/SspDb/dsd?Action=htmlpage&page=20 (Accessed 6 January 2024).
- INEI (2020) Censos Nacionales Agropecuario. [online]. Available from: https://www.gob.pe/36487-consultar-informacion-de-los-censos-realizados-por-el-inei-censos-nacionales-agropecuario (Accessed 6 January 2024).
- INEI (2018) Censos Nacionales de Población y Vivienda. [online]. Available from: https://www.gob.pe/36495-consultar-informacion-de-los-censos-realizados-por-el-inei-censos-nacionales-de-poblacion-y-vivienda (Accessed 6 January 2024).
- INEI (2023) *Perú: Formas de acceso al agua y saneamiento básico* [online]. Available from: https://www.inei.gob.pe/biblioteca-virtual/boletines/formas-de-acceso-al-agua-y-saneamiento-basico-9343/1/ (Accessed 29 March 2024).
- loris, A. A. R. (2012) The geography of multiple scarcities: urban development and water problems in Lima, Peru. *Geoforum*. [Online] 43 (3), 612–622.
- IPCC (2022a) Climate Change 2022 Impacts, Adaptation and Vulnerability: Working Group II Contribution to the Sixth Assessment Report of the Intergovernmental Panel on Climate

- Change. [Online]. Cambridge (UK): Cambridge University Press. Available from: https://www.cambridge.org/core/product/identifier/9781009325844/type/book (Accessed 9 January 2024).
- IPCC (2023) 'Sections', in Core Writing Team et al. (eds.) Climate Change 2023: Synthesis Report. Contribution of Working Groups I, II and III to the Sixth Assessment Report of the Intergovernmental Panel on Climate Change. [Online]. Geneva, Switzerland: Intergovernmental Panel on Climate Change (IPCC). pp. 35–115. Available from: https://www.ipcc.ch/report/ar6/syr/ (Accessed 14 October 2024).
- IPCC (2022b) 'Summary for policymakers', in H.-O. Pörtner et al. (eds.) Climate Change 2022: Impacts, Adaptation and Vulnerability. Contribution of Working Group II to the Sixth Assessment Report of the Intergovernmental Panel on Climate Change. [Online]. Cambridge, UK and New York, NY, USA: Cambridge University Press. pp. 3–33. Available from: https://www.cambridge.org/core/product/identifier/9781009325844/type/book (Accessed 15 February 2024).
- Jarvis, A. et al. (2008) *Hole-filled seamless SRTM data V4*. [online]. Available from: http://srtm.csi.cgiar.org (Accessed 13 August 2024).
- Jayakumar, D. et al. (2018) 'Chapter 27 Spatiotemporal variability of soil moisture and drought estimation using a distributed hydrological model', in Samui Pijush et al. (eds.) *Integrating Disaster Science and Management*. [Online]. Elsevier. pp. 451–460. Available from: https://www.sciencedirect.com/science/article/pii/B9780128120569000270 (Accessed 12 December 2024).
- Jezeer, R. E. et al. (2019) Influence of livelihood assets, experienced shocks and perceived risks on smallholder coffee farming practices in Peru. *Journal of Environmental Management*. [Online] 242, 496–506.
- Juhola, S. et al. (2024) A new dynamic framework is required to assess adaptation limits. *Global Environmental Change*. [Online] 87102884.
- Kalra, N. et al. (2015) Robust Decision-Making in the water sector: A Strategy for implementing Lima's long-term water resources master plan. Policy Research Working Papers. [Online]. The World Bank. Available from: https://hdl.handle.net/10986/22861 (Accessed 11 November 2024).
- Klinke, A. & Renn, O. (2012) Adaptive and integrative governance on risk and uncertainty. *Journal of Risk Research*. [Online] 15 (3), 273–292.
- Kwakkel, J. H. (2017) The Exploratory Modeling Workbench: An open source toolkit for exploratory modeling, scenario discovery, and (multi-objective) robust decision making. *Environmental Modelling & Software*. [Online] 96, 239–250.
- Kwakkel, J. H. & Pruyt, E. (2013) Exploratory Modeling and Analysis, an approach for model-based foresight under deep uncertainty. *Technological Forecasting and Social Change*. [Online] 80 (3), 419–431.
- Leal Filho, W. et al. (2021) Climate change adaptation on Small Island States: an assessment of limits and constraints. *Journal of Marine Science and Engineering*. [Online] 9 (6), 602.
- Lempert, R. (2019) 'Robust Decision Making (RDM)', in Vincent A. W. J. Marchau et al. (eds.) *Decision Making under Deep Uncertainty: From Theory to Practice*. [Online]. Cham: Springer

- International Publishing. p. [online]. Available from: http://link.springer.com/10.1007/978-3-030-05252-2 (Accessed 10 December 2023).
- Lempert, R. (2003) Uncertain Science... Uncertain World. *Eos, Transactions American Geophysical Union*. [Online] 84 (30), 285–286.
- Linacre, E. T. (1993) Data-sparse estimation of lake evaporation, using a simplified Penman equation. *Agricultural and Forest Meteorology*. [Online] 64 (3), 237–256.
- Llauca, H. et al. (2023) Constraining Flood Forecasting Uncertainties through Streamflow Data Assimilation in the Tropical Andes of Peru: Case of the Vilcanota River Basin. *Water*. [Online] 15 (22), 3944.
- Llauca, H. et al. (2021) PISCO_HyM_GR2M: a model of monthly water balance in Peru (1981–2020). *Water*. [Online] 13 (8), 1048.
- Locatelli, B. et al. (2016) Synergies between adaptation and mitigation in climate change finance. International Journal of Climate Change Strategies and Management. [Online] 8 (1), 112–128.
- MapBiomas Peru (2022) *Cobertura y uso*. [online]. Available from: https://peru.mapbiomas.org/colecciones-de-mapbiomas-peru/ (Accessed 23 June 2024).
- Marchau, V. A. W. J. et al. (eds.) (2019) *Decision Making under Deep Uncertainty: from theory to practice*. [Online]. Cham: Springer International Publishing. [online]. Available from: http://link.springer.com/10.1007/978-3-030-05252-2 (Accessed 10 December 2023).
- Mark, B. G. et al. (2010) Climate Change and Tropical Andean Glacier Recession: Evaluating Hydrologic Changes and Livelihood Vulnerability in the Cordillera Blanca, Peru. *Annals of the Association of American Geographers*. [Online] 100 (4), 794–805.
- Mark, B. G. et al. (2017) Glacier loss and hydro-social risks in the Peruvian Andes. *Global and Planetary Change*. [Online] 159, 61–76.
- Martinez, R. et al. (2011) 'Synthesis of the climate of the Tropical Andes', in S. K. Herzog et al. (eds.) *Climate change and biodiversity in the Tropical Andes*. Inter-American Institute of Global Change Research (IAI). 109.
- McNamara, K. E. et al. (2017) Identification of limits and barriers to climate change adaptation: case study of two islands in Torres Strait, Australia. *Geographical Research*. [Online] 55 (4), 438–455.
- McNamara, K. E. & Jackson, G. (2019a) Loss and damage: A review of the literature and directions for future research. *WIREs Climate Change*. [Online] 10 (2), 564.
- McNamara, K. E. & Jackson, G. (2019b) Loss and damage: A review of the literature and directions for future research. *WIREs Climate Change*. [Online] 10 (2), 564.
- Mechler, R. et al. (2020) Loss and Damage and limits to adaptation: recent IPCC insights and implications for climate science and policy. *Sustainability Science*. [Online] 15 (4), 1245–1251.
- Meza, H. M. et al. (2016) Información de caracterización de la subcuenca del río Quillcay. p.1–13. MINAM (2009) COBERTURAFIN1.

- MINAM (2015) Mapa nacional de cobertura vegetal (2013). [online]. Available from: https://www.minam.gob.pe/patrimonio-natural/wp-content/uploads/sites/6/2013/10/MAPA-NACIONAL-DE-COBERTURA-VEGETAL-FINAL.compressed.pdf (Accessed 6 January 2024).
- Moallemi, E. A. et al. (2020) Exploratory modeling for analyzing coupled human-natural systems under uncertainty. *Global Environmental Change*. [Online] 65, 102186.
- Moallemi, E. A. & Malekpour, S. (2018) A participatory exploratory modelling approach for long-term planning in energy transitions. *Energy Research & Social Science*. [Online] 35, 205–216.
- Moser, S. C. & Ekstrom, J. A. (2010) A framework to diagnose barriers to climate change adaptation. *Proceedings of the National Academy of Sciences*. [Online] 107 (51), 22026–22031.
- Motschmann, A. et al. (2020a) Losses and Damages connected to glacier retreat in the Cordillera Blanca, Peru. *Climatic Change*. [Online] 162 (2), 837–858.
- Motschmann, A. et al. (2020b) Towards integrated assessments of water risks in deglaciating mountain areas: water scarcity and GLOF risk in the Peruvian Andes. *Geoenvironmental Disasters*. [Online] 7 (1), 26.
- Muñoz, R. et al. (2024a) A framework for policy assessment using exploratory modeling and analysis: An application in flood control. *Climate Risk Management*. [Online] 45, 100635.
- Muñoz, R. et al. (2024b) Assessing water management strategies in data-scarce mountain regions under uncertain climate and socio-economic changes. *Water Resources Management*. [Online]. Available from: https://doi.org/10.1007/s11269-024-03853-5 (Accessed 29 April 2024).
- Muñoz, R. et al. (2021) Comparing model complexity for glacio-hydrological simulation in the datascarce Peruvian Andes. *Journal of Hydrology: Regional Studies*. [Online] 37, 100932.
- Muñoz, R., et al. (2024c) Supplementary material. Assessing water management strategies in data-scarce mountain regions under uncertain climate and socio-economic changes. *Water Resources Management*. [Online]. Available from: https://link.springer.com/10.1007/s11269-024-03853-5 (Accessed 5 July 2024).
- Neuburger, M. & Singer, K. (2016) 'Perus Bevölkerung: Das historische Gewordensein von Diskriminierungen und Privilegierungen', in *Die Welt verstehen: eine geographische Herausforderung, mit 25 Beiträgen eine Festschrift der Geographie Innsbruck für Axel Borsdorf.* Innsbrucker geographische Studien. Innsbruck: Geographie Innsbruck Selbstverl. pp. 307–324.
- Newman, J. & Milkovits, M. (2021a) *Feature Scoring* [online]. Available from: https://tmip-emat.github.io/source/emat.analysis/feature-scoring.html?highlight=feature%20scoring (Accessed 18 November 2024).
- Newman, J. & Milkovits, M. (2021b) *TMIP-EMAT documentation* [online]. Available from: https://tmip-emat.github.io/index.html (Accessed 24 October 2024).
- Ologeh, I. O. et al. (2018) 'Constraints and Limits to Climate Change Adaptation Efforts in Nigeria', in Walter Leal Filho & Johanna Nalau (eds.) *Limits to Climate Change Adaptation*. [Online]. Cham: Springer International Publishing. pp. 159–174. Available from: https://doi.org/10.1007/978-3-319-64599-5 9 (Accessed 15 March 2024).

- O'Neill, B. et al. (2022) 'Key Risks Across Sectors and Regions', in H.- O. Pörtner et al. (eds.) Climate Change 2022 Impacts, Adaptation and Vulnerability: Contribution of Working Group II to the Sixth Assessment Report of the Intergovernmental Panel on Climate Change. 1st edition [Online]. Cambridge, UK and New York, NY, USA: Cambridge University Press. Available from: https://www.cambridge.org/core/product/identifier/9781009325844/type/book (Accessed 13 December 2024).
- O'Neill, B. C. et al. (2014) A new scenario framework for climate change research: the concept of shared socioeconomic pathways. *Climatic Change*. [Online] 122 (3), 387–400.
- O'Neill, B. C. et al. (2017) The roads ahead: Narratives for shared socioeconomic pathways describing world futures in the 21st century. *Global Environmental Change*. [Online] 42, 169–180.
- Pabón-Caicedo, J. D. et al. (2020) Observed and projected hydroclimate changes in the Andes. Frontiers in Earth Science. [Online] 8. [online]. Available from: https://www.frontiersin.org/journals/earth-science/articles/10.3389/feart.2020.00061/full (Accessed 23 September 2024).
- PUB (2023) *Building our water future*. p.1–72. [online]. Available from: https://www.pub.gov.sg/-/media/PUB/PDF/To-Publish-PUB-SR-23-Final.pdf (Accessed 31 October 2024).
- Quesquén Rumiche, A. (2008) Propuesta de asignaciones de agua en bloque volúmenes anuales y mensuales, para la formalización de los derechos de uso de agua cuenca Alto Santa en la comisión de regantes Quillcay.
- Raes, D. (2009) *The ETo calculator Evapotranspiration from a reference surface*. [online]. Available from: https://www.fao.org/fileadmin/user_upload/faowater/docs/ReferenceManualETo.pdf (Accessed 19 September 2024).
- Raskin, P. D. et al. (1996) Water and sustainability. *Natural Resources Forum*. [Online] 20 (1), 1–15.
- Riahi, K. et al. (2017) The Shared Socioeconomic Pathways and their energy, land use, and greenhouse gas emissions implications: An overview. *Global Environmental Change*. [Online] 42, 153–168.
- Rivas, D. et al. (2014) Modelo de recursos hídricos de la subcuenca de Quillcay.
- Rodríguez Eraso, N. et al. (2013) Land use and land cover change in the Colombian Andes: dynamics and future scenarios. *Journal of Land Use Science*. [Online] 8 (2), 154–174.
- Salzmann, N. et al. (2013) Glacier changes and climate trends derived from multiple sources in the data scarce Cordillera Vilcanota region, southern Peruvian Andes. *The Cryosphere*. [Online] 7 (1), 103–118.
- Santofimia, E. et al. (2017) Acid rock drainage in Nevado Pastoruri glacier area (Huascarán National Park, Perú): hydrochemical and mineralogical characterization and associated environmental implications. *Environmental Science and Pollution Research*. [Online] 24 (32), 25243–25259.
- Schauwecker, S. et al. (2017) The freezing level in the tropical Andes, Peru: an indicator for present and future glacier extents. *Journal of Geophysical Research: Atmospheres*. [Online] 122 (10), 5172–5189.

- Scott, C. A. et al. (2021) Do ecosystem insecurity and social vulnerability lead to failure of water security? *Environmental Development*. [Online] 38, 100606.
- Sedapal (2022) Sedapal presentó registros de consumo de agua de los distritos de Lima y Callao [online]. Available from: https://www.gob.pe/institucion/sedapal/noticias/605439-sedapal-presento-registros-de-consumo-de-agua-de-los-distritos-de-lima-y-callao (Accessed 8 August 2024).
- Seehaus, T. et al. (2019) Changes of the tropical glaciers throughout Peru between 2000 and 2016 mass balance and area fluctuations. *The Cryosphere*. [Online] 13 (10), 2537–2556.
- SENAMHI (2020) SENAMHI HSR PISCO: Peruvian Interpolated data. [online]. Available from: https://iridl.ldeo.columbia.edu/SOURCES/.SENAMHI/.HSR/.PISCO/ (Accessed 6 January 2024).
- Singer, K. et al. (2017) 'Waktsa Markallaa: My Poor Land.', in *Water an atlas*. Guerrilla Cartography. p. 135.
- Song, J.-H. et al. (2020) Uncertainty in Irrigation Return Flow Estimation: Comparing Conceptual and Physically-Based Parameterization Approaches. *Water*. [Online] 12 (4), 1125.
- Song, Z. & Jia, S. (2023) Municipal Water Use Kuznets Curve. *Water Resources Management*. [Online] 37 (1), 235–249.
- Steg, L. (2023) Psychology of Climate Change. *Annual Review of Psychology*. [Online] 74 (1), 391–421.
- Stitelmann, O. Y. (2024) Loss and damage of climate change in tropical glacierized areas: from changes in water availability to GLOFs. Masters Degree thesis. Zurich: University of Zurich.
- Surminski, S. & Lopez, A. (2015) Concept of loss and damage of climate change a new challenge for climate decision-making? A climate science perspective. *Climate and Development*. [Online] 7 (3), 267–277.
- Taaime, N. et al. (2023) Worldwide development of agronomic management practices for quinoa cultivation: a systematic review. *Frontiers in Agronomy*. [Online] 5. Available from: https://www.frontiersin.org/journals/agronomy/articles/10.3389/fagro.2023.1215441/full (Accessed 10 July 2024).
- Terán-Chaves, C. A. et al. (2023) Assessing the Vulnerability of Maize Crop Productivity to Precipitation Anomalies: A Case Study in the Semiarid Region of Cesar, Colombia. *Water*. [Online] 15 (11), 2108.
- Thomas, A. et al. (2021) Global evidence of constraints and limits to human adaptation. *Regional Environmental Change*. [Online] 21 (3), 85.
- Vaghefi, S. A. et al. (2021) Using Decision Making under Deep Uncertainty (DMDU) approaches to support climate change adaptation of Swiss Ski Resorts. *Environmental Science & Policy*. [Online] 126, 65–78.
- Vázquez-Rowe, I. et al. (2019) Peru's road to climate action: are we on the right path? The role of life cycle methods to improve Peruvian national contributions. *Science of The Total Environment*. [Online] 659, 249–266.

- Vetter, T. et al. (2017) Evaluation of sources of uncertainty in projected hydrological changes under climate change in 12 large-scale river basins. *Climatic Change*. [Online] 141 (3), 419–433.
- Vilímek, V. et al. (eds.) (2024) *Geoenvironmental Changes in the Cordillera Blanca, Peru*. Geoenvironmental Disaster Reduction. [Online]. Cham: Springer International Publishing. [online]. Available from: https://link.springer.com/10.1007/978-3-031-58245-5 (Accessed 15 January 2025).
- Vuille, M. et al. (2008) Glacier mass balance variability in the Cordillera Blanca, Peru and its relationship with climate and the large-scale circulation. *Global and Planetary Change*. [Online] 62 (1), 14–28.
- van Vuuren, D. P. et al. (2011) The representative concentration pathways: an overview. *Climatic Change*. [Online] 109 (1), 5.
- Warner, B. P. (2016) Understanding actor-centered adaptation limits in smallholder agriculture in the Central American dry tropics. *Agriculture and Human Values*. [Online] 33 (4), 785–797.
- WCRP (2024) *CMIP Coupled Model Intercomparison Project* [online]. Available from: https://wcrp-cmip.org/ (Accessed 24 November 2024).
- Weibel, F. (2022) Effect of climate change on human health: Case studies from Switzerland. Masters Degree thesis. University of Zurich.
- Wheater, H. S. et al. (2022) Advances in modelling large river basins in cold regions with Modélisation Environmentale Communautaire—Surface and Hydrology (MESH), the Canadian hydrological land surface scheme. *Hydrological Processes*. [Online] 36 (4), e14557.

Note on the use of Al

ChatGPT was used to assist with various aspects of this work, particularly coding and writing. For coding, it helped to improve efficiency, understand unfamiliar data formats (e.g., netCDF), and translate conceptual logic into functional code segments. For writing, it helped refine the tone and style of some segments, ensure that the writing was concise and consistent with academic standards, and improve the clarity of complex ideas. To meet standards of correct English and Spanish, DeepL Write and Translate were also used.

9. Appendix

9.1. Data

9.1.1. GIS data

Table 14: Raw GIS data used for the analysis.

Filename	Publisher & Date	Temporal coverage (if indicated)	Variables	Type / Resolution / Extent
COBERTURAFIN1	(MINAM, 2009)		land cover classes: COBERTURA	Raster / 28m / WGS 84 / UTM zone 18S / Santa catch- ment
Cobertura y uso	(MapBiomas Peru, 2022)	1985-2022	land cover classes: COBERTURA Y USO	Raster / 30m / UTM zone 18S / Peru
YYYY_MM_DD_Sentinel- 2_L2A_B04 / _B08	(ESA, 2023a, 2023b)	21.08.2023, 04.03.2023	reflectance: 04 = Red 08 = NIR	Raster / 10m / UTM zone 18S / Quillcay cat- chment
glacier_inventory_1989 / _2010 / _2016 / _2020	(ANA, 2014, 2018b, 2018a, 2023)	1989, 2010, 2016, 2020	glacier area	Vector / - / / UTM zone 18S Cordillera Blanca
quillcay_catchment	delineated from: NASA. Shuttle Ra- dar Topography Mission (SRTM). (Jarvis et al., 2008)	2008	catchment area of Quill- cay river	Vector / - / UTM zone 18S / Quillcay catch- ment
santa_cov: Mapa nacional de cobertura vegetal	(MINAM, 2015)	2013	land cover classes: cobertura vegetal 2013	Vector / - / UTM zone 18S / Santa catch- ment
srtm_21_14	CIAT. Derived from: NASA. Shuttle Ra- dar Topography Mission (SRTM). (Jarvis et al., 2008)	2008	Elevation (DEM)	Raster / 90m / WGS84 / Santa catchment +
Huascaran National Park	(Esri, n.d.)	-	Area of National Park	Vector / UTM zone 18S

Table 15: Processed GIS data used in for the analysis.

Name	Modification	Original data
X_clipped	clipped to quillcay_catchment	quillcay_catchment
quillcay_nNP	quillcay_catchment that is NOT inside the	Huascaran National Park
	Huascarán National Park	
aug_NDVI	recalculated Sentinel B04 / _B08	YYYY_MM_DD_Sentinel-2_L2A_B04 / _B08
mar_NDVI	(21.08.2023, 04. 03. 2023) to the NDVI	
agri	reclassification based on land cover classes :	COBERTURAFIN1_clipped
	1 : area that has similar c-values than agricul-	
	ture (irrigated / non-irrigated)	
	0 : remaining area	

9.1.2. Historical data

Table 16: Raw historical data. The variables are color-coded according to their impact on the water balance: Variables that influence supply = blue; demand = orange; both = yellow.

Name	Publisher & date	Temporal cover- age (if indicated)	Variables	Type / Resolution / Extent
BASD-CMIP6_PE (Fernandez-Palo- mino et al., 2023)	(Fernandez-Palomino et al., 2024)	(years: 1981- 2014)	temperature (min./max., daily) precipitation (daily)	 gcms = ["CanESM5", "IPSL-CM6A-LR", "MPI-ESM1-2- HR", "CNRM- CM6-1", "CNRM- ESM2-1", "EC- Earth3", "GFDL- ESM4", "MI- ROC6", "MRI- ESM2-0", "UKESM1-0-LL"] variables = ["pr", "tasmin", "tasmax"] NetCDF (Raster) Resolution: 1d, 10km
PISCOv2p1 / PIS- COv1p1	(SENAMHI, 2020)	1981 - 2020	temperatureprecipitationevapotran- spiration	NetCDF (Raster) Resolution: 1d/1m, 10km
Historical Glacier Surface	(ANA, 2014, 2018b, 2018a)	1989, 2010, 2016	area (km2)	Vector data
Historical population "datos_x4_pop_historical" (Census and governmental projections)	(INEI, 2018)	1981, 1993, 2007, 2017	-	district scale: Huaraz & Independencia
Historical irrigated areas "da-tos_x5_area_irr_historical"	(INEI, 2020) (Quesquén Rumiche, 2008)	1994, 2012, 2008	area (km2)	district scale: Huaraz & Independencia

Table 17: Processed historical data. The variables are color-coded according to their impact on the water balance: Variables that influence supply = blue; demand = orange; both = yellow.

Name	Variables	Modification	Original data
Reference Evapotranspiration	eto: =evapotranspiration, [mm/day, frequency: monthly]	calculated with FAO calculator (python package)	BASD-CMIP6: min. & max. temperature Assumptions on: wind-speed, humidity, radiation
Precipitation Minimal temperature Maximal temperature	pp [mm/month] tasmin [°C] tasmax [°C]	sum(daily mean precipitation in the catchment) mean(daily mean temperature in the catchment) →bias-correction with PISCO	BASD-CMIP6_PE (scenario: historical) PISCOv2p1 / PIS-COv1p1
Historical forest areas "datos_x6_area_for_historical"	area (km2)	forest where value = 3 → forest fraction from 1985, 1990, 1995, 2000, 2005, 2010.	Cobertura y uso (MapBiomas Peru, 2022)

9.1.3. Future projections

Table 18: Raw future scenarios. The variables are color-coded according to their impact on the water balance: Variables that influence supply = blue; demand = orange; both = yellow.

Name	Publisher (linked: access)	Date	Variables	Type / Resolution / Extent
BASD-CMIP6_PE (Fernandez-Palo- mino et al., 2023)	(Fernandez-Palomino et al., 2024)	2015 - 2050	• temperature (min./max., [°C])	• Experiment: SSP1- 2.6, SSP3-7.0, SSP5-8.5
			precipitation, [mm/d]	gcms = same as historical
iamc_db_popula- tion _PER	(Riahi et al., 2017; IIASA, 2018)	2010 – 2050 (+5yr)	population [mil- lion]	Region: PeruSSP1-5Baseline scenarios
iamc_db_cropland _LAM	(Riahi et al., 2017; IIASA, 2018)	2010 – 2050 (+10yr)	cropland area [million ha]	Region: R32LAM-M (Latin America – medium and high income) SSP1-5 Baseline scenarios

Table 19: Processed future scenarios. The variables are color-coded according to their impact on the water balance: Variables that influence supply = blue; demand = orange; both = yellow.

Name	Variables	Modification	Original data
grouped climate	date: [DD.MM.YYYY]	• [2015, 2050]	• -
variables datos clim 1-30	• month: [M]	date modification	• -
(datos_clim_*scenario*)	days_in_month: =number of days in the month	date modification	• -
single climate variables datos pp 1-30	x_pp: =precipitation, [mm/month]	bias-corrected	BASD-CMIP6_PE
datos_eto_1-30 datos_agla_1-30	 t_min: =minimal monthly temperature, [°C] 	 bias-corrected 	BASD-CMIP6_PE
(extracted from datos_clim_1-30)	 t_max: =max. monthly tem- perature, [°C] 	bias-corrected	BASD-CMIP6_PE
	x_eto: =evapotranspiration, [mm/day]	calculate with dif- ferent t_min / t_max values ac- cording to the dif- ferent scenarios	BASD-CMIP6_PE: t_min, t_max Assumptions on wind speed, radiation, humid- ity
	evap =lake evaporation, [mm/day]. (only required if reservoirs are included)	 calculate with different t and altitude (Linacre, 1993) 	BASD-CMIP6_PE: t_min, t_max
	x_area_gla: =glacier area, [km2]	based on ΔT: calculate FLH (=flh, flh_area), the impact on the a_gla which has 17% of its surface below the FLH	BASD-CMIP6_P: t_min, t_max glacier_inventory_2016 srtm_21_14 (DEM)
	mf: =melting factor	• -	artificial factor (cali- brated from Shaman)
	net_irr_dem := net water allocation for irrigation, [m3/d/ha] with an efficiency of 35%. (socioeconomic data!, together with climate data due to data structure.)	transform to m3/d/ha based on efficiency and irri- gation block area	 datos_x5_area_irr_historical" irrigation demand and irrigation block area from Rivas, Cuéllar and McKinney, 2014
	qeco := environmental flow requirement	50% of min. monthly observed runoff from 1981 - 2014	PISCO v1p1

Name	Variables	Modification	Original data
datos_socioec	 x4_pop := population as function of the district frac- tion inside the catchment 	cumulative change from 2015-2050 [%] expressed by a range from min. to max. change based on SSP- projections 1-5	iamc_db_popula- tion_PER
	x5_area_irr: =irrigated area in the catchment, assuming a constant ratio between irrigated and non-irrigated area	cumulative change from 2015-2050 [%] expressed by a range from min. to max. change based on SSP-projections 1-5	iamc_db_cropland_LAM

9.2. Statistics

9.2.1. Trend detection

For trend detection in temperature, precipitation and discharge time series a Mann-Kendall was used, as it performs well with every distribution.

Table 20: P-values from the Mann-Kendall test (α = 0.05) applied to historic (1981-2014) and average scenario (2015 - 2050, 2020 – 2050 for simulated discharge) time series. Simulated historical runoff data were used to isolate the contributions of climate scenarios from discrepancies between simulated and observed data.

Climate variable	historical	SSP 1-2.6	SSP 3-7.0	SSP5-8.5
Annual average temperature (°C)	p-value: 9.46e-08 trend: increasing	p-value: 1.56e-11 trend: increasing	p-value: 8.62e-13 trend: increasing	p-value: 9.28e-14 trend: increasing
Total annual precipitation (mm)	p-value: 1.23e-01 trend: no trend	p-value: 9.0e-03 trend: increasing	p-value:1.0e-03 trend: increasing	p-value: 1.0e-03 trend: increasing
Annual average dis- charge (m³/s)	p-value: 0.98 trend: no trend	p-value: 0.36 trend: no trend	p-value:0.95 trend: no trend	p-value: 0.36 trend: no trend
Dry season average discharge (m³/s)	p-value: 2.2e-05 trend: decreasing	p-value: 0.02 trend: decreasing	p-value: 1.07e-03 trend: decreasing	p-value: 5.96e-04 trend: decreasing

9.2.2. Statistical differences between historical and projected data

Based on preliminary tests for normality and homogeneity of variances, Welch's ANOVA was used for normally distributed data, while the Kruskal-Wallis test was used for non-normal distributions to assess central tendency. Post-hoc analyses were performed using the Games-Howell test or the Wilcoxon rank-sum test, respectively.

Table 21: P-values for statistical significance and post hoc test results are reported for significant findings, with a significance level of $\alpha = 0.05$ for all tests.

Climate variable	Statistical difference?	Post-hoc test	
Annual average temperature (°C)	Welch's ANOVA p-value: 4.59e-32 significant difference: YES	Games-Howell Historical – SSP 1-2.6: Historical – SSP 3-7.0: Historical – SSP 5-8.5:	significant p-value 0 2.66e-14 0

Climate variable	Statistical difference?	Post-hoc test		
Total annual precipitation (mm)	Welch's ANOVA p-value: 0.02 significant difference: YES	Games-Howell Historical – SSP 1-2.6: Historical – SSP 5-8.5:	significant p-value 0.03 0.03	
Annual average dis- charge (m³/s)	Welch's ANOVA p-value: 0.98 significant difference: NO	-	-	
Dry season average discharge (m³/s)	Welch's ANOVA p-value: 4.46e-26 significant difference: YES	Games-Howell Historical – SSP 1-2.6: Historical – SSP 3-7.0: Historical – SSP 5-8.5:	significant p-value 5.14e-10 6.58e-12 8.12e-12	

9.3. Additional figures

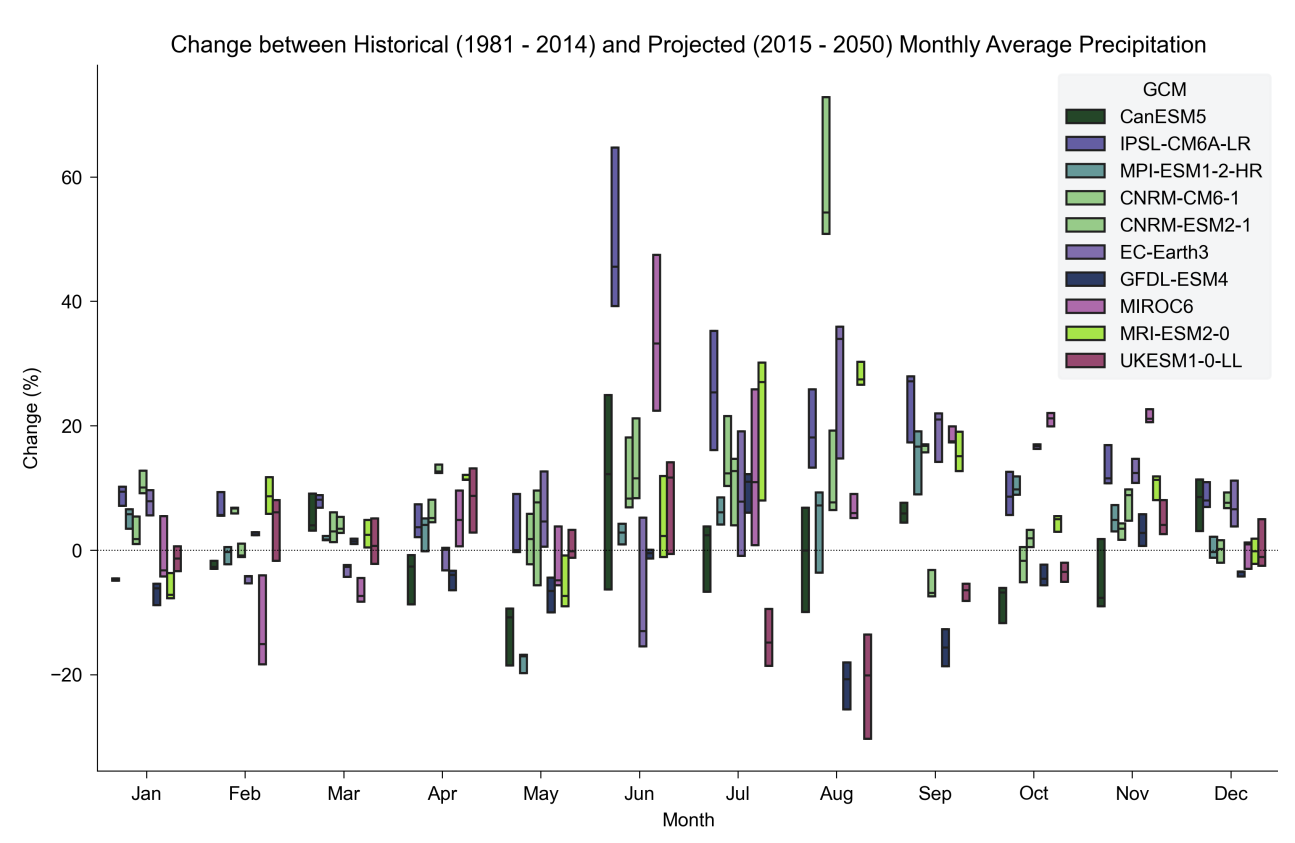


Figure 35: Comparison between historical and future precipitation patterns. The box groups 50% of the data equally around the median (horizontal line) and the whiskers extend to the 10% and 90% of the data respectively (own illustration).

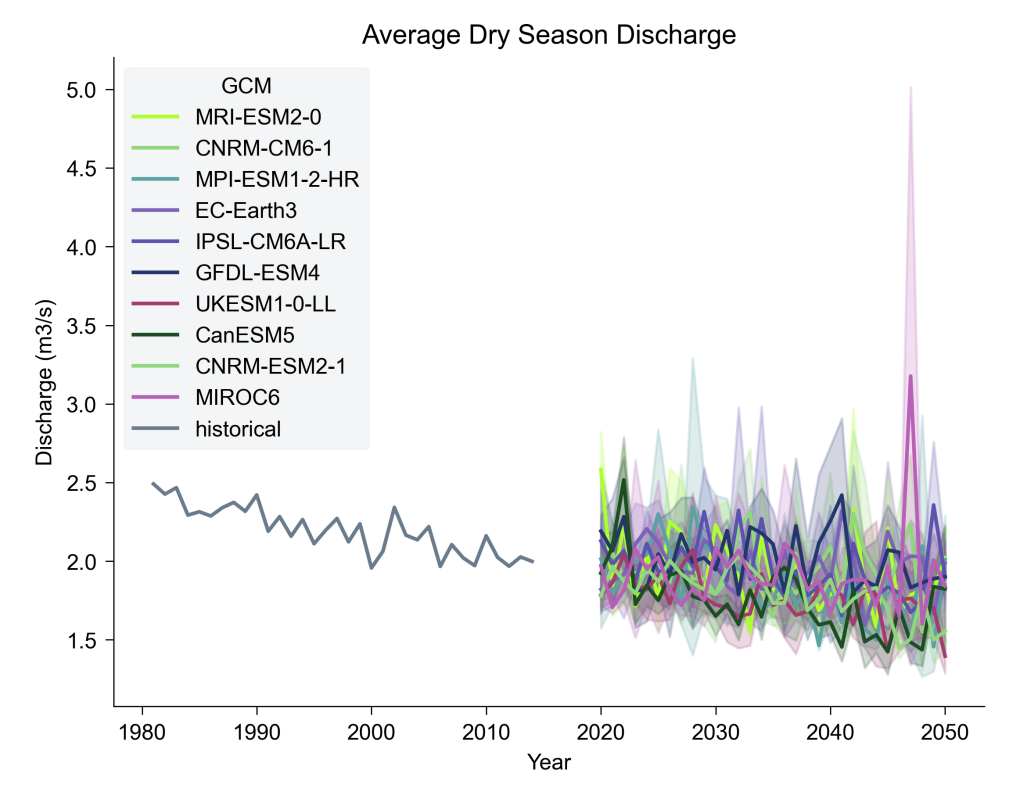


Figure 36: Average dry season discharge. Both datasets are based on the three different climate scenarios and simulated historical data. The bold line represents the SSP average for each GCM, whilst the shaded areas illustrate the standard deviation (own illustrations)

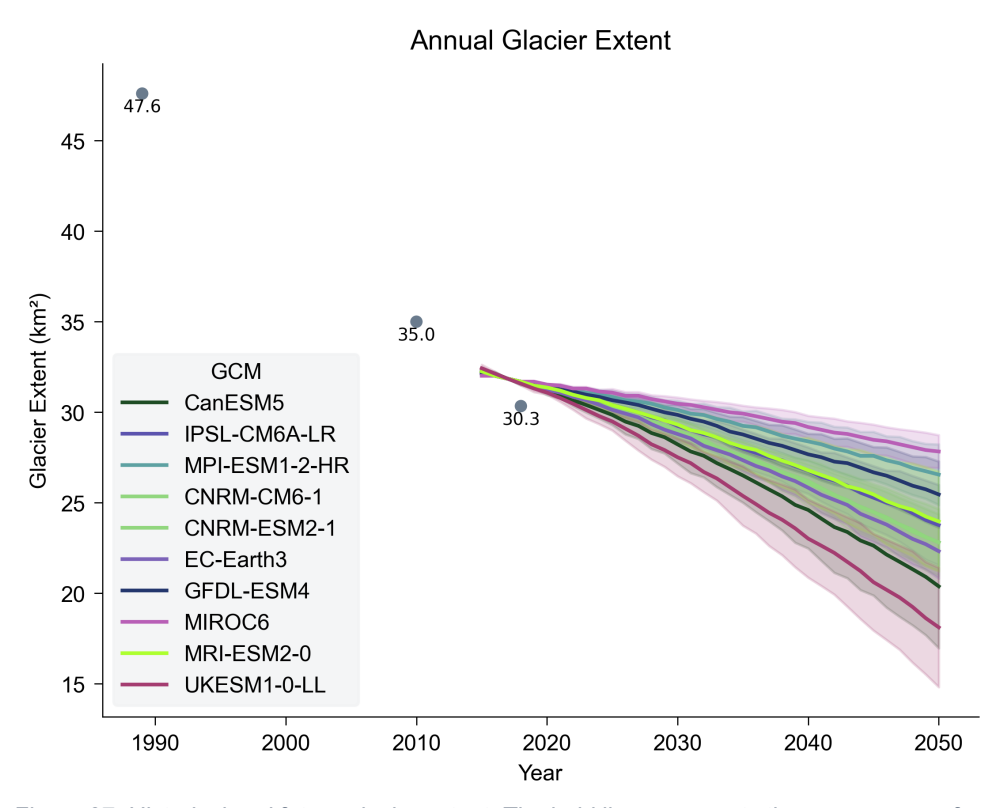


Figure 37: Historical and future glacier extent. The bold line represents the average area for each GCM, whilst the shaded areas illustrate the standard deviation (own illustration).

10. Personal Declaration

I hereby declare that the submitted thesis is the result of my own, independent work. All external sources are explicitly acknowledged in the thesis.

29.01.2024, Zurich

Fiona Federer

Tedor